Ion source surface activity in high pressure electron capture mass spectrometry
by Christopher Martin Pace

A thesis submitted in partial fulfillment of the requirements for the degree of Master of Science in Chemistry
Montana State University
© Copyright by Christopher Martin Pace (1988)

Abstract:
The negative ion mass spectra of 61 Environmental Protection Agency (EEA) priority pollutants using high pressure electron capture mass spectrometry (HPECMS) revealed that many of the compounds produced ions that could not have been formed by classical resonance and dissociative electron capture. Two general types of unusual ions arose out of the initial examination of the negative ion mass spectra produced by the pollutants. One of the two types of unusual ions was produced by many of the polychlorinated pollutants. These unusual ions corresponded to [M-Z+nH-nCl]^- where M is the parent analyte molecule and Z is either a fragment of M whose mass depends on its composition or is zero. The value of n was found to range between 1 and 5. The other type of unusual ion observed corresponded to [M+R]^- where R was thought to be predominantly CH2,CH3, or some other small alkyl species. Most of the polycyclic aromatic hydrocarbons (PAH's) examined displayed unusual ions of the type [M+R]^-. Normalized reconstructed single ion chromatograms (NRSIC) are shown to provide a useful probe into the nature of the two types of unusual ions discussed here. From examining the HPEC mass spectra and NRSIC at various ion source conditions, it is shown that both types of unusual ions result from interactions of an analyte species with the ion source wall. The theory of HPECMS shows that reactions occurring at the ion source surface provide a likely pathway for the production of unusual negative ions.

ION SOURCE SURFACE ACTIVITY IN HIGH PRESSURE ELECTRON CAPTURE MASS SPECTROMETRY

by

Christopher Martin Pace

A thesis submitted in partial fulfillment
of the requirements for the degree

of

Master of Science

in

Chemistry

MONTANA STATE UNIVERSITY
Bozeman, Montana

March 1988

N378
P1132

APPROVAL

of a thesis submitted by

Christopher Martin Pace

This thesis has been read by each member of the thesis committee and has been found to be satisfactory regarding content, English usage, format, citations, bibliographic style, and consistency, and is ready for submission to the College of Graduate Studies.

3/9/88
Date

Eric Grimsrud
Chairperson, Graduate Committee

Approved for the Major Department

3-9-88
Date

Bradford Pollard
Head, Chemistry Department

Approved for the College of Graduate Studies

3-18-88
Date

M P Malone
Graduate Dean

STATEMENT OF PERMISSION TO USE

In presenting this thesis in partial fulfillment of the requirements for a master's degree at Montana State University, I agree that the Library shall make it available to borrowers under rules of the Library. Brief quotations from this thesis are allowable without special permission, provided that accurate acknowledgment of source is made.

Permission for extensive quotation from or reproduction of this thesis may be granted by my major professor, or in his absence, by the Dean of Libraries when, in the opinion of either, the proposed use of the material is for scholarly purposes. Any copying or use of the material in this thesis for financial gain shall not be allowed without my written permission.

Signature 

Date 3-9-88

ACKNOWLEDGMENT

This research was funded in part by Cooperative Agreement CR-813424 with the U.S. Environmental Protection Agency, Environmental Research Laboratory, Athens, Georgia; and the National Science Foundation under Grant No. CHE-854029.

TABLE OF CONTENTS

	Page
INTRODUCTION	1
Background	1
Theory	11
Formation of Negative Ions	11
Positive Ions, Radicals, and Electrons	13
Diffusion to the Walls	16
Ion Source Surface Activity	17
Ventilation	19
Steady State Equations	20
Chemical Events versus Ventilation	23
STATEMENT OF PROBLEM	25
EXPERIMENTAL PROCEDURES	26
RESULTS AND DISCUSSION	28
Unusual Ions of the Type $[M-Z+nH-Cl]^-$	35
Endrin Aldehyde	35
Heptachlor Epoxide	53
Dieldrin	58
Heptachlor	61
Endrin	66
Endosulfan Sulfate	70
Hexachlorocyclopentadiene	75
Mirex	78
Pentac	81
Hexachlorobenzene	84
Polychlorinated Biphenyls (PCB's)	89
Ions of the Type $[M+R]^-$	92
Fluorene	94
Fluoranthene	100
Benzo(b)fluoranthene	106
Benzo(k)fluoranthene	109
SUMMARY	113
REFERENCES CITED	115
APPENDIX	118

LIST OF TABLES

Table		Page
1.	Values for Components of Equations 27 and 28 at 473 K, 0.3 Torr, 200 μA, and 200 eV	22
2.	Time Required for Two Body Reactions Inside the Ion Source at 473 K, 0.3 Torr, 200 μA, and 200 eV	23
3.	Time Required for Single Body Processes Inside the Ion Source at 473 K, 0.3 Torr, 200μA, and 200 eV	23
4.	EPA Priority Pollutants Examined by HPECMS	29
5.	Polychlorinated Compounds Investigated That Show Ions of the Type $[M-Z+nH-nCl]^-$	35
6.	Tabulated HPEC Mass Spectra for Endrin Aldehyde	38
7.	Effect of Pressure at a Constant Temperature of 100°C on the Formation of the Unsual Ions of Endrin Aldehyde	39
8.	Effect of the Emission Current at 100°C and 0.45 Torr on the Formation of the Unusual Ions of Endrin Aldehyde	40
9.	Tabulated HPEC Mass Spectra for Four PAH's	93
10.	Tabulated HPEC Mass Spectra for Heptachlor Epoxide	119
11.	Tabluated HPEC Mass Spectra for Dieldrin	119
12.	Tabulated HPEC Mass Spectra for Heptachlor	120
13.	Tabulated HPEC Mass Spectra for Endrin	120
14.	Tabulated HPEC Mass Spectra for Endosulfan Sulfate	121
15.	Tabulated HPEC Mass Spectra for Mirex	121

LIST OF TABLES - Continued

Table		Page
16.	Tabulated HPEC Mass Spectra for Pentac	122
17.	Tabulated HPEC Mass Spectra for Hexachlorobenzene	122

LIST OF FIGURES

Figure		Page
1.	The Proposed Mechanism for Unusual Ion Production Suggested by Stemmler and Hites	6
2.	The Proposed Mechanism for Unusual Ion Production Suggested by Sears, Campbell and Grimsrud	8
3.	HPEC Mass Spectrum of α-Hexachlorocyclohexane at 95°C and 0.3 Torr	31
4.	NRSIC for α-Hexachlorocyclohexane at 95°C and 0.3 Torr	32
5.	NRSIC for α-Hexachlorocyclohexane at 195°C and 0.3 Torr	33
6.	NRSIC for α-Hexachlorocyclohexane at 220°C and 0.3 Torr	34
7.	HPEC Mass Spectrum of Endrin Aldehyde at 85°C and 0.3 Torr	36
8.	NRSIC for Endrin Aldehyde at 85°C and 0.3 Torr	41
9.	NRSIC for Endrin Aldhyde at 100°C and 0.1 Torr	43
10.	NRSIC for Endrin Aldehyde at 100°C and 0.2 Torr	44
11.	NRSIC for Endrin Aldehyde at 100°C and 0.3 Torr	45
12.	NRSIC for Endrin Aldehyde at 100°C and 0.5 Torr	46
13.	NRSIC for Endrin Aldehyde at 175°C and 0.2 Torr	47
14.	NRSIC for Endrin Aldehyde for 175°C and 0.3 Torr	48

LIST OF FIGURES - Continued

Figure		Page
15.	Suggested Mechanism for the Formation of Negative Ions from Endrin Aldehyde	53
16.	HPEC Mass Spectrum of Heptachlor Epoxide at 80°C and 0.3 Torr	54
17.	NRSIC for Heptachlor Epoxide at 80°C and 0.3 Torr	56
18.	NRSIC for Heptachlor Epoxide at 100°C and 0.1 Torr	57
19.	Suggested Mechanism for the Formation of Negative Ions from Heptachlor Expoxide	58
20.	HPEC Mass Spectrum of Dieldrin at 85°C and 0.3 Torr	59
21.	NRSIC for Dieldrin at 85°C and 0.3 Torr	60
22.	Suggested Mechanism for the Formation of Negative Ions from Dieldrin	61
23.	HPEC Mass Spectrum of Heptachlor at 80°C and 0.3 Torr	63
24.	NRSIC for Heptachlor at 175°C and 0.3 Torr	64
25.	NRSIC for Heptachlor at 175°C and 0.45 Torr	65
26.	Suggested Mechanism for the Formation of Negative Ions from Heptachlor	66
27.	HPEC Mass Spectrum of Endrin at 80°C and 0.3 Torr	67
28.	NRSIC for Endrin at 80°C and 0.3 Torr	68
29.	Suggested Mechanism for the Formation of Negative Ions from Endrin	69
30.	HPEC Mass Spectrum of Endosulfan Sulfate at 100°C and 0.3 Torr	71
31.	NRSIC for Endosulfan Sulfate at 100°C and 0.3 Torr	72

LIST OF FIGURES - Continued

Figure		Page
32.	NRSIC for Endosulfan Sulfate at 220°C and 0.3 Torr	73
33.	Suggested Mechanism for the Formation of Negative Ions from Endosulfan Sulfate	74
34.	HPEC Mass Spectrum of Hexachlorocyclopentadiene at 90°C and 0.3 Torr	76
35.	NRSIC for Hexachlorocyclopentadiene at 90°C and 0.3 Torr	77
36.	Suggested Mechanism for the Formation of Negative Ions from Hexachlorocyclopentadiene	78
37.	HPEC Mass Spectrum of Mirex at 175°C and 0.2 Torr	79
38.	NRSIC for Mirex at 175°C and 0.2 Torr	80
39.	Suggested Mechanism for the Formation of Negative Ions from Mirex	82
40.	HPEC Mass Spectrum of Pentac at 100°C and 0.3 Torr	83
41.	NRSIC for Pentac at 100°C and 0.3 Torr	85
42.	Suggested Mechanism for the formation of Negative Ions from Pentac	86
43.	HPEC Mass Spectrum of Hexachlorobenzene at 100°C and 0.3 Torr	87
44.	NRSIC for Hexachlorobenzene at 100°C and 0.3 Torr	88
45.	Suggested Mechanism for the Formation of Negative Ions from Hexachlorobenzene	89
46.	HPEC Mass Spectrum of a PCB Containing 8 Chlorines at 100°C and 0.3 Torr	90
47.	NRSIC for a PCB Containing 8 Chlorines at 100°C and 0.3 Torr	91

LIST OF FIGURES - Continued

Figure		Page
48.	Suggested Mechanism for the Formation of Negative Ions from a PCB Containing 8 Chlorines	92
49.	HPEC Mass Spectrum of Fluorene at 260°C and 0.3 Torr	95
50.	NRSIC for Fluorene at 175°C and 0.3 Torr	97
51.	NRSIC for Fluorene at 200°C and 0.3 Torr	98
52.	NRSIC for Fluorene at 260°C and 0.3 Torr	99
53.	Suggested Mechanism for the Formation of Negative Ions from Fluorene	100
54.	HPEC Mass Spectrum of Fluoranthene at 260°C and 0.3 Torr	101
55.	NRSIC for Fluoranthene at 100°C and 0.2 Torr	103
56.	NRSIC for Fluoranthene at 180°C and 0.2 Torr	104
57.	NRSIC for Fluoranthene at 200°C and 0.3 Torr	105
58.	Suggested Mechanism for the Formation of Negative Ions from Fluoranthene	106
59.	HPEC Mass Spectrum of Benzo(b)fluoranthene at 250°C and 0.3 Torr	107
60.	NRSIC for Benzo(b)fluoranthene at 220°C and 0.2 Torr	108
61.	Suggested Mechanism for the Formation of Negative Ions from Benzo(b)fluoranthene	109
62.	HPEC Mass Spectrum of Benzo(k)fluoranthene at 250°C and 0.3 Torr	110
63.	NRSIC for Benzo(k)fluoranthene at 250°C and 0.3 Torr	111
64.	Suggested Mechanism for the Formation of Negative Ions from Benzo(k)fluoranthene	112

ABSTRACT

The negative ion mass spectra of 61 Environmental Protection Agency (EPA) priority pollutants using high pressure electron capture mass spectrometry (HPECMS) revealed that many of the compounds produced ions that could not have been formed by classical resonance and dissociative electron capture. Two general types of unusual ions arose out of the initial examination of the negative ion mass spectra produced by the pollutants. One of the two types of unusual ions was produced by many of the polychlorinated pollutants. These unusual ions corresponded to $[M-Z+nH-nCl]^-$ where M is the parent analyte molecule and Z is either a fragment of M whose mass depends on its composition or is zero. The value of n was found to range between 1 and 5. The other type of unusual ion observed corresponded to $[M+R]^-$ where R was thought to be predominantly CH_2, CH_3, or some other small alkyl species. Most of the polycyclic aromatic hydrocarbons (PAH's) examined displayed unusual ions of the type $[M+R]^-$. Normalized reconstructed single ion chromatograms (NRSIC) are shown to provide a useful probe into the nature of the two types of unusual ions discussed here. From examining the HPEC mass spectra and NRSIC at various ion source conditions, it is shown that both types of unusual ions result from interactions of an analyte species with the ion source wall. The theory of HPECMS shows that reactions occurring at the ion source surface provide a likely pathway for the production of unusual negative ions.

INTRODUCTION

Background

High Pressure Electron Capture Mass Spectrometry (HPECMS) is a term used to describe the analytical method of detecting negative ions produced in a chemical ionization (CI) ion source containing about 0.1 to 1.0 Torr of buffer gas. This method of mass spectrometry evolved from its counterpart, Positive Chemical Ionization Mass Spectrometry (PCIMS), developed by Munson and Field[1] in 1966. While the production and detection of positive ions was well understood in 1966, negative ion mass spectrometry was not. The slower development of negative ion mass spectrometry was due in part to a lack of instruments capable of detecting negative ions. One of the first reports of HPECMS was in 1972 when Dougherty and Dalton[2] published their negative ion mass spectra of 10 polycyclic chlorinated insecticides using methane as the buffer gas. Since this time, and especially in the last decade, HPECMS has evolved into a widely used technique. HPECMS in conjunction with capillary column gas chromatography has become a powerful tool to those working in areas of chemistry where a need exists for a highly sensitive and/or selective means of compound identification.

The reason for the success of HPECMS stems from the reaction of thermalized gas phase electrons with gas phase molecules. It has been shown[3] that the sensitivity of HPECMS versus PCIMS depends to a large degree upon the second order rate coefficients of the primary reactions involved. The second order rate coefficient for electron-molecule reactions is up to two orders of magnitude greater than that of the positive ion-molecule reactions associated with PCIMS.[4] In order for an organic molecule to undergo electron capture, it must possess a positive electron affinity (EA)[5-8] and be able to stabilize its excess energy, obtained from the electron capture process, by collisions with neutral gas molecules before electron autodetachment can occur.[7,8] Only a small fraction of all organic molecules possess a positive EA, thus making HPECMS a very useful tool for detecting certain compounds in complex matrixes.[3,9] In some instances it is possible to derivatize a compound with a negative or slightly positive EA to form one which captures electrons readily.[10] One example of the derivatization technique is in the quantitation of octopamines and synephrines in urine[11] where the molecules were first derivatized with pentafluoropropionic anhydride.

The buffer gas in the HPECMS ion source serves two purposes. First, the buffer gas provides a medium in

which the energy of the initial electron beam and that of the secondary electrons produced by the beam are quickly reduced by collisions with neutral buffer gas molecules. This produces a large population of low energy electrons[12] increasing the probability of electron capture occurring. Secondly, the buffer gas provides collisional stabilization to the initially formed excited negative ion.[13] Several different monotomic and diatomic gases, including He, Ne, Ar, Kr, Xe, N_2, CH_4, $i\text{-}C_4H_{10}$ and CO_2, have been used as the buffer gas in HPECMS.[13] All of the above gases have unique characteristics. In the remainder of this work we will be concerned primarily with methane as the buffer gas.

Although many of the organic molecules that capture electrons do so by the classical resonance and/or dissociative electron capture processes, some organic molecules exhibit HPEC mass spectra that must have had their origins from reactions other than or in addition to electron capture.[12] Several reasons can be stated for the appearance of unusual ions observed in the HPEC mass spectra of certain compounds. First, the electron capture process is sufficiently fast as to allow several events to occur during the residence time that the analyte molecule spends in the ion source.[8] The high source pressure can possibly cause reactions between analyte molecules and buffer gas ions[12] and between analyte molecules and buffer

gas radicals prior to ionization.[14,15] Both gas phase ions and radicals are produced in high abundance by irradiation of the buffer gas with the primary electron beam. Finally, the presence of trace impurities, such as oxygen and water, that find their way into the ion source of the mass spectrometer can possibly lead to the formation of unusual ions.[12] The processes leading to the formation of negative ions inside the HPEC ion source are strongly dependent upon experimental parameters such as temperature, pressure, emission current, and the energy of the primary electron source.[16]

Numerous examples appear in the literature which exhibit HPEC mass spectra that arose from processes other than simple resonance and/or dissociative electron capture. The HPEC mass spectra of the polycyclic chlorinated insecticides published by Dougherty and Dalton[2] displayed unusual ions of the type $[M+O-Cl]^-$ and $[M+Cl]^-$ (where M is the parent analyte molecule). The $[M+O-Cl]^-$ ion appears elsewhere in the literature[6,16,17] and has been shown[18] to be a displacement reaction between the molecular anion, M^-, and trace amounts of oxygen present in the mass spectrometer.

The $[M+Cl]^-$ ion mentioned above is thought to arise from reaction between the parent molecule and the primary dissociative electron capture product, chloride ion.[19] The $[M+Cl]^-$ ion in this case can be minimized, if not

eliminated, by reducing the sample concentration initially introduced into the ion source.[19] The introduction of analyte molecules under normal capillary column GC/MS conditions will, under most conditions, eliminate the production of $[M+Cl]^-$ ions. Kassel, Kayganich and Watson[20] displayed HPEC mass spectra that also contained $[M+Cl]^-$ ions, but in this case the analyte molecules did not contain any chlorine atoms. Here the ion source was pretreated with carbon tetrachloride (CCl_4) for a short time (five minutes) before being returned to the normal mode of HPECMS operation, methane at 1 Torr. A five- to ten-fold increase in relative response for a wide range of compounds was observed when the CCl_4 pretreatment method was applied. The unusual $[M+Cl]^-$ ions were described as arising from a chloride radical ($Cl^{\cdot}$) attachment prior to ionization by electron capture. The source of the $Cl^{\cdot}$ radical was thought to be the metallic surfaces inside the ion source which had been pretreated with CCl_4. The observation of very low levels of Cl^- ions and the decrease in the $[M+Cl]^-$ ion with increases in both time and temperature strongly supported the idea of $Cl^{\cdot}$ species bound to the source walls. The authors summed up this work with the following:

> For unsaturated organic compounds there appears to be sufficient interaction between analyte, $Cl^{\cdot}$ radicals, and the source volume surface for production of very intense $[M+Cl]^-$ ions.

Jones, et. al.,[21] have also reported the presence of $Cl^{\cdot}$ radicals on iron surfaces, following treatment with CCl_4.

The HPEC mass spectra published by Stemmler and Hites[19] of 24 hexachlorocyclopentadiene derivatives displayed unusual ions of the type $[M+nH-nCl]^-$ where n was shown to range between 1 and 5 for many of the compounds. In addition to ions resulting from both a single and series of 34 mass unit losses from the parent molecule, a close inspection of this work reveals that the loss of 34 mass units can also occur from fragment ions. Figure 1 is the proposed route to the production of the $[M+nH-nCl]^-$ ions as suggested by Stemmler and Hites. This figure shows an addition-elimination reaction which could occur prior to ionization by electron capture. A series of addition-elimination reactions occurring prior to electron capture could account for the multiple losses of 34 mass units. When fully deuterated methane was used as the buffer gas, both $[M+H-Cl]^-$ and $[M+D-Cl]^-$ ions were observed.

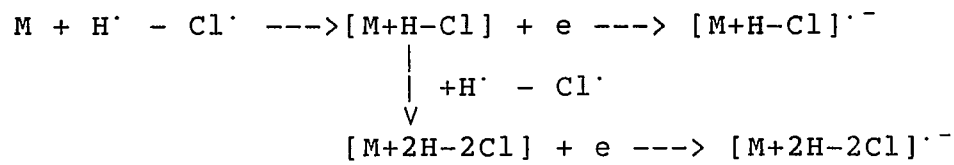


Figure 1. The Proposed Mechanism for Unusual Ion Production Suggested by Stemmler and Hites.

The $[M+nH-nX]^-$ ion, where X refers to a halogen, is prevalent in the HPEC mass spectra of many polyhalogenated organic molecules.[8,16,17,22,23]

Sears, Campbell and Grimsrud[8] recently published a paper which addressed the formation of unusual ions of the type $[M+nH-nX]^-$ and concluded that these ions resulted from interaction of the species of interest with the walls of the ion source. Evidence supporting this idea was presented and will be briefly described here.

When the compound fluoranil was introduced into the ion source of a mass spectrometer which had previously been filled with methane under normal HPECMS conditions, the electron impact (EI) spectrum of this compound displayed an ion which was not present in the EI spectrum when the compound was introduced into a clean ion source. This ion corresponded to the molecular ion plus two hydrogens, $[M+2H]^+$. The $[M+2H]^+$ ion was thought to result from a reaction where a double bond containing two halogens was hydrogenated. Other evidence shown in this work displayed the apparent sticking of certain species to the ion source walls. The sticking effect was displayed by the use of normalized reconstructed single ion chromatograms (NRSIC) which showed that the unusual ions of the type $[M+nH-nX]^-$ were persisting in time well after the disappearance of the parent molecular anion, M^-. This result suggested that some species adhere to the walls of

the ion source for some time after the analyte passed through the source. The mechanism proposed by Sears, Campbell and Grimsrud for the production of the $[M+nH-nX]^-$ ions is shown in Figure 2 and takes the above evidence into consideration.

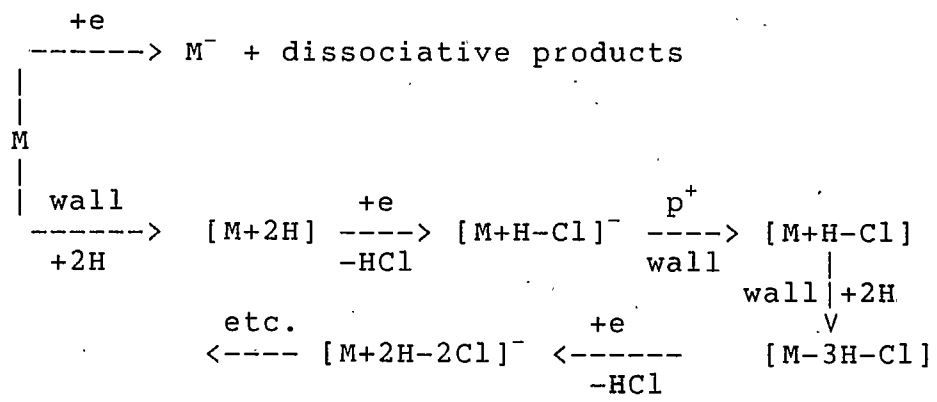


Figure 2. The Proposed Mechanism for Unusual Ion Production Suggested by Sears, Campbell and Grimsrud.

Also, in this same study the HPEC mass spectra of trifluoroacetic derivatives of isomers of aminoanthracene and aminophenanthrene were shown to contain unusual ions of the type $[M-0]^-$. These ions are considered unusual because the only oxygen present in these molecules is doubly bonded to a carbon atom. The $[M-0]^-$ ion was drastically reduced in abundance by adding triethylamine to the methane buffer gas. Triethylamine has a very high proton affinity and reacts quickly with the positive reagent ions found in the methane plasma by abstraction of

a proton. The protonated amines, thereby formed, do not react with the analyte. Their conclusion was that the unusual ion in this case arose from a positive ion-molecule reaction followed by neutralization and then electron capture. These researchers also applied triethylamine to the compounds discussed above that show unusual ions of the type $[M+nH-nX]^-$. They found that no changes in the spectra were observed, indicating that these ions do not depend on positive ion-molecule interactions.

Another type of unusual ion found in HPECMS literature is the ion corresponding to $[M+R]^-$, where R is a hydrogen or other alkyl species. McEwen and Rudat[15] were the first investigators to report radical addition reactions taking place in the ion source of a mass spectrometer under HPECMS conditions. They used 7,7,8,8-tetracyanoquinodimethane (TCNQ) as a radical trap inside the ion source and showed that this compound gave complex HPEC mass spectra which displayed ions of the type $[M+R]^-$, where R in this case was predominantly $\cdot H$, $\cdot CH_3$, and $\cdot C_2H_5$. They concluded that the addition products observed for TCNQ under HPECMS conditions were due to the gas phase addition of radicals prior to electron capture.

Other examples appear in the literature where it is believed that the $[M+R]^-$ ions observed resulted from gas phase radical attachment prior to electron capture. A study done by Stockl and Budzikiewicz[14] concerning

molecule-radical reactions under HPECMS conditions showed that 4-hydroxyquinoline-2-carboxylic acid, phenzaine-1-carboxylic acid, and related compounds produced spectra that included ions of the type $[M+C_nH_{2n}]^-$. They concluded that these ions resulted from methyl radical ($\cdot CH_3$) attack on the analyte molecule followed by abstraction of a hydrogen by another radical species ($R\cdot$) prior to ionization. Hilpert, Byrd, and Vogt[24] showed that some of the polycyclic aromatic hydrocarbons (PAH's) they tested produced HPEC mass spectra that included ions of the type $[M+CH_2]^-$. An interesting feature of the work shown by these investigators was the differing relative abundance of the $[M+CH_2]^-$ ions between different compounds. The studies of other investigators[25,26] on the HPEC mass spectra produced by PAH's exhibit general disagreement with respect to the ionization process involved.

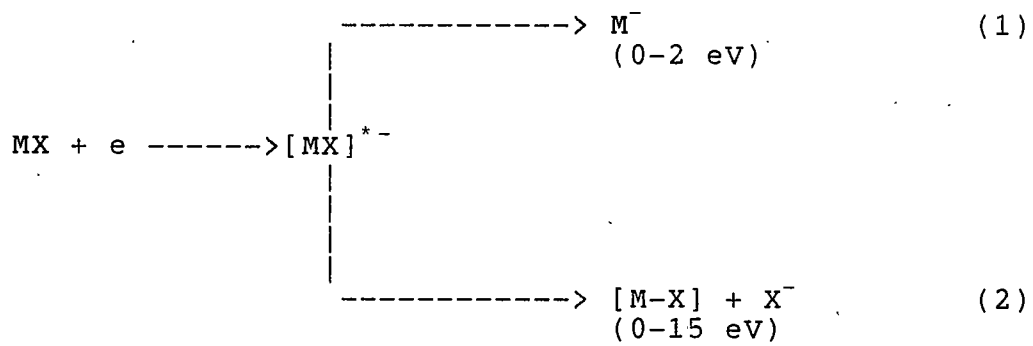
The examples given above of unusual ions occurring in HPECMS indicate that the ion source is a place where chemical events, in addition to resonance and dissociative electron capture, can be responsible for the observed spectra. In order to determine the origins of the unusual ions found in the HPEC mass spectra of some of the EPA priority pollutants examined in Chapter 4 of this study, a detailed look at the existing theory concerning the possible chemical events occurring inside the CI ion source will be presented.

Theory

According to the present theory of HPECMS, several chemical events are possible inside the ion source that can potentially lead to the negative ions detected. These chemical events will be systematically reviewed in the following sections. After the review of chemical events, the importance of each will be presented.

Formation of Negative Ions

Negative ions may be formed by resonance and dissociative electron capture.[7] These processes are shown by reactions 1 and 2:



(1)

(2)

Reaction 1, resonance electron capture, occurs between molecules having a positive electron affinity and electrons which have energies in the range of 0-2 electron volts (eV). The vibrationally excited negative ion initially produced, $[MX]^{*-}$, must be stabilized by collisions with neutral gas molecules before it undergoes

autodetachment of the electron or dissociation. Reaction 2, dissociative electron capture, can occur by a rapid bond cleavage or by a slower process which may involve a molecular rearrangement.[7] These reactions occur between analyte molecules and electrons with energies in the range of 0-15 eV. The electrons inside the ion source under HPECMS conditions are thought to be of near thermal energy (0 eV).[8] In addition to the electron's energy, the product generated by electron capture can also be dependent upon the ion source temperature and pressure. For some molecules higher ion source temperature promotes dissociative electron capture resulting in an increase in fragment ions, such as Cl^- for chlorinated compounds, while lower temperatures favor the production of molecular anions formed by the resonance electron capture process.[17] Other molecules, such as the PAH's, show a much smaller degree of HPEC mass spectral variation with changes in temperature.[26] Increasing the ion source pressure will increase the number of ion-electron pairs that are produced until the electron beam is stopped by gas molecules. Increasing the ion source pressure will also increase the collisional frequency, affecting the rate of electron thermalization and collisional stabilization of the vibrationally excited negative ions. In most cases increasing the ion source pressure increases the negative ion response until a maxima is reached.[5,13] The second

order rate coefficient for the electron capture process is around $2x10^{-7}$ cm^3 $molecule^{-1}$ sec^{-1} for molecules which undergo this process most rapidly,[4] and a wide range of coefficients can generally be expected.

Positive Ions, Radicals, and Electrons

The HPEC ion source contains between 0.1 and 1.0 Torr methane which is used for the purpose of reducing the energy of the initial electron beam and to provide collisional stabilization of the negative ions formed by electron capture.[13] The interaction of the electron beam with neutral methane gas molecules inside the ion source produces a high abundance of positive ions, radicals, and low energy electrons.[13,15] As indicated in equations 3 and 4:

$$CH_4 + e \text{ -----> } CH_4^+ + 2e \quad (3)$$

$$CH_4 + e \text{ -----> } CH_3^+ + H^{\cdot} + 2e \quad (4)$$

formation of each positive ion is accompanied by the production of a low energy electron. Each ionizing event removes about 30 eV from the bombarding electron,[27] typically between 70-300 eV, and the energy of the incident electron beam is further reduced by additional nonionizing collisions with neutral methane molecules.[28] The production rate, S, of positive ions and low energy electrons is given by:

$$S \text{ (pairs/sec)} = 2.1 \times 10^{11} \text{ (I x E)} \quad (5)$$

where I (μA) is the intensity of the electron beam entering the ion source and E (eV) is its energy. For the ion source used in this study the value of I has been estimated to be 5% of the set emission current.[8] The positive ions produced by reactions 3 and 4 are rapidly converted into CH_5^+ and $C_2H_5^+$ ions[1] as shown below:

$$CH_4^+ + CH_4 \text{ -----> } CH_5^+ + \cdot CH_3 \quad (6)$$

$$CH_3^+ + CH_4 \text{ -----> } C_2H_5^+ + H_2 \quad (7)$$

Recombination of positive ions with electrons also occurs under HPECMS conditions[15] producing radical and neutral products. Examples of recombination are given by equations 8-10:

$$C_2H_5^+ + e \text{ -----> } \cdot C_2H_5 \quad (8)$$

$$CH_5^+ + e \text{ -----> } \cdot CH_3 + H_2 \quad (9)$$

$$CH_5^+ + e \text{ -----> } \cdot H + CH_4 \quad (10)$$

The production rate for radical species, S_R, can be obtained by modification of equation 5. The modification takes into account the observation made from equations 3, 4 and 6 through 10 that between 2 and 3 radicals are produced for every positive ion-electron pair produced by the interaction of the primary electron beam with methane gas molecules. The production rate for radicals inside the HPEC ion source is given by:

$$S_R \text{ (radicals/sec)} = 5.3\times10^{11} \text{ (I x E)} \quad (11)$$

where I (μA) and E (eV) are the same as equation 5.

The second order rate coefficients for positive ion-molecule reactions under HPECMS conditions are around 2×10^{-9} cm^3 $molecule^{-1}$ sec^{-1} for exothermic reactions.[4] For radical-molecule reactions the second order rate coefficient is around 1×10^{-10} cm^3 $radicals^{-1}$ sec^{-1} for the very fastest of these reactions.[15]

In addition to reacting with neutral molecules, positive ions can also recombine with electrons or negative ions. The second order rate coefficient for positive ion-electron recombination, α_e, has been shown to be fairly constant for different organic positive ions[29] and is given by:

$$\alpha_e \text{ } (cm^3 \text{ } sec^{-1}) = 9\times10^{-7} \text{ } (300/T)^{1/2} \quad (12)$$

where T (K) is the temperature of the ion source. For positive ion-negative ion recombinations under HPECMS conditions, the second order rate coefficients, α_-, have been shown to be approximately equal for all reactions of this type regardless of the interacting species.[30] The second order rate coefficient for all positive ion-negative ion recombinations is given by:[30]

$$\alpha_- \text{ } (cm^3 sec^{-1}) = 6.8\times10^{-7} \text{ } T^{-0.4} \quad (13)$$

The radical species produced inside the ion source can undergo radical-radical recombination. The second order rate coefficient for methyl-methyl radical recombination, K_R, will be used for all recombinations of this type and is 4×10^{-11} cm^3 $radicals^{-1}$ sec^{-1}.[31]

Diffusion to the Walls

An ion source operated under HPECMS conditions fits Langmuir's definition of a plasma,[32] and the diffusional characteristics of charged species are ambipolar as opposed to free. The chemical species present in the ion source can diffuse through the plasma and come into contact with the source wall. A charged species upon contact with an ion source wall will lose its charge. The rate coefficient for the diffusion process depends upon whether the species under consideration is charged or neutral. For positive ions, negative ions and electrons the rate coefficient for diffusion is given by $D_a r_o^{-2}$, where D_a is the ambipolar diffusion coefficient[8] and r_o is the characteristic diffusion length[33] of the ion source. The ambipolar diffusion coefficient, D_a, is used here for all charged species because the ionic plasma does not permit the free diffusion of individual species. Inside the ion source of the HPEC mass spectrometer a positive ion will diffuse twice as fast as the electrostatically free positive ion, and the electron will diffuse 500 times

slower than when free in order to meet the conditions of charge neutrality required by ionic plasmas of this type.[3] An equation for D_a has been provided,[8] which is strongly dependent on changes in both temperature and pressure and is given by:

$$D_a \ (cm^2 sec^{-1}) = 0.11 \ (T/273)^2 \ (760/P) \qquad (14)$$

where T (K) is the temperature of the ion source and P (Torr) is the pressure.

For neutral molecules and radicals the rate coefficient for diffusion is given by Dr_o^{-2}, where D is the diffusion coefficient for neutrals[34] and r_o is the characteristic diffusion length[33] of the ion source. An equation for D has been provided[8,34] and is given by:

$$D \ (cm^2 sec^{-1}) = 0.063 \ (T/273)^{3/2} \ (760/P) \qquad (15)$$

The characteristic diffusion length, r_o, has been estimated[8] at 0.13 cm for the ion source used in this work.

Ion Source Surface Activity

If a species is chemically altered upon contact with the metallic surface (or wall) inside the ion source and subsequently detected as a negative ion, there then is a need to know what type of activity takes place at this surface. For most gas-metal combinations absorption is a

remarkably efficient process, and the probability that a normal backgound constituent of a vacuum system, such O_2, CO, N_2 or H_2, will become adsorbed during a single collision with a clean metal surface (the "sticking probability") is high, often between 0.1 and 1.[35] When the methane plasma interacts with the typical HPEC ion source of stainless steel construction, a series of surface reactions are possible. Some of the surface reactions that could possibly take place at the methane plasma-metal interface[36] are shown below:

$$CH_4 \text{ <----> } CH_4(\text{adsorbed}) \quad (16)$$

$$CH_4(\text{ad}) \text{ <----> } CH_3(\text{ad}) + H(\text{ad}) \quad (17)$$

$$CH_3(\text{ad}) \text{ <----> } CH_2(\text{ad}) + H(\text{ad}) \quad (18)$$

$$CH_2(\text{ad}) \text{ <----> } CH(\text{ad}) + H(\text{ad}) \quad (19)$$

$$CH(\text{ad}) \text{ <----> } C(\text{ad}) + H(\text{ad}) \quad (20)$$

$$C(\text{ad}) \text{ <----> } C(\text{dissolved}) \quad (21)$$

$$H_2 \text{ <----> } 2H(\text{ad}) \quad (22)$$

From equations 16 through 22 it can been seen that the ion source surface has on it a complex array of methane derived species. In addition to the methane gas interaction with the ion source surface, it can now be envisioned that some of the radicals and positive ions shown earlier to be produced inside the ion source under HPECMS conditions could also adsorb onto the surface.

If an analyte species, neutral or charged, comes into contact with the ion source wall there are several possible outcomes. The species could potentially react with one of the methane derived species thought to be present on the source surface followed by desorption and possible electron capture to result in the observation of an unusal ion.

Another fate of collision of an analyte species with the ion source surface might be a dissociative reaction which consumes the species of interest as was shown[37] to be the case for ethylene and selected halogeno-substituted alkenes on an iron surface at 300 K. The species could also adsorb onto the ion source surface then desorb without any change in structure.

If any sticking is occurring at the ion source surface by analyte species, a means of showing this type of behavior is needed. The normalized reconstructed single ion chromatogram (NRSIC) is probably the best method available for this type of observation and will be used in this study.

Ventilation

For the chemical events described earlier to occur inside the ion source they must do so before the species of interest is vented from the source. The rate coefficient for ventilation is given by F/V where

F (cm^3 sec^{-1}) is the volumetric flow rate of gas through the detector and V (cm^3) is the source volume. The volumetric flow rate is determined from an equation by Dushman[38] and is shown below:

$$F = 3.64 \times 10^3 \; A \; (T/M)^{1/2} \qquad (24)$$

where A (cm^2) is the sum of the electron beam entrance aperture and the ion exit slit, T (K) is the temperature of the ion source, and M is the molecular weight of the buffer gas. The volumetric flow rate is independent of the ion source pressure and is equal to the conductance out of the source. For the ion source used in this work the value of A is 0.018 cm^2, and the value of M is 16, the molecular weight of methane.

Steady State Equations

In order to determine the importance of the chemical events lisited earlier in this chapter, the concentration of electrons, positive ions and radicals needs to be determined. The equation Siegal[3] derived for the positive ion concentration under CI conditions in the absence of sample molecules and assuming steady state conditions is given by:

$$\frac{d[I^+]}{dt} = S - \frac{F}{V}[I^+] - \frac{Da}{r_o^2}[I^+] - \alpha_e [I^+][e] = 0 \qquad (25)$$

where all the terms for this equation have been described earlier. A similar equation can be derived[15] to calculate the steady state radical population in a CI plasma and is given by:

$$\frac{d[R]}{dt} = S_R - \frac{F}{V}[R] - \frac{kD}{r_o^2}[R] - K_R[R]^2 = 0 \qquad (26)$$

where k is the reactivity between radicals and the ion source walls. For the case in which every collision with the wall results in loss of the radical, k=1. The other terms found in equation 26 have been described earlier in this chapter.

Equations 25 and 26 can be rearranged into quadratic equations and subsequently solved. In solving equation 25 the positive ion and electron concentrations were taken as being equal as was shown in an earlier section of this chapter. For equation 26 it will be assumed that all radicals upon contact with the source suface will not be destroyed, k=0. The resulting equations in terms of positive ion and electron concentration and radical concentration are shown by:

$$[e] = [I^+] = \frac{-\left(\frac{D_a}{r_o^2} + \frac{F}{V}\right) + \left[\left(\frac{D_a}{r_o^2} + \frac{F}{V}\right)^2 + \frac{4\alpha_e S}{V}\right]^{1/2}}{2\alpha_e} \qquad (27)$$

$$[R] = \frac{-\left(\frac{F}{V}\right) + \left[\left(\frac{F}{V}\right)^2 + \frac{4K_R S_R}{V}\right]^{1/2}}{2 K_R} \qquad (28)$$

where the values of the components of each equation have been given in absolute or equation form in previous sections of this chapter. Table 1 lists the value of each component of equations 27 and 28 at the specified ion source conditions. From the values given in Table 1 the concentration of positive ions and electrons is found to be 8×10^9 pairs cm^{-3}, and the concentration of radicals is 2×10^{12} radicals cm^{-3}. Thus at these conditions the radicals exceed positive ions and electrons by a factor of 250.

Table 1. Values for Components of Equations 27 and 28 at 473 K, 0.3 Torr, 200 μA, and 200 eV.

Component	Value
F	356 cm^3 sec^{-1}
V	1 cm^3
S	4.2×10^{14} pairs sec^{-1}
S_R	1.1×10^{15} radicals sec^{-1}
D_a	8.3×10^2 cm^2 sec^{-1}
D	3.6×10^2 cm^2 sec^{-1}
r_o^2	0.0169 cm^2
α_e	7×10^{-7} cm^3 sec^{-1}
K_R	4×10^{-11} cm^3 $radicals^{-1}$ sec^{-1}

Chemical Events versus Ventilation

From the concentrations of positive ions, electrons, and radicals found in the previous section, it is now possible to determine the time needed for individual chemical events to occur inside the ion source. Table 2 lists the time that is needed, by way of pseudo first order rate constants, for the two-body reactions at the ion source conditions given. Table 3 lists the time required for single body events to occur inside the ion source.

Table 2. Time Required for Two Body Reactions Inside the Ion Source at 473 K, 0.3 Torr, 200 μA, and 200 eV.

Event	Rate Const. $cm^3\ sec^{-1}$	Time Req. (msec)
Electron capture	$2x10^{-7}$	0.5
Positive ion-molecule	$2x10^{-9}$	60
Radical-molecule(K_R)	$1x10^{-7}$	5
Positive ion-electron(α_e)	$7x10^{-7}$	0.2
Positive ion-negative ion (α_-)	$5.8x10^{-8}$	2

Table 3. Time Required for Single Body Processes Inside the Ion Source at 473 K, 0.3 Torr, 200 μA, and 200 eV.

Event	Rate Const. sec^{-1}	Time Req. (msec)
Ventilation(F/V)	356	3
Neutral Diffusion(Dr_o^{-2})	$2.1x10^4$	0.05
Charged Diffusion($D_a r_o^{-2}$)	$4.9x10^4$	0.02

It is apparent that the time required for ventilation, about 3 msec, is slow enough to allow several reactions to occur while the analyte is still inside the ion source. For example, the analyte molecule could diffuse to the source wall (0.05 msec), desorb and capture an electron (0.5 msec), then diffuse to the source wall again (0.02 msec) followed by desorption and electron capture. This sequence of diffusion, desorption, and electron capture could theoretically occur approximately six times before the analyte is vented from the source.

Because the rates of reactions given earlier were for specific cases the values given in Table 2 could possibly be in large error for certain cases. Nevertheless, this view of ion source events has proven to be useful in the past[8] and will be used in this work to help explain the unusual ions found to be present in the HPEC mass spectra of a number of the EPA priority pollutants.

STATEMENT OF PROBLEM

In the previous chapter the current literature concerning the observation of unusual ions in HPECMS was presented which showed that events other than electron capture must have been responsible for the unusual ions. The current theory concerning HPECMS was then presented and clearly showed that many chemical events in addition to electron capture can possibly occur inside an ion source operated under HPECMS conditions. The objective of this study was to examine the HPEC mass spectra of a majority of the EPA priority pollutants[39] and to use the present theory of HPECMS described in the Introduction to explain any unusual ions observed.

EXPERIMENTAL PROCEDURES

All HPEC mass spectra and chromatograms shown in this study were obtained on a VG 7070E-HF double focusing mass spectrometer which was directly coupled to a Varian 3700 gas chromatograph using a 30 m x 0.25 mm DB-5 fused silica column (J&W Scientific, Rancho Cordova, California). Helium was used as the GC carrier gas at a flow rate of about 1 to 2 cm^3 - atm sec^{-1}. The flow rate of methane gas through another port depended upon the ion source pressure desired and was typically ten times greater than the flow of helium. Ion source pressure was determined with a MKS 270B capacitive manometer. In this study source pressures between 0.1 and 0.5 Torr were used. The opening where the direct insertion probe entered the source was plugged to avoid variations in source conductance. The ion source temperature was determined by a thermocouple which was attached to the ion source block. Source temperatures between 80°C and 260°C were used. The electron energy was either 200 eV or 250 eV and the emission current was either 200 μA or 500 μA. The detection of negative ions was achieved by the use of a conversion dynode and an analog electron multiplier.

All compounds used in this study were obtained from Chemical Services, Inc., West Chester, Pennsylvania. Methanol was used as the solvent except in the case of the polynuclear aromatic hydrocarbons (PAH's) where toluene was used. All compounds were introduced into the ion source via the capillary column in the splitless mode for 30 seconds at concentrations between 1 and 10 ng/μL.

RESULTS AND DISCUSSION

This study began with the examination of the HPEC mass spectra produced by the EPA priority pollutants listed in Table 4. From this initial examination two distinct types of spectra arose which displayed negative ions that could not have resulted from the classical resonance and dissociative electron capture processes alone. One of the two types of spectra mentioned above shows unusual ions of the type $[M-Z+nH-nCl]^-$, where M is the analyte molecule and Z is either a fragment of M whose mass depends on its composition or is zero. A number of the polychlorinated pollutants listed in Table 4 display negative ions corresponding to $[M-Z+nH-nCl]^-$. The other type of unusual negative ions observed in the spectra of some of the EPA priority pollutants corresponds to $[M+R]^-$, where R is thought to be H, CH_2, CH_3 or some other small alkyl species. Most of the PAH's listed in Table 4 show ions of the type $[M+R]^-$.

The normalized reconstructed single ion chromatograms (NRSIC), which were mentioned briefly in Chapter 1, will be used extensively throughout this study to prove the existence of interactions between analyte species and the ion source walls. Theoretically, the ions produced in the

Table 4. EPA Priority Pollutants Examined by HPECMS.

1. 1,2,4-Trichlorobenzene
2. Hexachlorobenzene
3. Hexachloroethane
4. Bis(2-chlorethyl)ether
5. 4-Chloro-3-methylphenol
6. 2-Chlorophenol
7. o-Dichlorobenzene
8. m-Dichlorobenzene
9. p-Dichlorobenzene
10. 2,4-Dichlorophenol
11. Bis(2-chloroisopropyl)ether
12. Bis(2-chloroethoxy)methane
13. Hexachlorobutadiene
14. Hexachlorocyclopentadiene
15. Pentachlorophenol
16. Tetrachloroethylene
17. Aldrin
18. Dieldrin
19. 4,4'-DDT
20. 4,4'-DDE
21. 4,4'-DDD
22. Endosulfan sulfate
23. Endrin
24. Endrin aldehyde
25. Heptachlor
26. Heptachlor epoxide
27. Hexachlorocyclohexane (BHC-α)
28. Hexachlorocyclohexane (BHC-β)
29. Hexachlorocyclohexane (BHC-γ)
30. Hexachlorocyclohexane (BHC-Δ)
31. Chlordane
    (technical mixture and metabolites)
32. PCB 1221
33. PCB 1248
34. PCB 1260
35. Acenaphthene
36. Fluoranthene
37. Benzo(a)pyrene
38. Benzo(b)fluoranthene
39. Benzo(k)fluoranthene
40. Acenaphthylene
41. Anthracene
42. 1,12-Benzoperylene
43. Fluorene
44. Phenanthrene
45. 1,2:5,6-Dibenzanthracene
46. Ideno (1,2,3-C,D) pyrene
47. Pyrene
48. Bis(2-ethylhexyl)phthalate
49. Butyl benzyl phthalate
50. Di-n-butyl phthalate
51. Diethyl phthalate
52. Dimethyl phthalate
53. 2,4-Dinitrotoluene
54. 2,6-Dinitrotoluene
55. Nitrobenzene
56. 2-Nitrophenol
57. 2,4-Dinitrophenol
58. N-Nitrosodiphenylamine
59. N-Nitrosodi-n-propylamine
60. Phenol
61. Isophorone

gas phase inside the mass spectrometer by a single compound should be vented from the ion source at approximately the same time. All NRSIC should then follow the same chromatogram. But because a mass spectrometer focuses individual ions on the detector, it is the electronics that limit how fast the mass range of interest can be scanned. If the scan rate is fast enough, all ions coming from the ion source at the same time should reach the detector at approximately the same time.

An experiment will now be presented that will prove the validity of the NRSIC for detecting wall reactions. The HPEC mass spectrum of α-hexachlorocyclohexane is shown in Figure 3 at 95°C and 0.3 Torr. Figure 3 shows that this polychlorinated molecule does not display unusual ions of the type $[M-Z+nH-nCl]^-$. The NRSIC for this compound are shown in Figures 4 through 6 at various ion source conditions. From these figures it is apparent that all negative ions produced by hexachlorocyclohexane have very similar single ion chromatograms. This suggests that all ions exited the ion source at the same time.

Each type of unusual ion mentioned above will now be discussed in terms of the results to be presented and the theory presented in the Introduction.

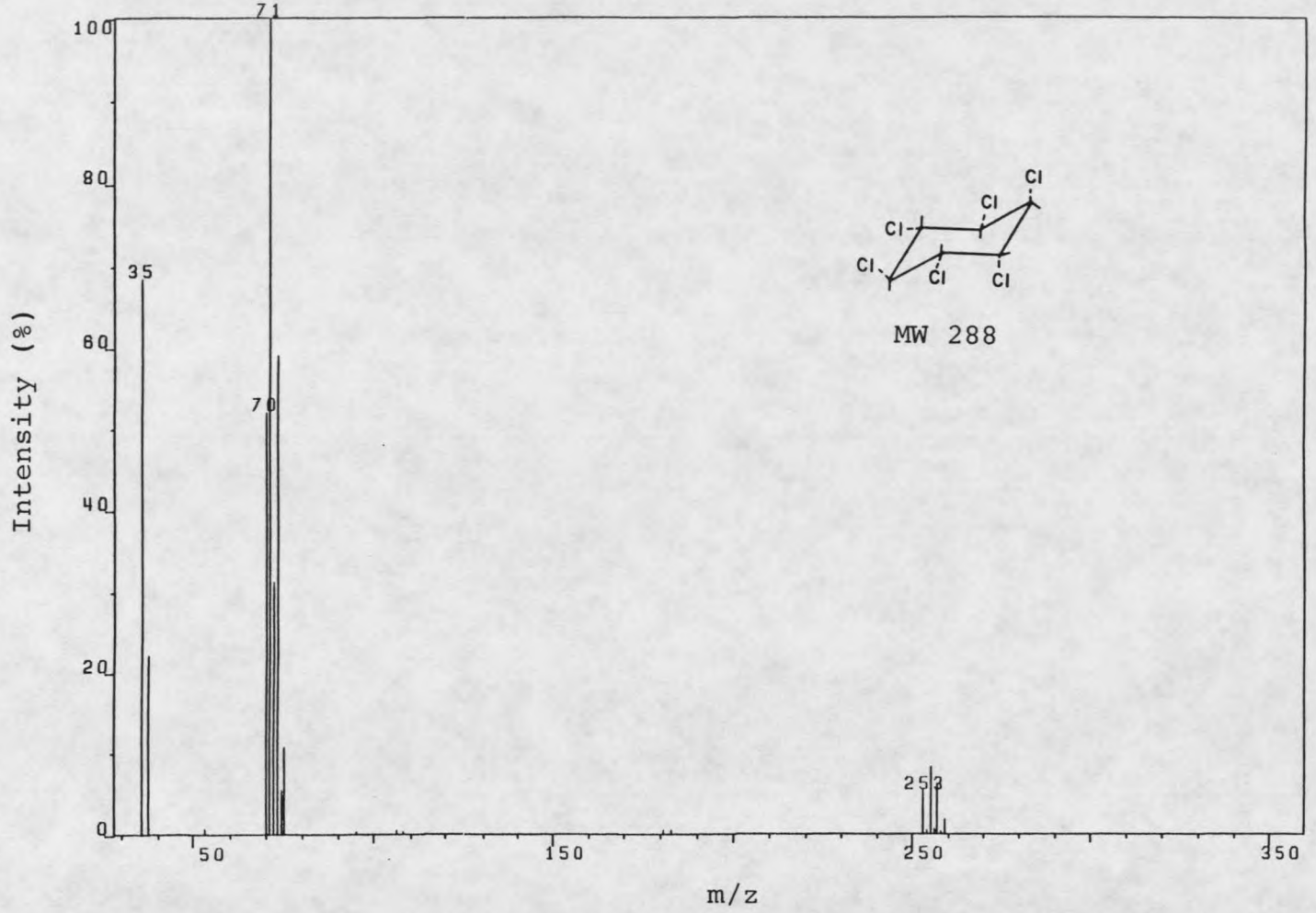


Figure 3. HPEC Mass Spectrum of α-Hexachlorocyclohexane at 95°C and 0.3 Torr.

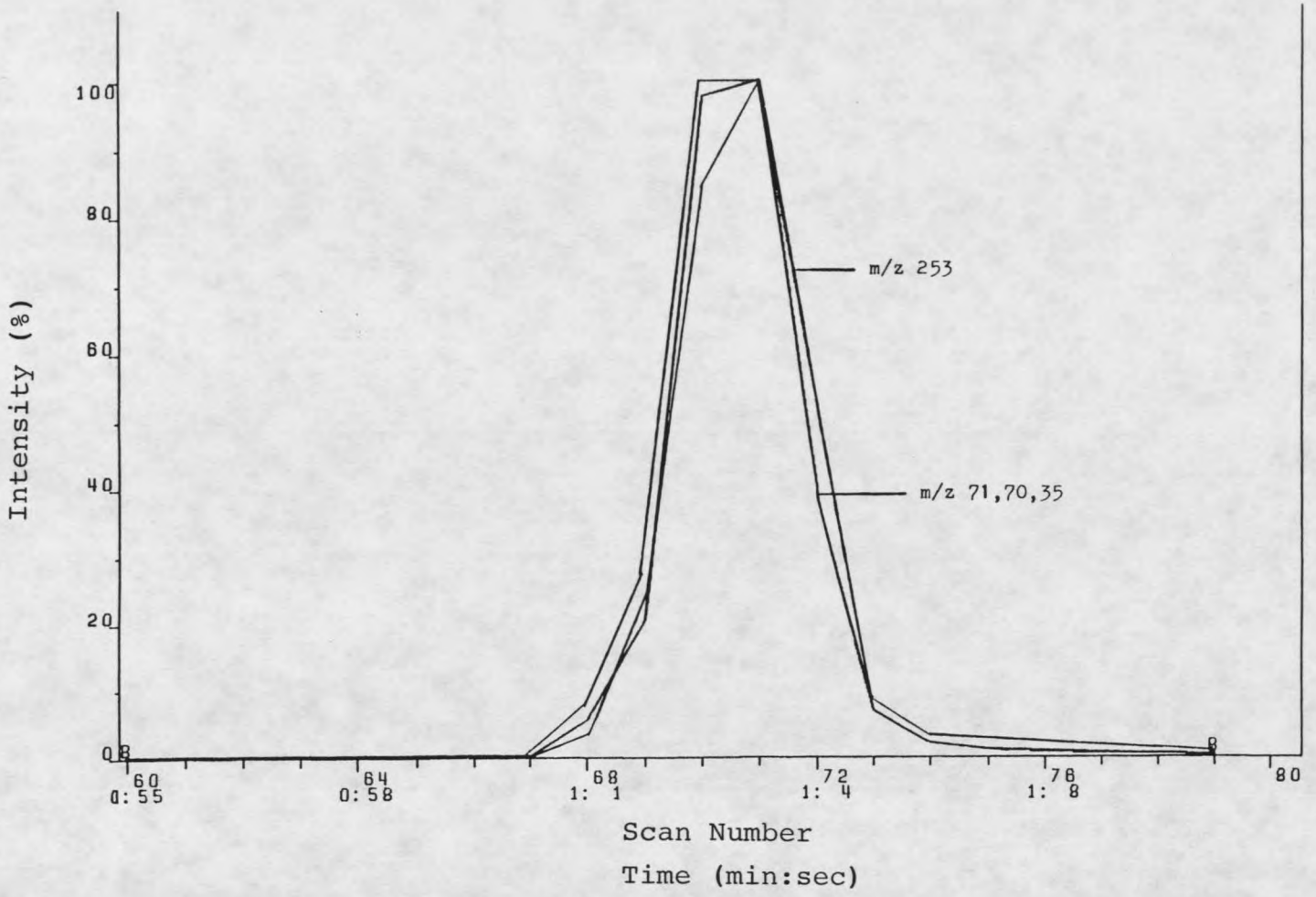


Figure 4. NRSIC for α-Hexachlorocyclohexane at 95°C and 0.3 Torr.

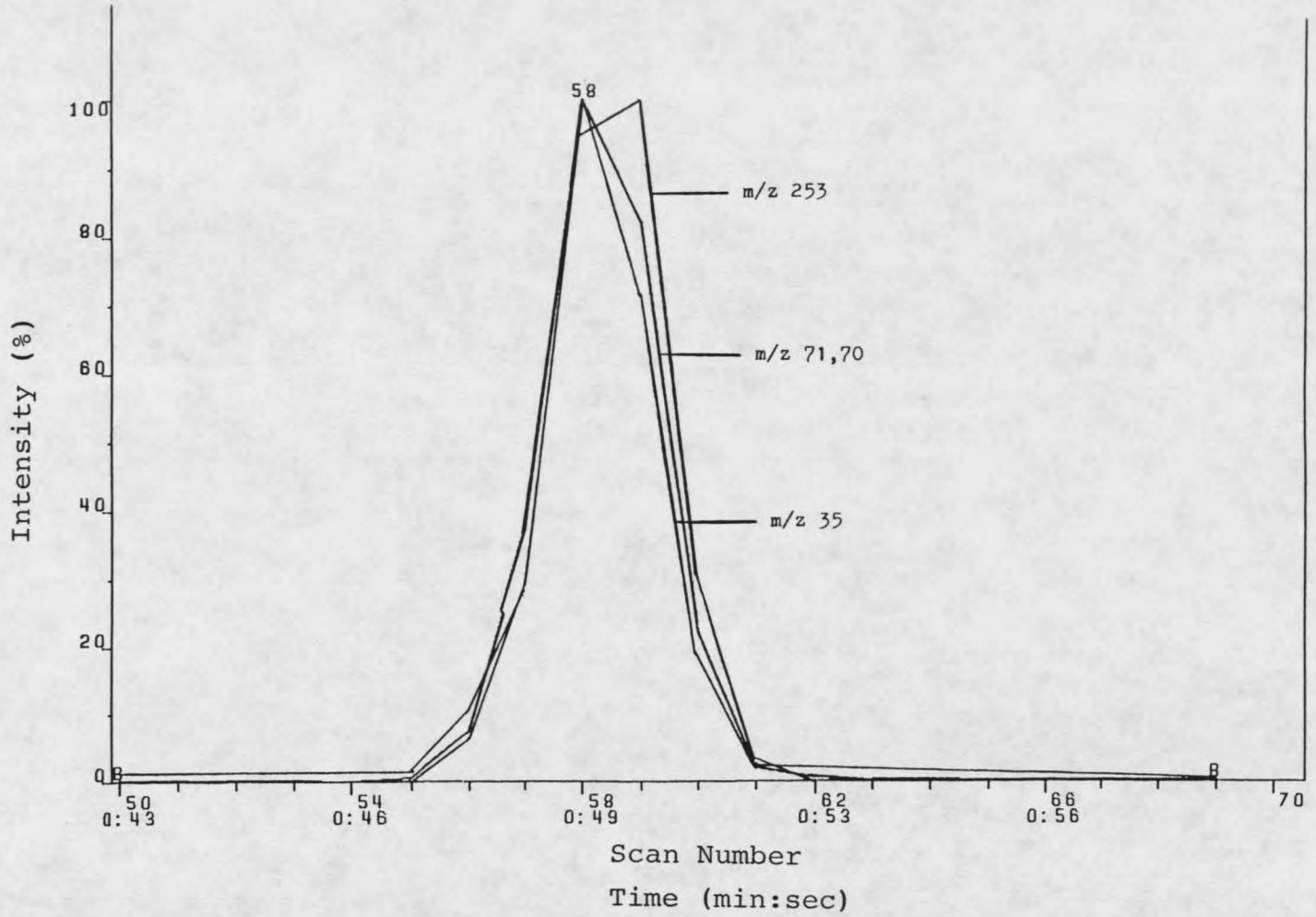


Figure 5. NRSIC for α-Hexachlorocyclohexane at 195°C and 0.3 Torr.

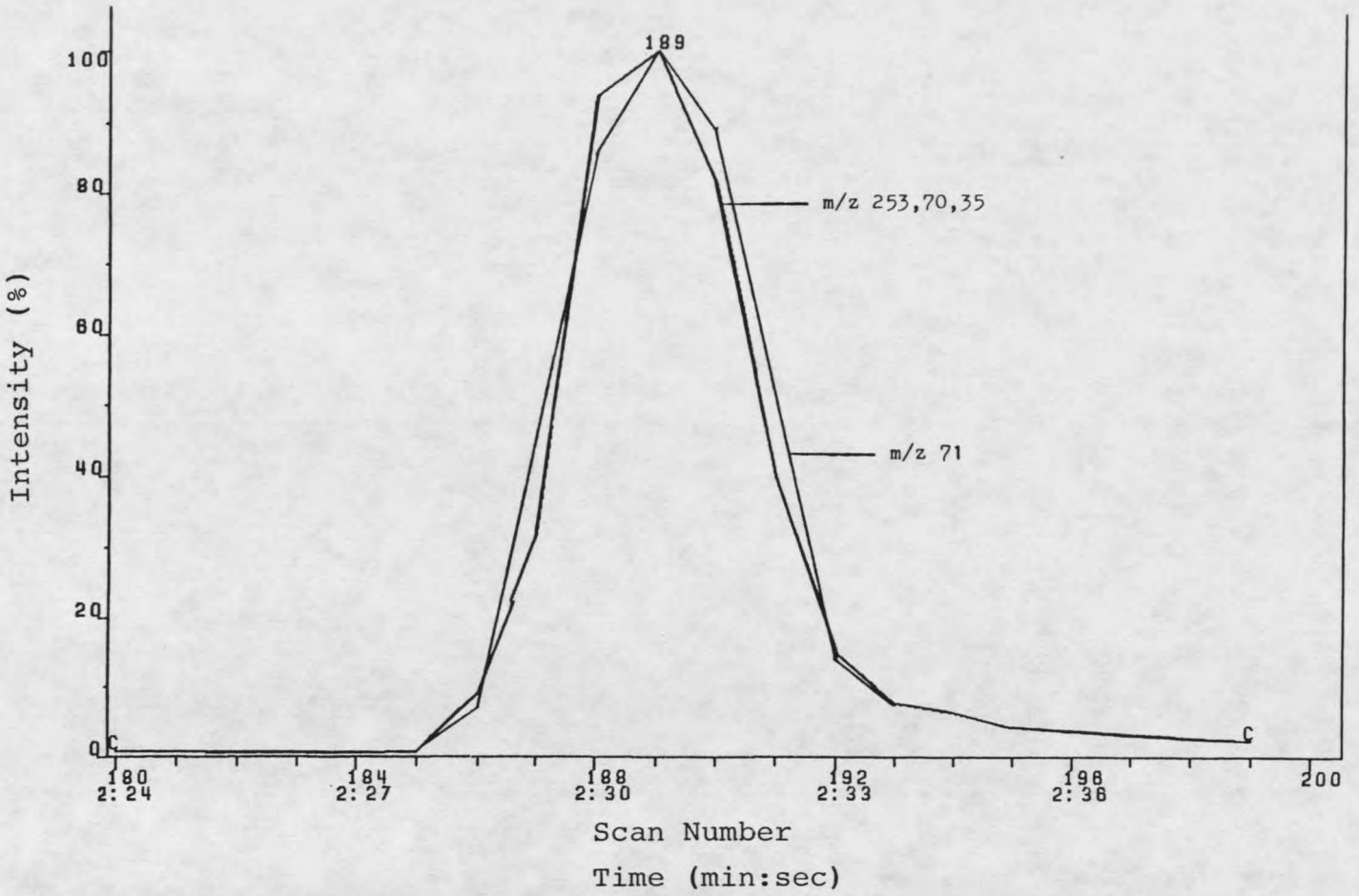


Figure 6. NRSIC for α-Hexachlorocyclohexane at 220°C and 0.3 Torr.

Unusual Ions of the Type $[M-Z+nH-nCl]^-$

The polychlorinated compounds investigated that produce unusual ions of the type $[M-Z+nH-nCl]^-$ are listed in Table 5. The first examples of unusual negative ions that will be considered are produced by α-hexachlorocyclopentadiene and its derivatives (Table 5, compounds 1-11).

Table 5. Polychlorinated Compounds Investigated That Show Ions of the Type $[M-Z+nH-nCl]^-$.

1.	Endrin aldehyde
2.	Heptachlor epoxide
3.	Dieldrin
4.	Heptachlor
5.	Endrin
6.	Endosulfan sulfate
7.	Mirex
8.	Pentac
9.	Aldrin
10.	Chlordane (technical mixture and metabolites)
11.	Hexachlorocyclopentadiene
12.	Hexachlorobenzene
13.	PCB 1260
14.	Pentachlorophenol
15.	Hexachlorobutadiene

Endrin Aldehyde

The HPEC mass spectrum of endrin aldehyde is shown in Figure 7 at 85°C and 0.3 Torr methane. The resonance electron capture product is represented by the isotopic chlorine cluster from m/z 378 to m/z 388 (where m/z is defined as the mass to charge ratio). For simplicity only the ion resulting from the ^{35}Cl isotope will be used in

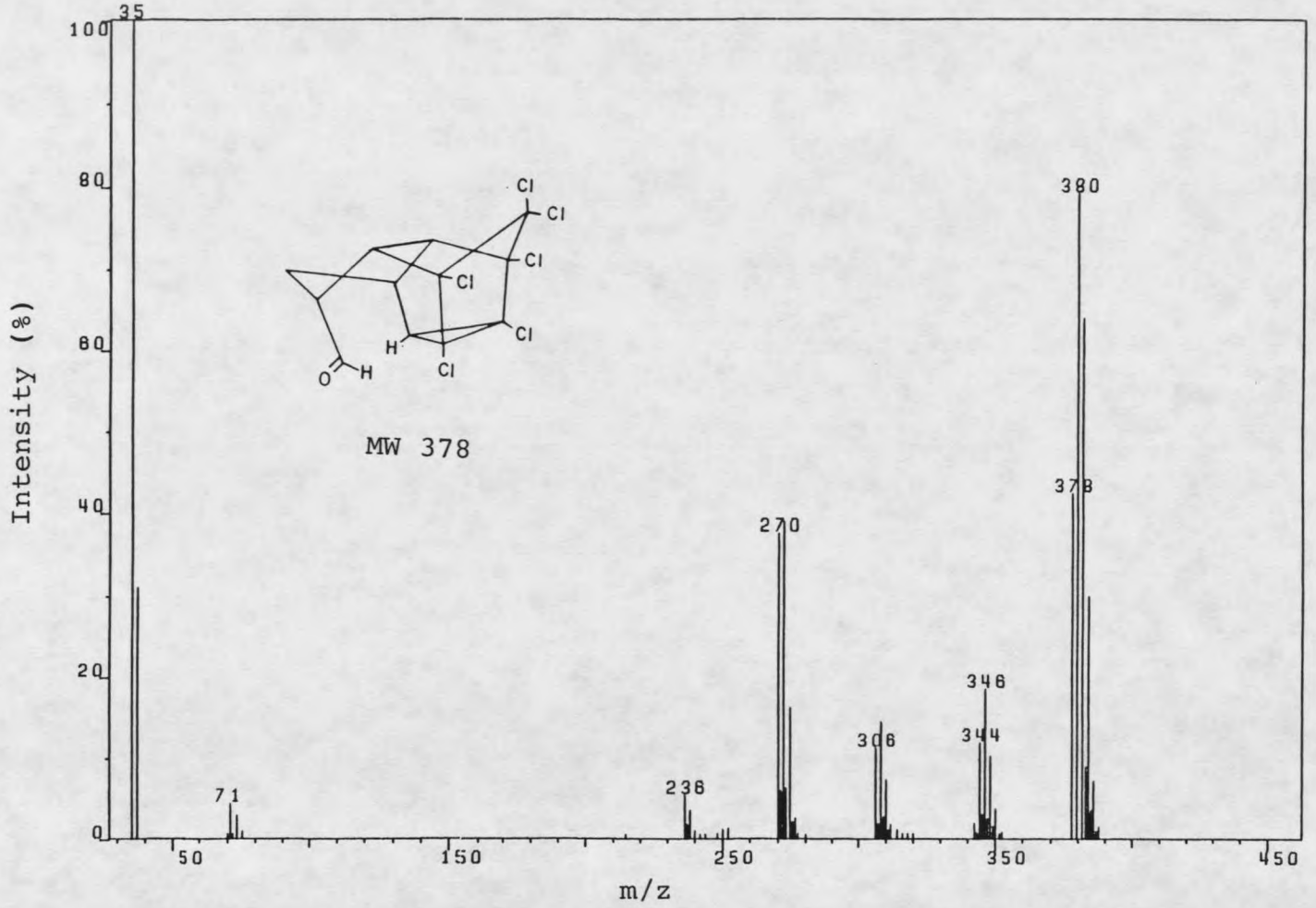


Figure 7. HPEC Mass Spectrum for Endrin Aldehyde at 85°C and 0.3 Torr.

describing the spectra presented in this study. Following the molecular anion at m/z 378, the ion of the next highest mass shown in Figure 7 appears at m/z 344. The ion at m/z 344 corresponds to the addition of a hydrogen and loss of a chlorine. This ion, represented as $[M+H-Cl]^-$, is unexpected when the buffer gas is supposedly used only for the purposes of producing low energy electrons and collisional stabilization to the newly formed excited negative ions. Following the ion at m/z 344 there appear ions at m/z 306 and m/z 270 which are probably the result of dissociative electron capture processes in which two and three HCl units were lost. The next significant ion observed in Figure 7, when viewing from high to low mass, comes at m/z 236. This ion, corresponding to $[M-Z+H-Cl]^-$ where Z is 3HCl units in this case, is another unusual ion observed in the HPEC mass spectrum of endrin aldehyde. The low mass end of the spectrum of this compound displays ions at m/z 71 and m/z 35. The species at m/z 35 corresponds to the Cl^- ion which is produced by dissociative electron capture and is often of high abundance in the HPEC mass spectra of chlorinated molecules. The species at m/z 71, corresponding to the HCl_2^- ion, is thought to arise from a secondary reaction involving the Cl^- ion and the analyte molecule.[2]

The effect of varying the temperature, pressure, and emission current of the ion source on the HPEC mass

Table 6. Tabulated HPEC Mass Spectra for Endrin Aldehyde.

Source Conditions			Negative Ions						
T°C	P(Torr)	Ec(mA)	378	344	306	270	236	71	35
85	0.3	0.2	42.2	11.8	11.2	37.5	5.4	4.4	100
100	0.1	0.5	17.6	4.2	23.8	51.5	3.7	4.7	100
100	0.2	0.2	41.6	7.0	23.4	54.3	5.2	5.3	100
100	0.3	0.2	25.5	7.7	9.7	28.8	4.1	3.8	100
100	0.5	0.2	32.6	9.4	12.7	34.5	6.2	2.5	100
175	0.2	0.5	10.0	15.4	28.6	63.7	30.3	4.2	100
175	0.3	0.2	5.1	5.2	13.0	31.8	9.4	3.4	100
175	0.45	0.2	5.7	7.5	12.6	34.7	15.3	2.9	100
175	0.45	0.5	4.0	6.4	10.2	28.3	14.7	3.0	100
220	0.3	0.2	-	1.5	9.3	27.7	9.6	3.8	100

spectra of endrin aldehyde is shown in Table 6. This table shows that as the temperature of the ion source is increased the abundance of the molecular anion decreases relative to the Cl^- ion. The observation that dissociative electron capture processes for chlorinated molecules increase relative to resonance electron capture as temperature increases inside the ion source was expected, as described in the Introduction.

How the change in pressure, while maintaining a constant temperature, affects the ratio of unusual ions versus the molecular anion in the HPEC mass spectra of endrin aldehyde is displayed in Table 7. It does not appear that there are any patterns for the formation of the unusual ions as compared to the molecular anion in the pressure range shown in Table 7.

Table 7. Effect of Pressure at a Constant Temperature of 100°C on the Formation of the Unusual Ions of Endrin Aldehyde.

Source Conditions	Unusual Ions versus M^-	
P(Torr)	344/378	236/378
0.1	0.24	0.21
0.2	0.17	0.13
0.3	0.30	0.16
0.5	0.29	0.19

When the emission current is varied, the positive ion, electron, and radical populations all respond as was shown in equations 5 and 11 in the Introduction. Table 8 shows the effect on the abundance of the unusual ions compared to the molecular anion when the emission current is changed from 200 μA to 500 μA. It appears from Table 8 that as the emission current is increased, the ratio of unusual ions compared to the molecular anion also increases.

Table 8. Effect of Emission Current at 100°C and 0.45 Torr on the Formation of the Unusual Ions of Endrin Aldehyde.

Source Conditions	Unusual Ions versus M^-	
Emission Current(μA)	344/378	236/378
200	1.3	2.7
500	1.6	3.7

Figure 8 displays the overlap of the significant ions found in the spectrum of endrin aldehyde at 85°C and 0.3 Torr methane using NRSIC. In Figure 8 the unusual ions at m/z 344 and m/z 236 persist for a longer period of time than some of the other ions. This figure also suggests that m/z 35 and m/z 71 also are formed from species which hang up on the ion source walls. The ions at m/z 378, m/z 306, and m/z 270 all follow the same reconstructed

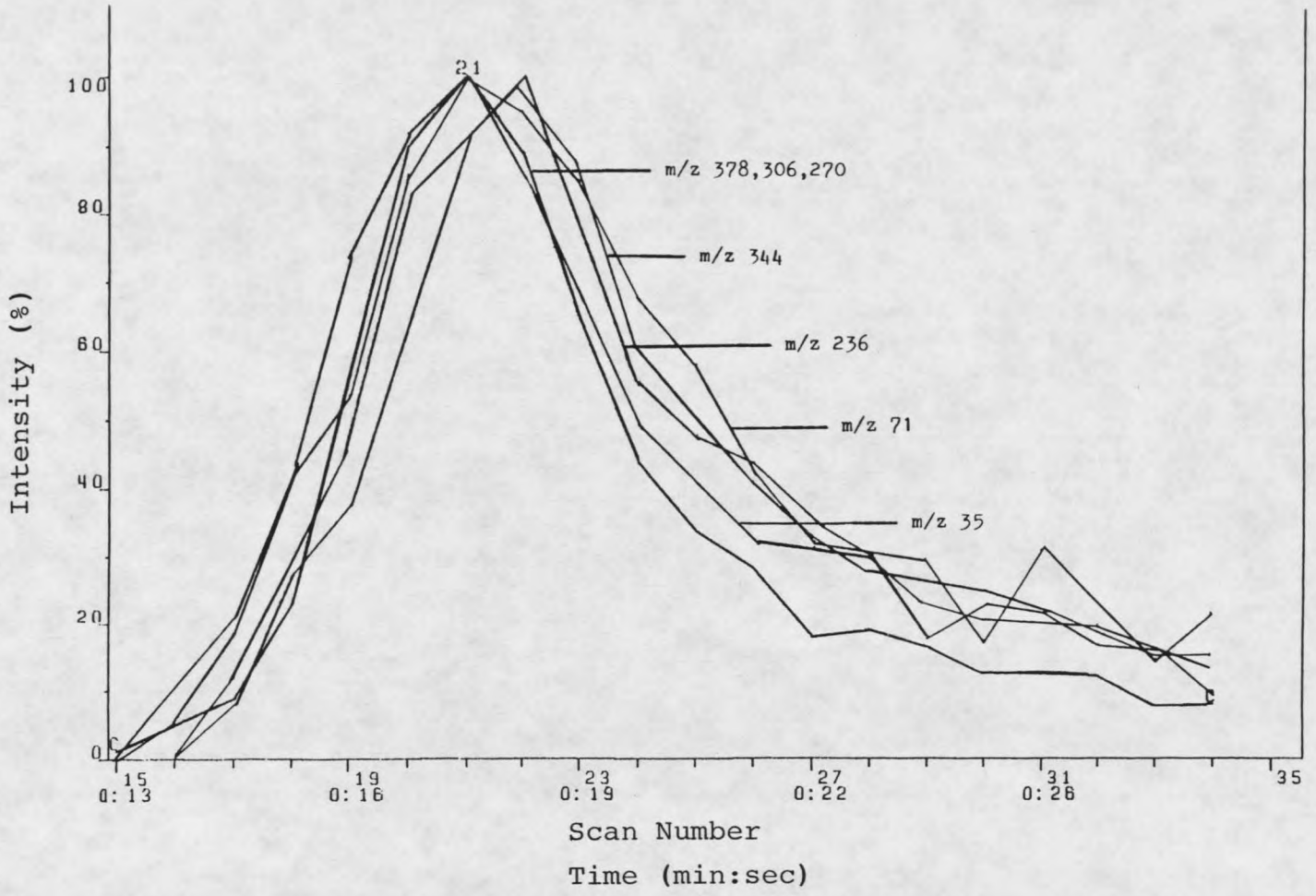


Figure 8. NRSIC for Endrin Aldehyde at 85°C and 0.3 Torr.

chromatogram suggesting that they were formed at the same time and probably by direct electron capture of the analyte.

Before offering an explanation on the possible ionization process of endrin aldehyde under HPECMS conditions, the NRSIC corresponding to some of the tabulated spectra (Table 6) for endrin aldehyde will be presented. Figures 8 through 14 are the NRSIC of this compound at selected conditions.

A trend in the appearance of the NRSIC for changes in both pressure and temperature are visible in Figures 8 through 14. At a constant temperature of 100°C and pressures ranging from 0.1 Torr to 0.5 Torr (Figures 9 through 12) the trend is for the NRSIC to go from wide tailing peaks to nearly gaussian shaped peaks. Although each of the ions seems to tail somewhat in all cases, the unusual ions tail significantly longer than the other ions.

The effect of changing the temperature on the NRSIC is shown in Figures 8, 11 and 14, where the temperatures are 85°C, 100°C and 175°C and a constant pressure of 0.3 Torr methane has been maintained. These figures show that variations in tailing are not nearly as extreme for temperature changes as they are for changes in pressure. There is a general trend for all ions to approach a more gaussian shaped profile as the temperature is increased.

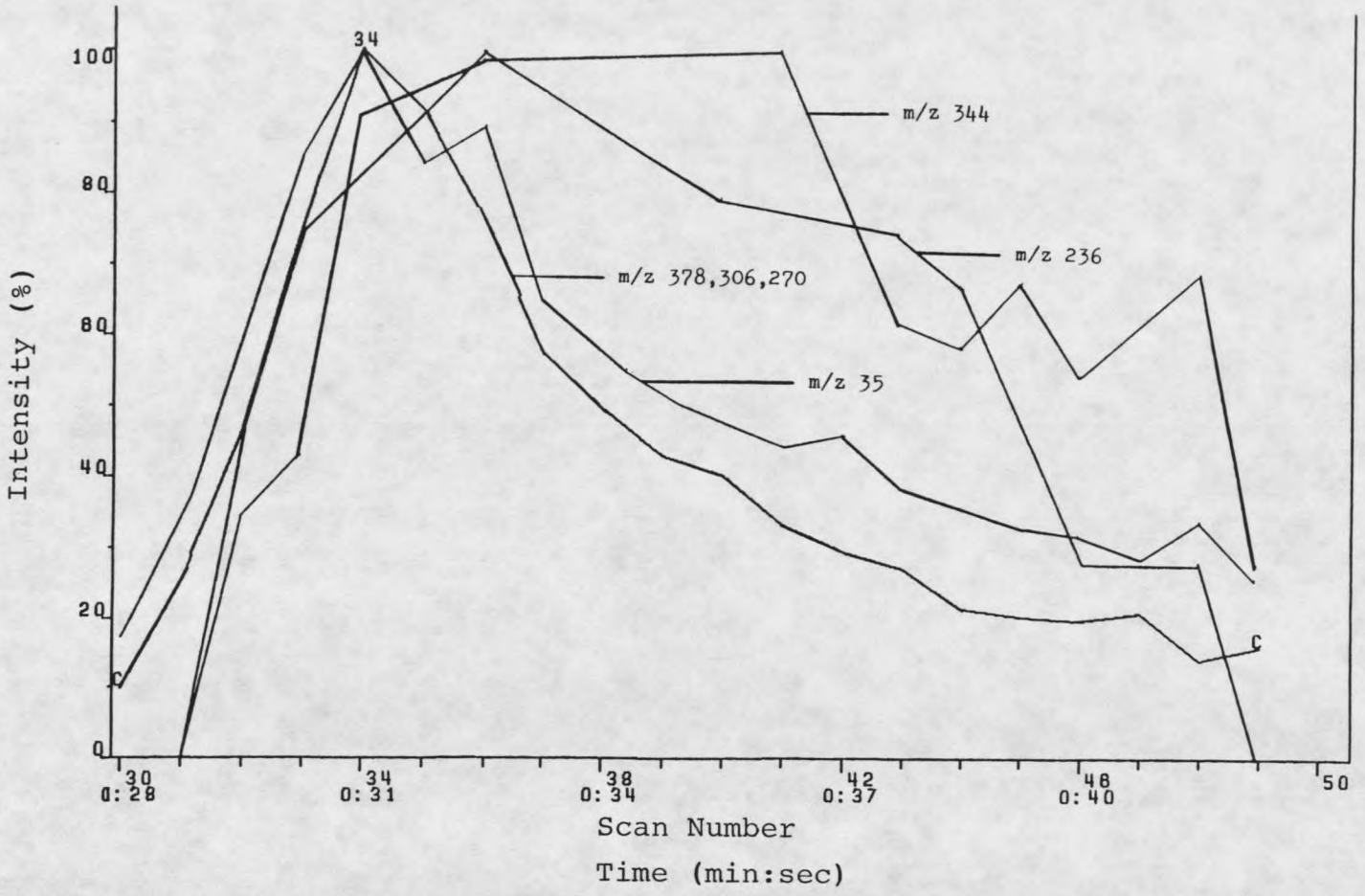


Figure 9. NRSIC for Endrin Aldehyde at 100°C and 0.1 Torr.

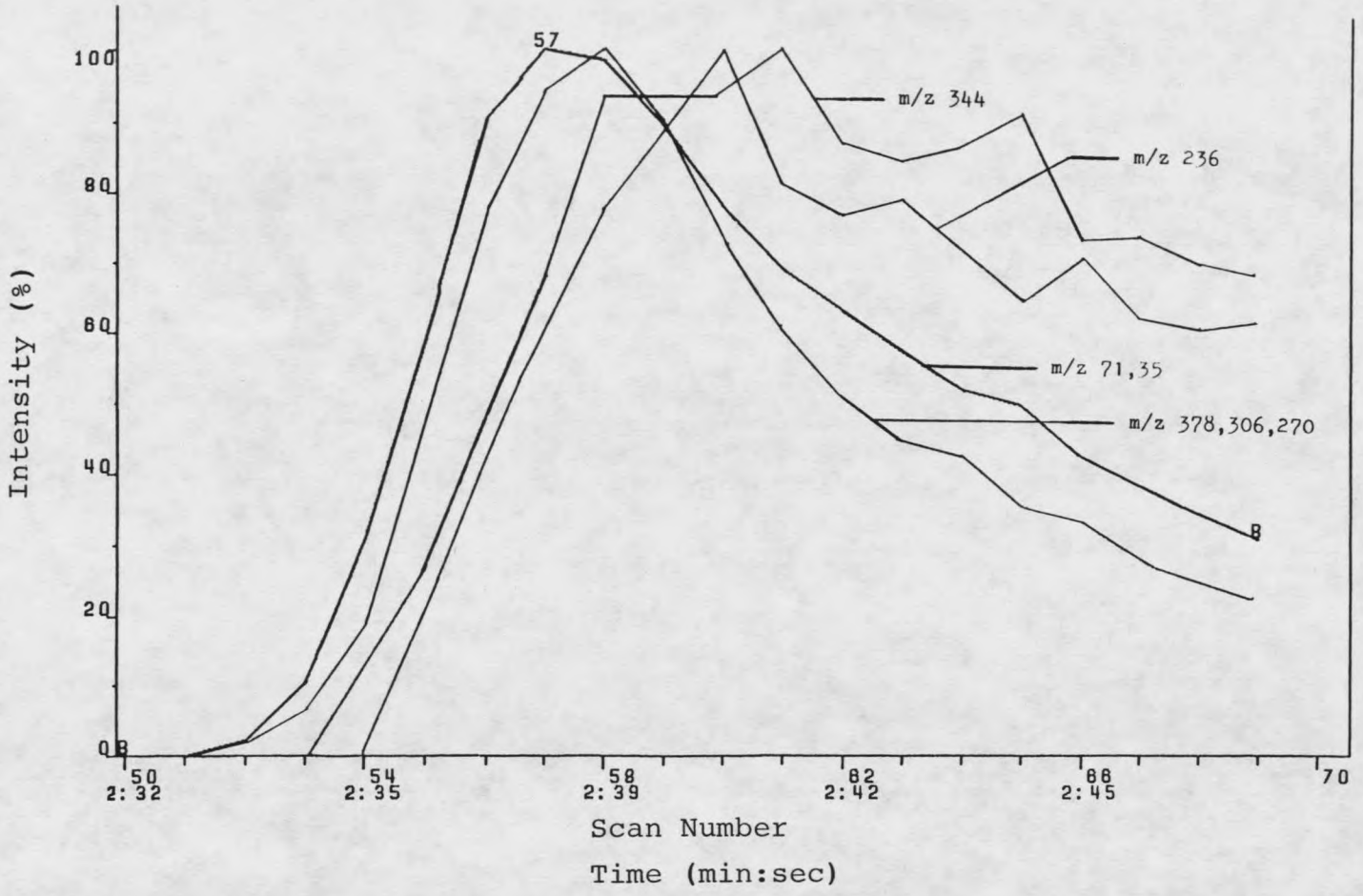


Figure 10. NRSIC for Endrin Aldehyde at 100°C and 0.2 Torr.

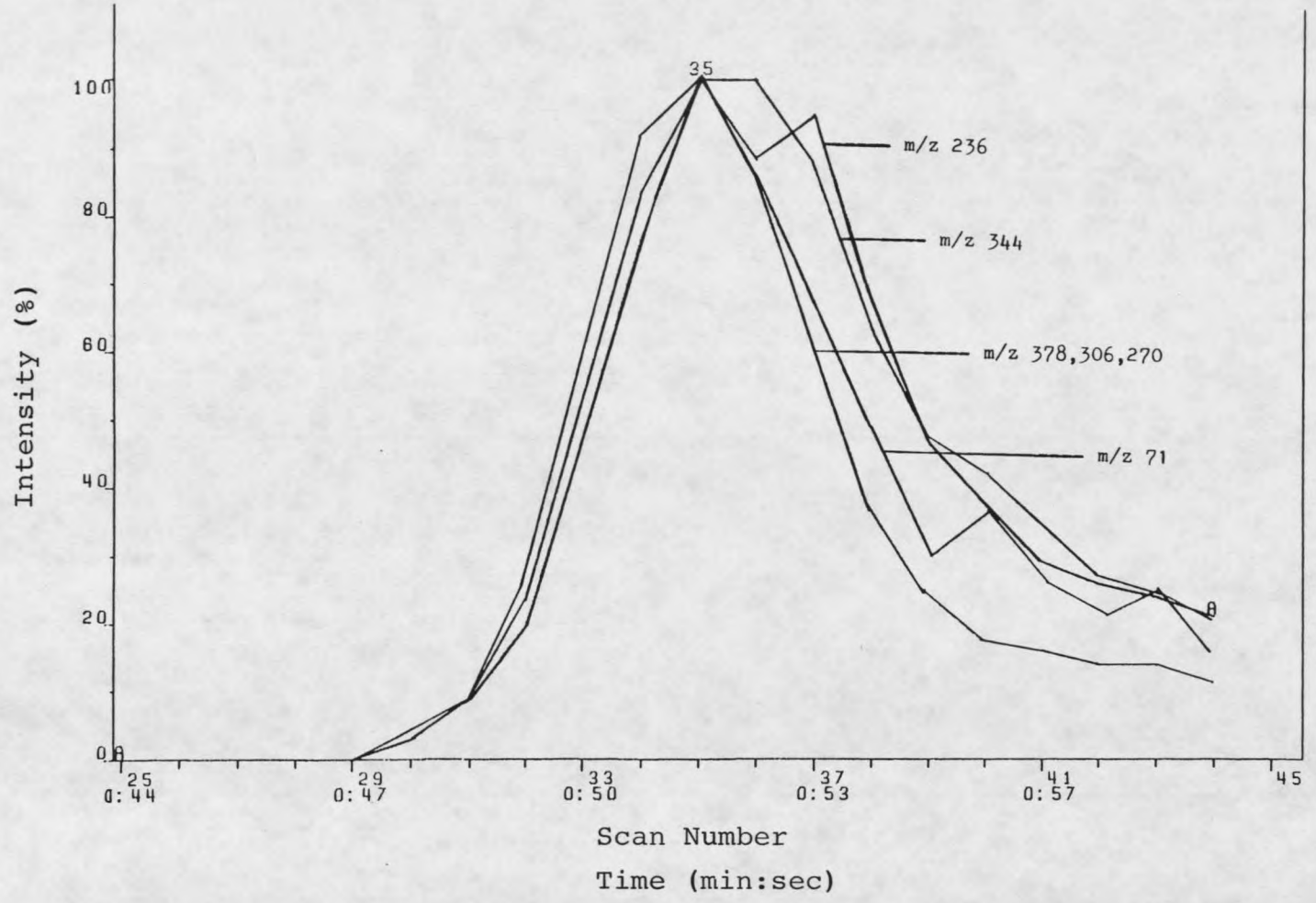


Figure 11. NRSIC for Endrin Aldehyde at 100°C and 0.3 Torr.

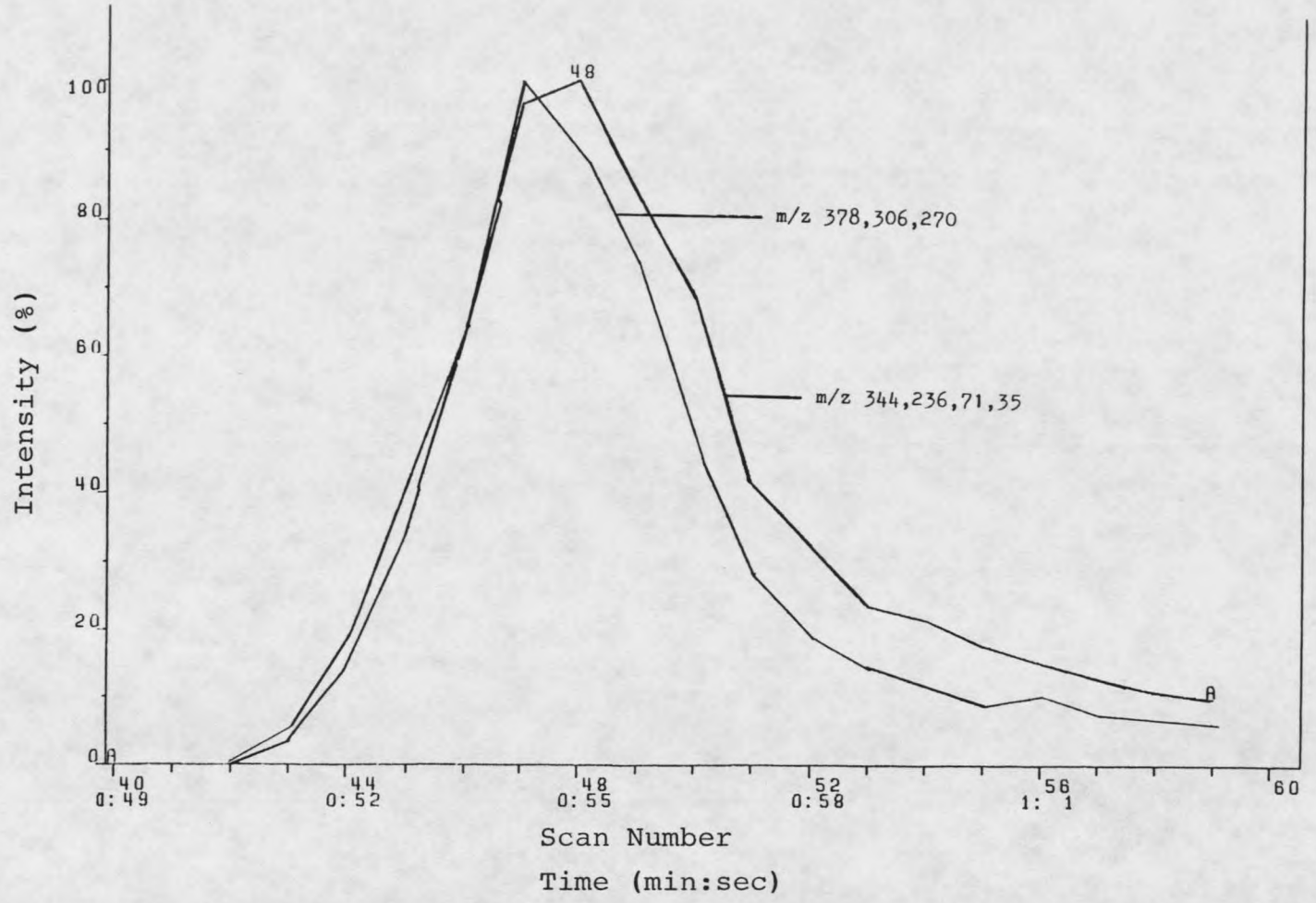


Figure 12. NRSIC for Endrin Aldehyde at 100°C and 0.5 Torr.

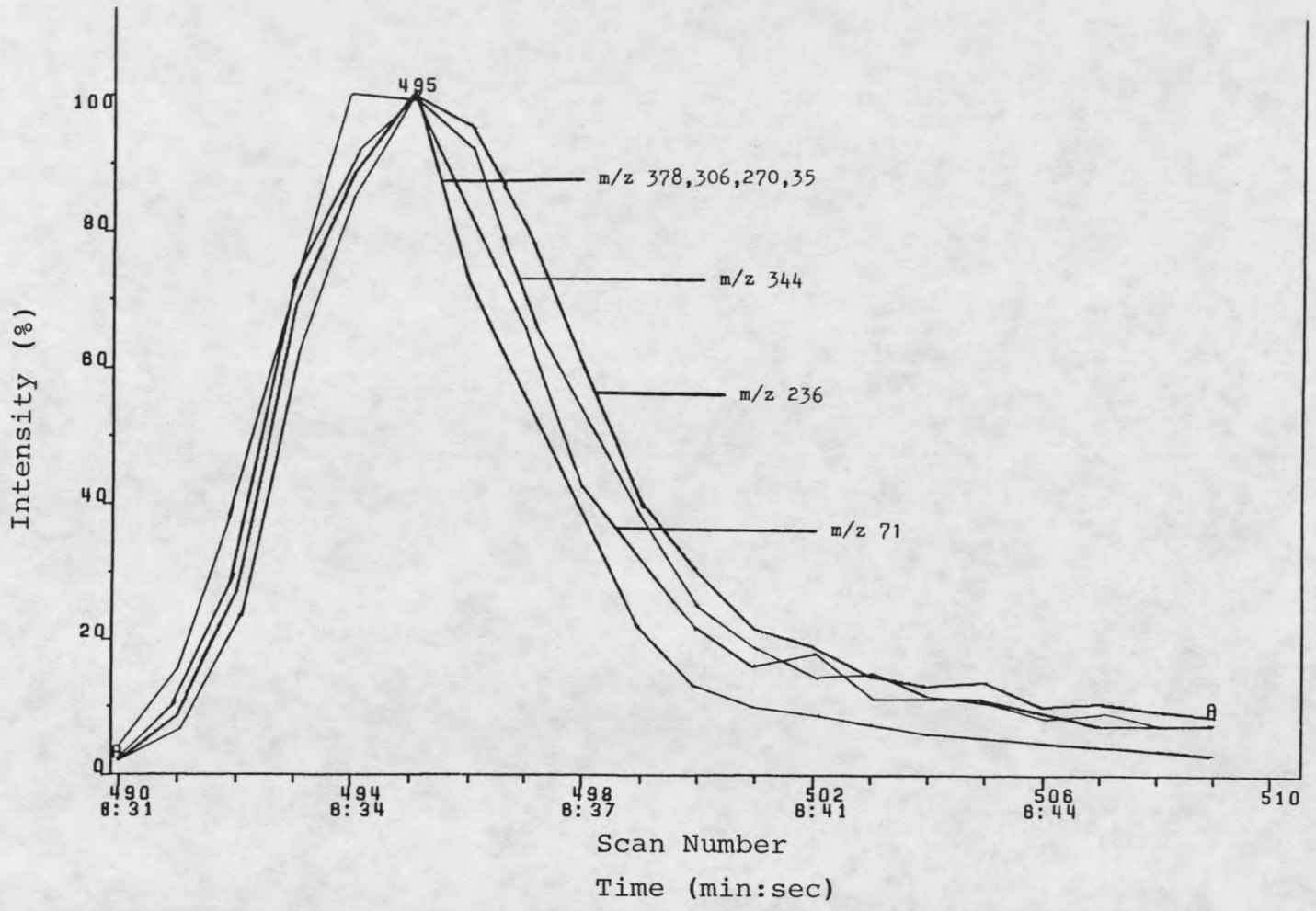


Figure 13. NRSIC for Endrin Aldehyde at 175°C and 0.2 Torr.

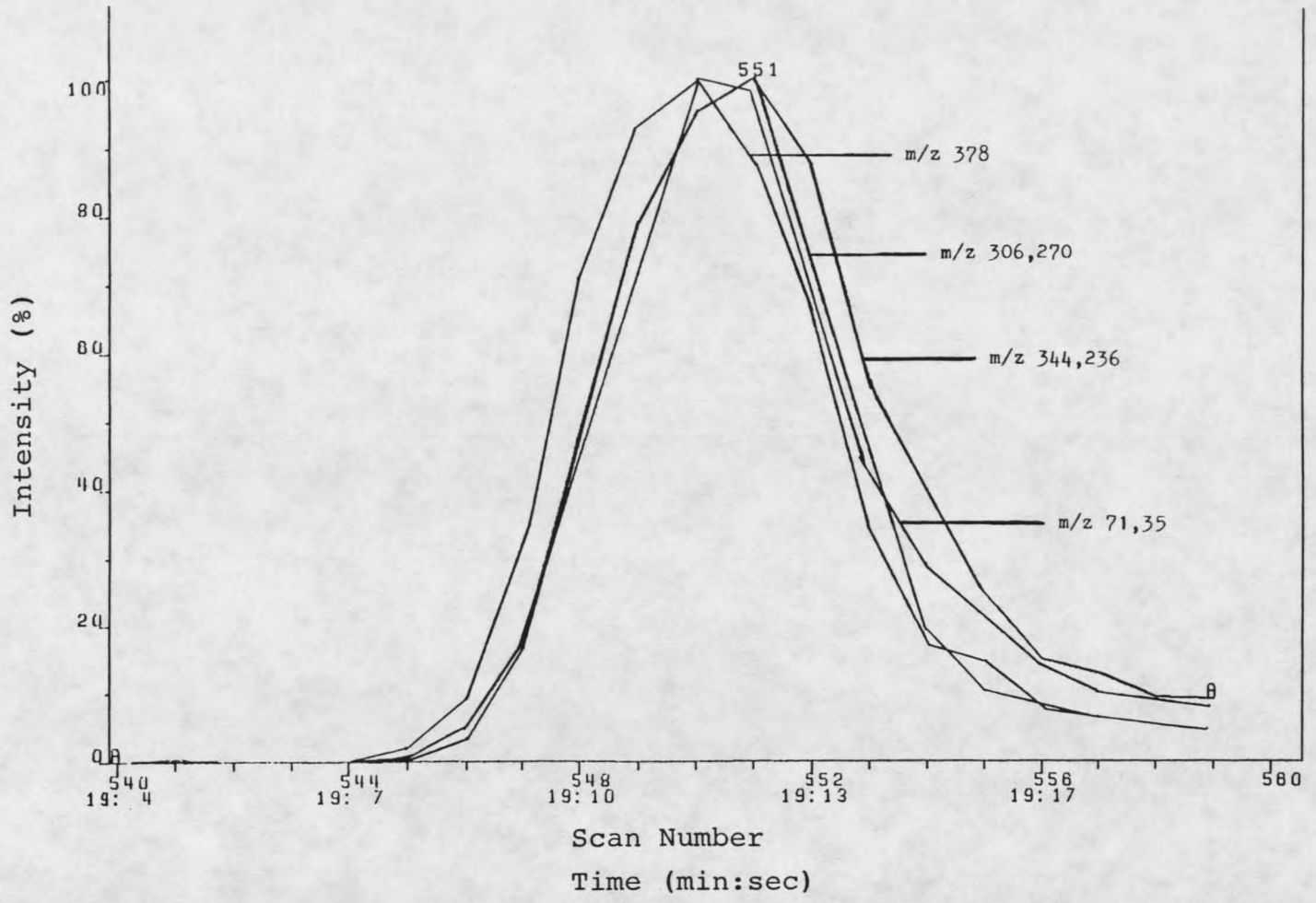


Figure 14. NRSIC for Endrin Aldehyde at 175°C and 0.3 Torr.

The literature and theory discussed in the Introduction suggested that an analyte species (charged or neutral) could become adsorbed onto the surface inside the ion source and react with methane derived species also adsorbed onto the surface. The temperature and pressure effects on the NRSIC can also be described in terms of this adsorbing of the analyte species to the ion source walls. As the temperature of the source increases, the desorption rate of chemical species increases also.[21] This increase in the desorption rate would explain why the tailing effect observed in the NRSIC decreases with increasing temperature.

A more difficult problem arises when trying to explain the dramatic changes in the NRSIC with decreasing pressure. In theory the rate of diffusion increases with decreasing pressure. With an ion source temperature of 100°C the life-time against diffusion to the wall for neutral species increases from 22 μsec at 0.1 Torr to 111 μsec at 0.5 Torr.

Another possible explanation for the drastic tailing of ions at low pressures displayed by the NRSIC is that at lower pressures there are fewer total species present in the methane plasma. Because of the lower concentration of species at lower source pressures there is a lower probability of an analyte species, once adsorbed onto the source surface, being knocked off the surface by a

colliding species. The combination of an increased diffusion rate and a decreased concentration of methane present in the ion source at low pressures is probably the best explanation for the observation of ions tailing more at low pressure than at high pressure in the NRSIC.

While the tailing associated with all ions at various source temperatures and pressures has been addressed, the reason why the unusual ions tail more has not. Theory shows that diffusion for charged and neutral species are roughly the same (0.02 msec and 0.05 msec at 100°C) when compared to the other chemical events possible inside the ion source. An analyte species could possibly diffuse to the source wall about 15 times in the amount of time it takes for a fast electron capture reaction to take place. Therefore, all analyte species should come into contact with the source walls before being vented from the source. The analyte species could adsorb onto the source wall in a variable way where the time it takes to desorb is almost always longer for species which are undergoing reactions that form the unusual ions as compared to simple adsorption-desorption. The reconstructed chromatograms observed would then show the unusual ions tailing as this study indicates. Now the question arises as to why the ions at m/z 35 and m/z 71 seem to tail after the molecular anion has passed. One possible explanation is that an analyte species could have its structure altered by the

adsorption-desorption process in such a way that the ionization process forming the m/z 35 and m/z 71 ions is then more probable.

Before giving a pictorial representation of the ion forming processes associated with endrin aldehyde, a need exists for knowing what type of reaction takes place at the ion source surface. Evidence given in the Introduction showed that fluorinil, a compound whose spectra also show ions of the type $[M-Z+nH-nX]^-$ (where X in this case is a fluorine atom), displays an electron impact (EI) mass spectrum in which there is an ion corresponding to $[M+2H]^+$ (the molecular species plus two hydrogens) when the ion source had been previously operated under HPECMS conditions. The $[M+2H]^+$ ion was shown not to exist in the clean ion source, suggesting it arose from methane derived species on the ion source walls.

The same type of experiment was applied to several of the chlorinated compounds shown in this study to produce ions of the type $[M-Z+nH-nCl]^-$, but due to the low abundance or absence of molecular ions, the presence of $[M+2H]^+$ ions in the EI spectra could not be confirmed.

In the remainder of this study it will be assumed, because of the work by others described above, that the unusual ions of the type $[M-Z+nH-nCl]^-$ arose in part from a wall reaction in which an [M+2H] species was produced.

Figure 15 is the suggested mechanism by which the negative ions shown in the NRSIC of Figure 10 are produced. This mechanism shows a reaction where the gas phase parent analyte molecule, M(g), can adsorb onto an ion source wall producing the wall adsorbed parent analyte molecule, M(w). Once adsorbed onto the source wall the M(w) species is shown to have three possible routes to ionization. First, M(w) can desorb, and then capture an electron, producing the resonance and dissociative electron capture products at m/z 378, m/z 306, and m/z 270. Another option for M(w) is to be structurally altered in some way to produce the unknown neutral species, W. The W species is shown in Figure 15 to desorb from the ion source wall and produce Cl^- and HCl_2^- ions upon electron capture. If the alteration of M(w) into W takes a longer period of time than simple adsorption-desorption, then the persistence of m/z 35 and m/z 71 in Figure 10 is explained. Finally, the fate of M(w) could be the conversion into [M+2H] by a reaction in which the parent analyte molecule has gained two hydrogens. The [M+2H] species is shown in Figure 15 to desorb from the source wall and undergo a dissociative electron capture reaction resulting in the unusual ion at m/z 344. The ion at m/z 236 is shown in Figure 15 as arising from the ion at m/z 270. The ion at m/z 270 could have come into contact with the source wall, picked up two hydrogens and

then captured an electron followed by a dissociative loss of an HCl unit. Although not shown in Figure 15, negative ions in addition to m/z 270 could also become adsorbed on the ion source walls.

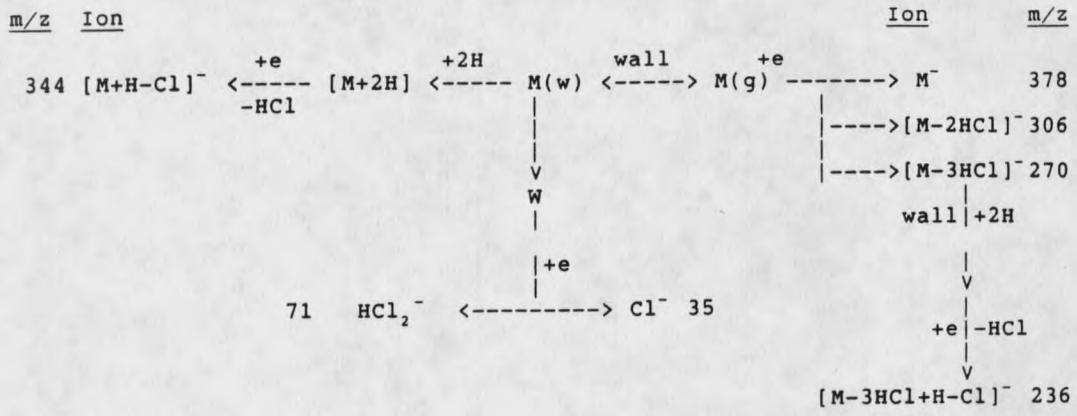


Figure 15. Suggested Mechanism for the Formation of Negative Ions from Endrin Aldehyde.

This detailed discussion for endrin aldehyde will be used to help explain the remainder of the compounds that display surface reactions which were investigated in this study.

Heptachlor Epoxide

The next compound that will be presented which displays unusual ions of type $[M-Z+nH-nCl]^-$ in its HPEC mass spectra is heptachlor epoxide. Figure 16 is the HPEC mass spectrum of heptachlor epoxide at 80°C and 0.3 Torr methane. The ion at m/z 235 shows up quite often in the

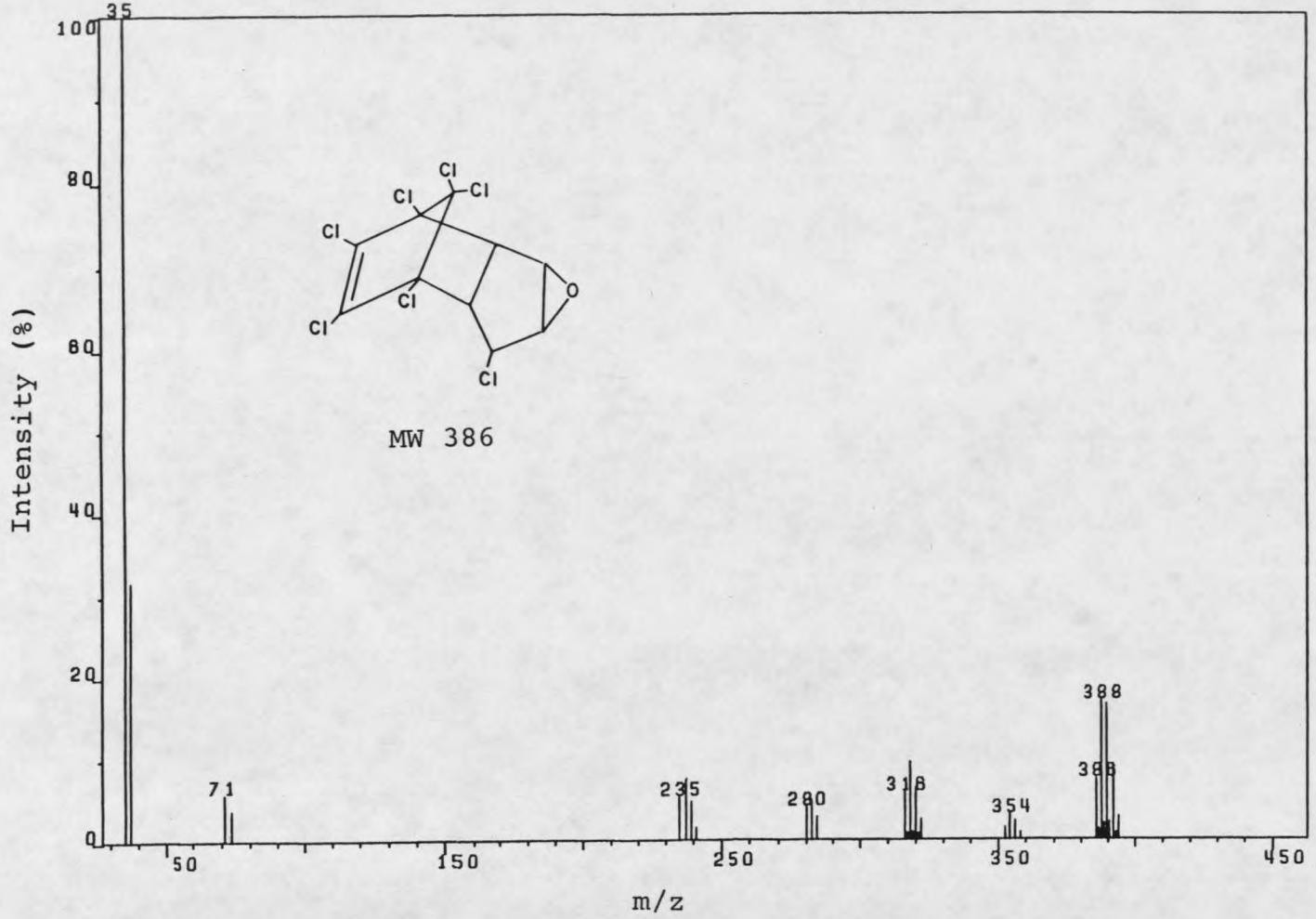


Figure 16. HPEC Mass Spectrum of Heptachlor Epoxide at 80°C and 0.3 Torr.

HPEC mass spectra of hexachlorocyclopentadiene derivatives. It is thought[19] that this ion arises from a gas phase retro-diels alder reaction which produces the aromatic pentachlorocyclopentadiene anion, $PCCPD^-$. The tabulated spectra for this compound at various ion source temperatures, pressures, and emission currents are displayed in the Appendix. The NRSIC of heptachlor epoxide at two different source conditions are shown in Figures 17 and 18.

From Figure 17 it appears that the negative ion at m/z 352 arose from the [M+2H] species thought to be produced at the surface of the ion source. Again, as was the case for endrin aldehyde, the ion at m/z 71 is present in the HPEC mass spectra of heptachlor epoxide and seems to tail somewhat after the molecular anion. The Cl^- ion appears to persist in the ion source for a longer period of time than the molecular anion in Figure 17. But in Figure 18 the Cl^- ion is shown to have the same chromatogram as the molecular anion.

An interesting feature in Figures 17 and 18 is that m/z 316 and m/z 280 appear to have almost identical reconstructed chromatograms. This suggests that the species which formed these ions desorbed from the ion source wall at the same time, while m/z 352, or $[M+H-Cl]^-$, has a reconstructed chromatogram that follows a totally different pathway. Figure 19 is the suggested mechanism

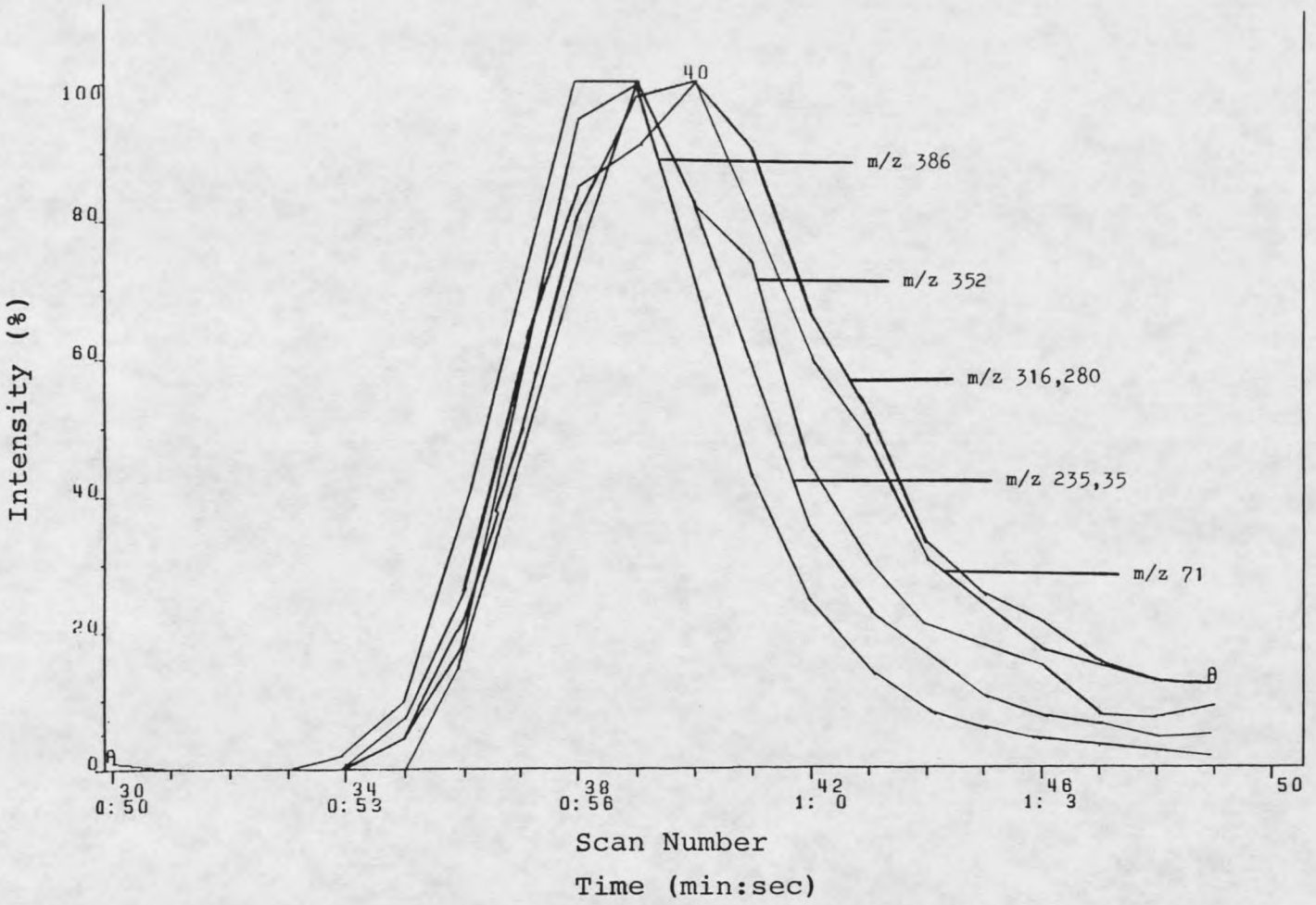


Figure 17. NRSIC for Heptachlor Epoxide at 80°C and 0.3 Torr.

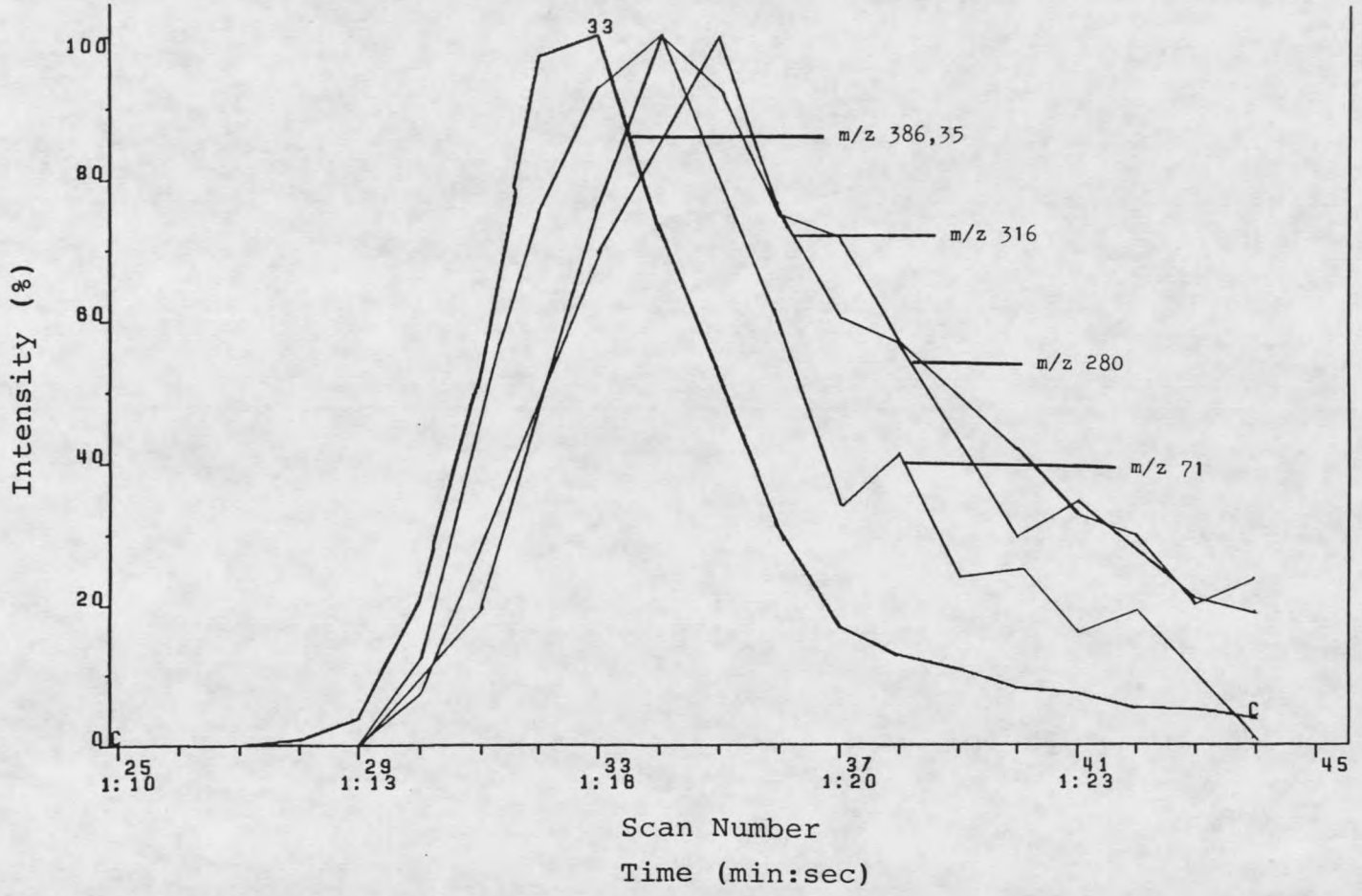


Figure 18. NRSIC for Heptachlor Epoxide at 100°C and 0.1 Torr.

for the production of negative ions observed in the HPEC mass spectra of heptachlor epoxide. This figure was constructed from observations made from Figures 17 and 18. Because m/z 35 is shown to have the same chromatogram as m/z 386 in Figure 18, it will be assumed that the Cl^- ion was produced by a direct dissociative electron capture of the parent analyte molecule.

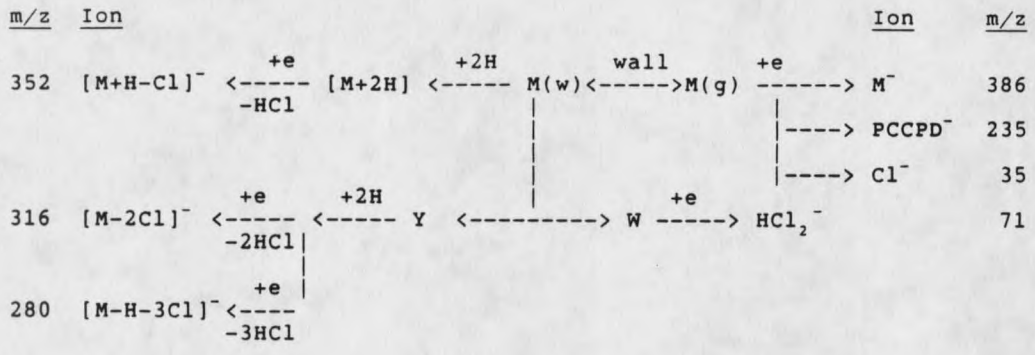


Figure 19. Suggested Mechanism for the Formation of Negative Ions from Heptachlor Epoxide.

Dieldrin

Dieldrin is the next hexachlorocyclopentadiene derivative that will be investigated. Figure 20 is the HPEC mass spectrum of this compound at 85°C and 0.3 Torr. The tabulated spectra for this compound at various ion source conditions are shown in the Appendix. Figure 20 shows the molecular anion at m/z 378 with an unusual ion following at m/z 344 corresponding to $[M+H-Cl]^-$.

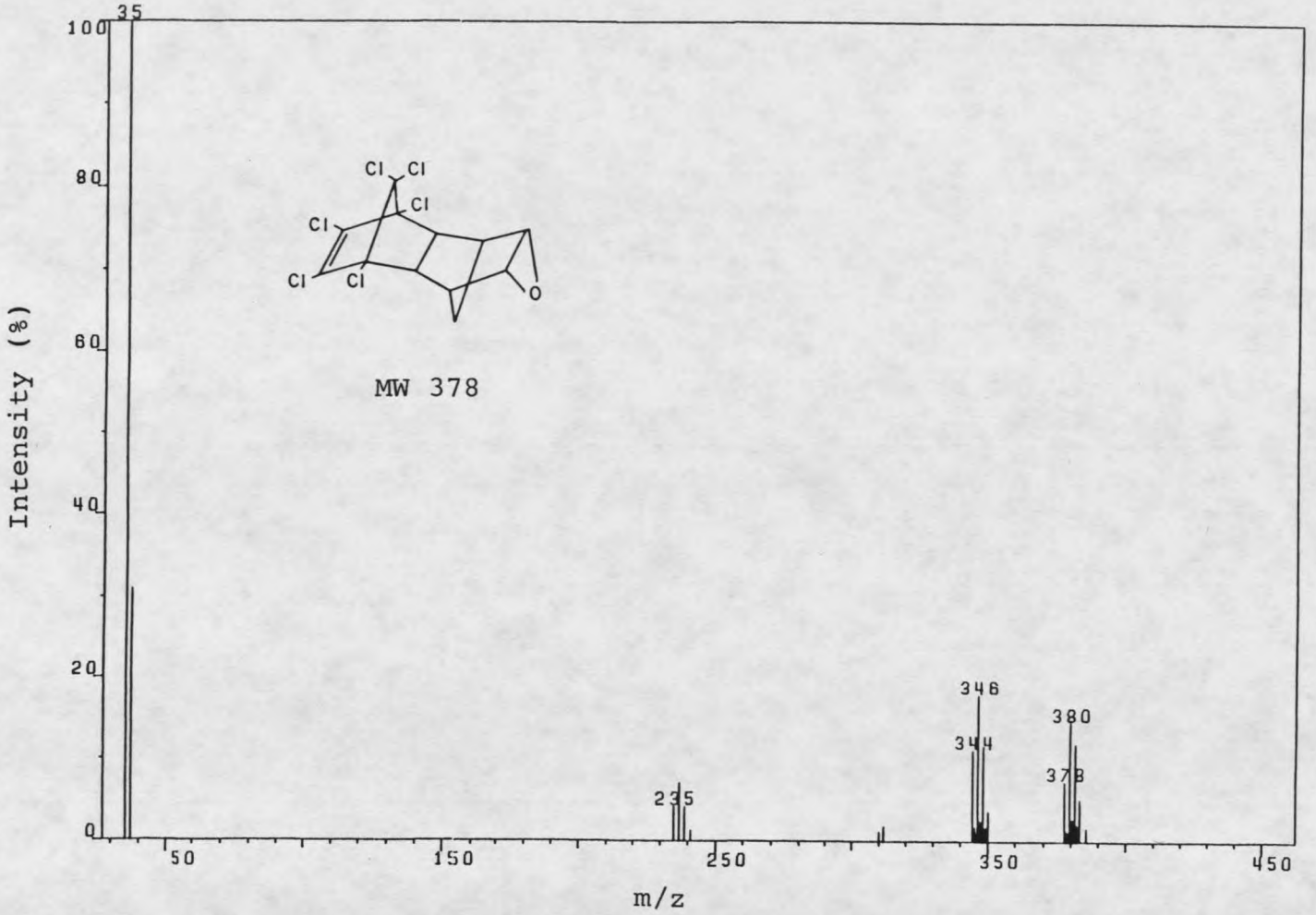


Figure 20. HPEC Mass Spectrum of Dieldrin at 85°C and 0.3 Torr.

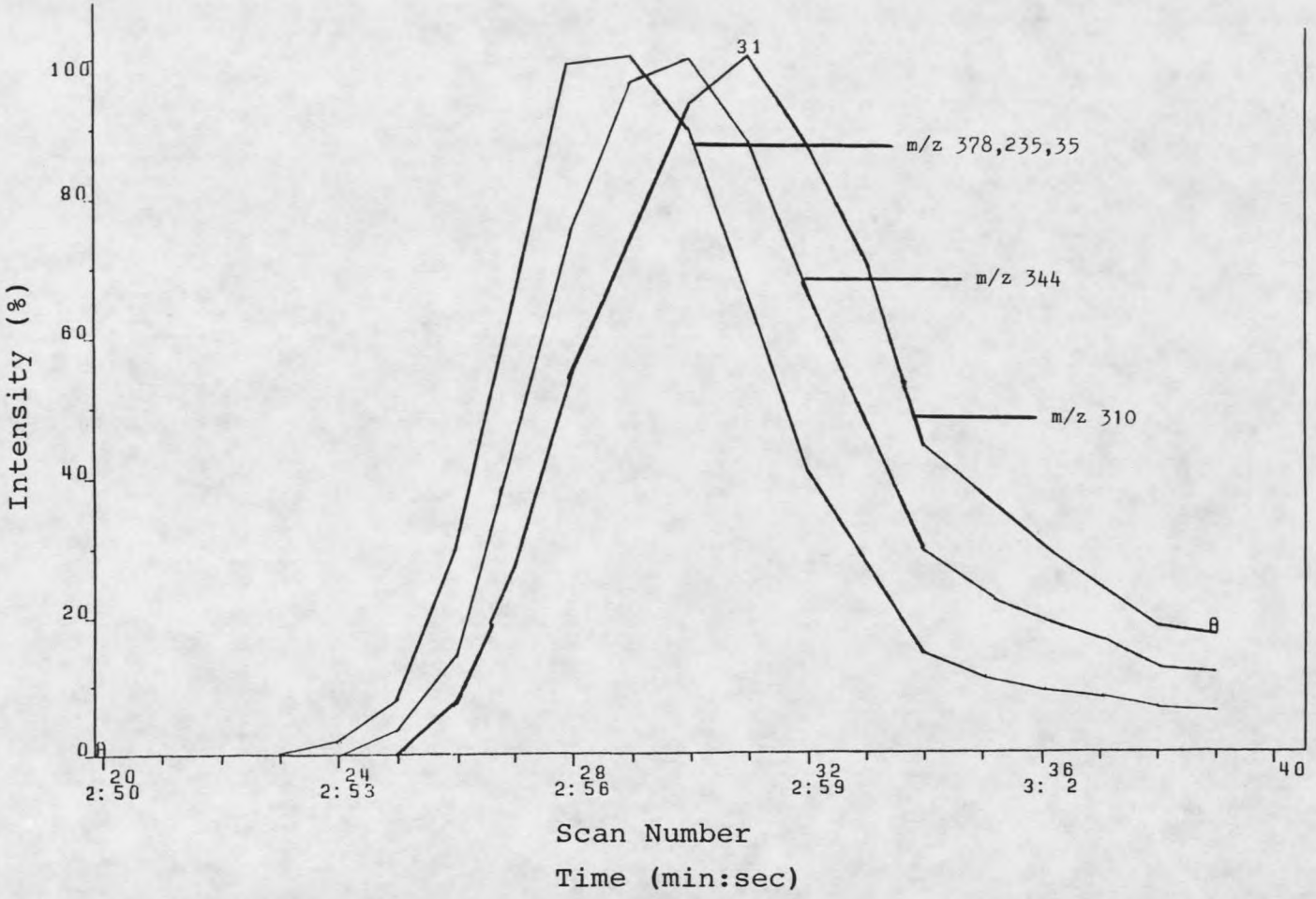


Figure 21. NRSIC for Dieldrin at 85°C and 0.3 Torr.

Following the ion at m/z 344, the next ion of highest mass appears at m/z 310 and is represented as $[M+2H-2Cl]^-$. The remaining two ions are probably the result of dissociative electron capture and appear at m/z 235 and m/z 35 in Figure 20. The NRSIC for this compound are shown in Figure 21 at 85°C and 0.3 Torr methane. Figure 21 shows that the molecular anion, $PCCPD^-$ and Cl^- ions all follow the same reconstructed chromatogram. In contrast, m/z 344 tails after these three ions, and m/z 310 tails after m/z 344. If the ion at m/z 344 were to react with the wall a second time, the ion at m/z 310 should, therefore, reach the detector later. The suggested ionization route for dieldrin is presented in Figure 22.

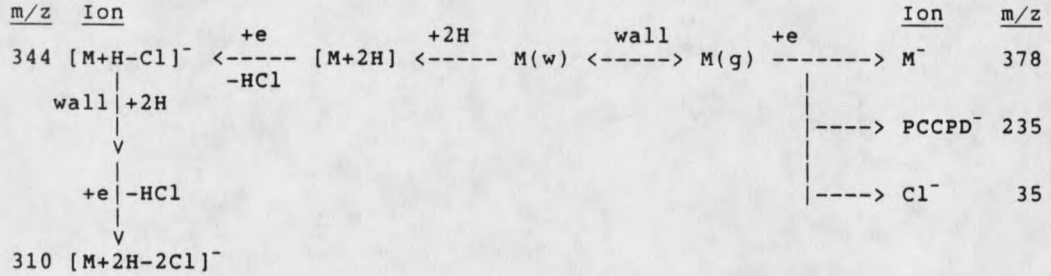


Figure 22. Suggested Mechanism for the Formation of Negative Ions from Dieldrin.

Heptachlor

Figure 23 is the HPEC mass spectrum of heptachlor at 80°C and 0.3 Torr methane. This figure shows that the dissociative pathway producing the Cl^- ion dominates even

at the low source temperature shown. The molecular anion is barely visible at m/z 370. Following the molecular anion is what is thought to be a dissociative electron capture product in which two HCl units were lost; it appears at m/z 298. The ions at m/z 264 and m/z 230 are multiple losses of 34 mass units from the ion at m/z 298, and both represent unusual ions of the type $[M-Z+nH-nCl]^-$. In addition to the ions already mentioned, ions corresponding to $PCCPD^-$, HCl_2^-, and Cl^- also are present in the HPEC mass spectra of this compound. The tabulated spectra at various source conditions are presented in the Appendix.

The NRSIC for this compound at two sets of different source conditions are shown in Figures 24 and 25. Figure 24 shows that an ion corresponding to m/z 196 appears in the spectra of this compound under the conditions listed. This is another unusual ion of the same type being discussed and is 34 mass units less than the species at m/z 230. Figure 24 also suggests that the unusual ions were formed by a multi-step process in which a single species reacted with the source surface several times.

Figure 25, at 175°C and 0.45 Torr, shows how increasing the pressure causes all reconstructed chromatograms to approach the same profile as would be expected for fast adsorption-desorption or gas phase reactions.

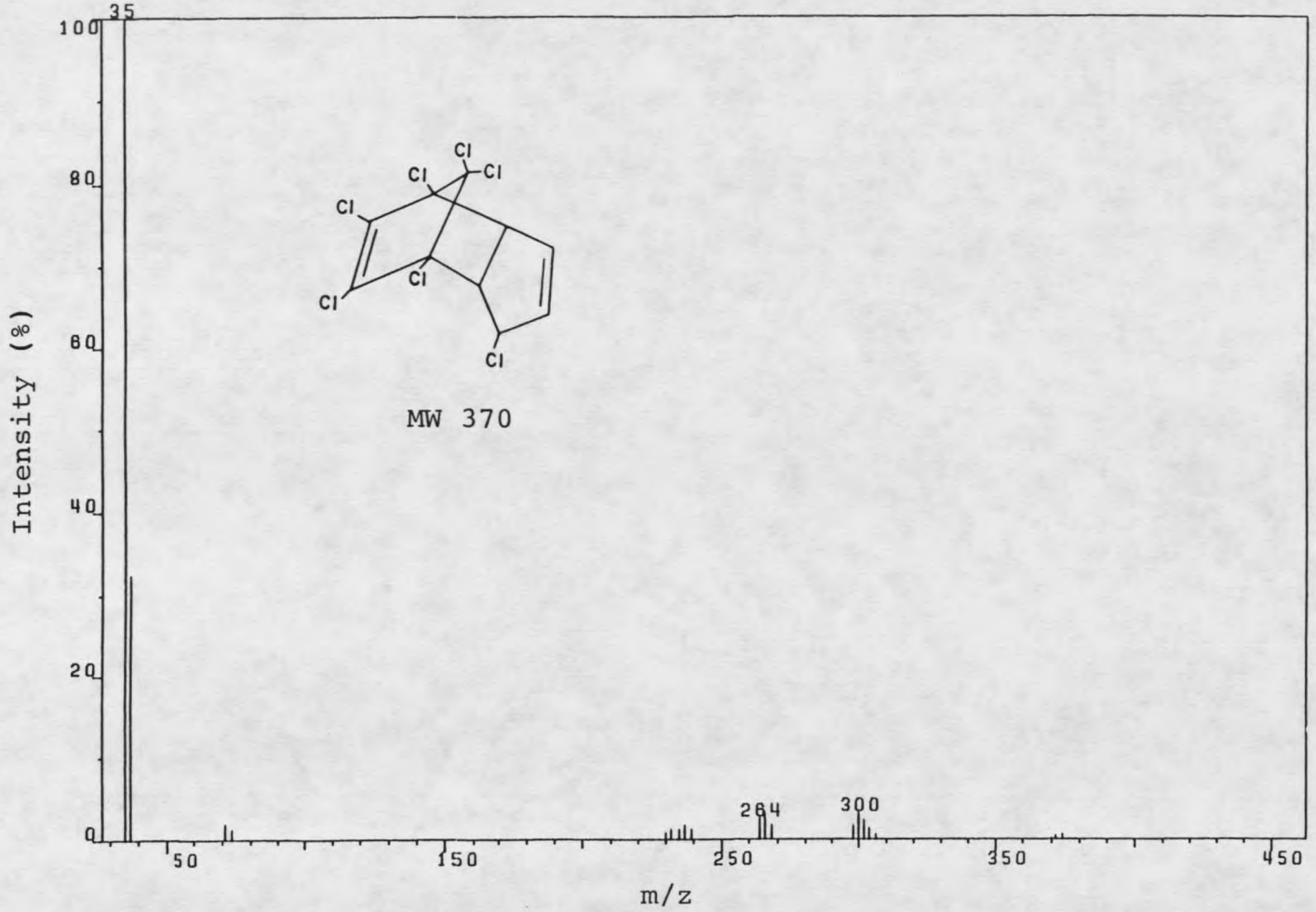


Figure 23. HPEC Mass Spectrum of Heptachlor at 80°C and 0.3 Torr.

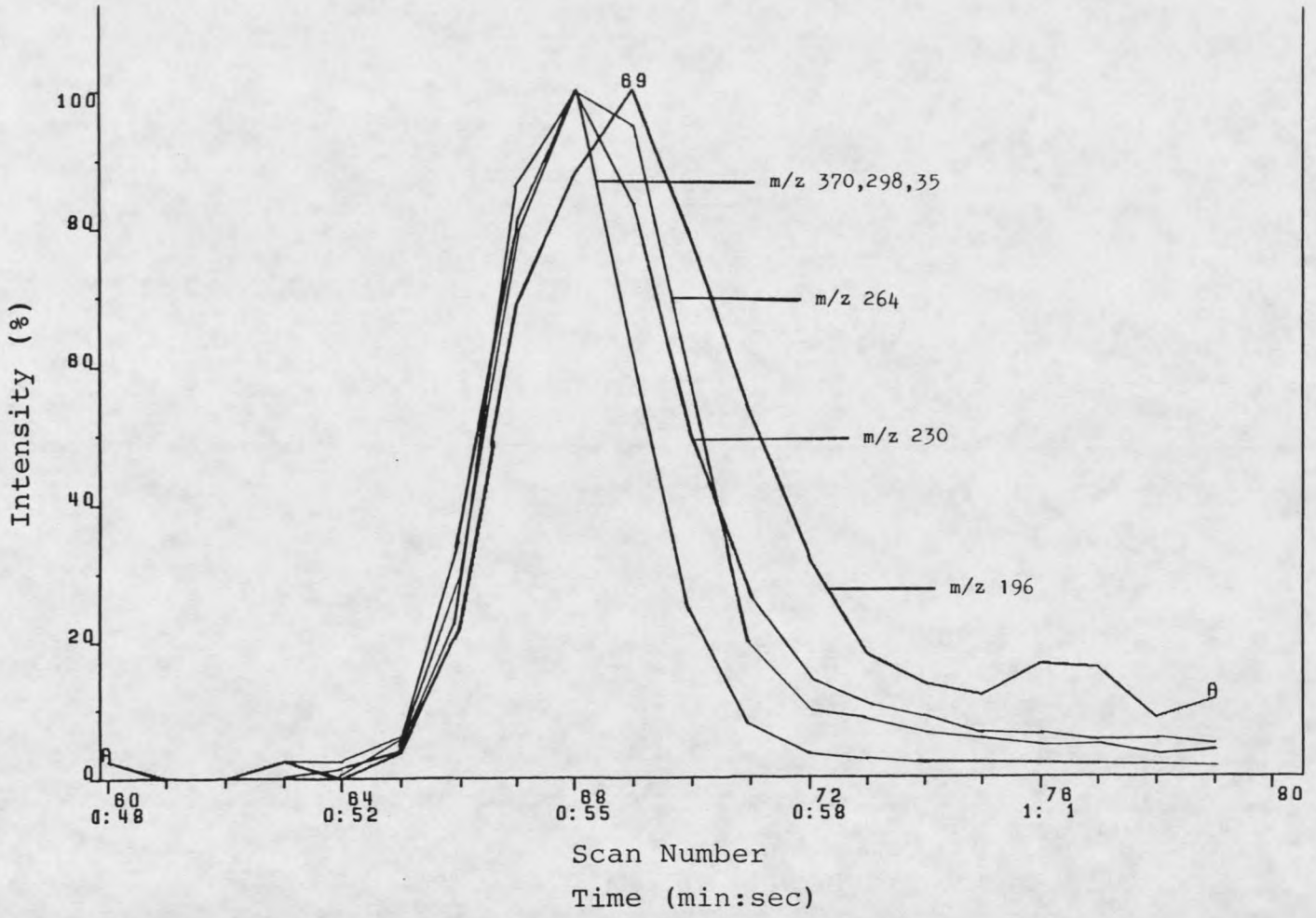


Figure 24. NRSIC for Heptachlor at 175°C and 0.3 Torr.

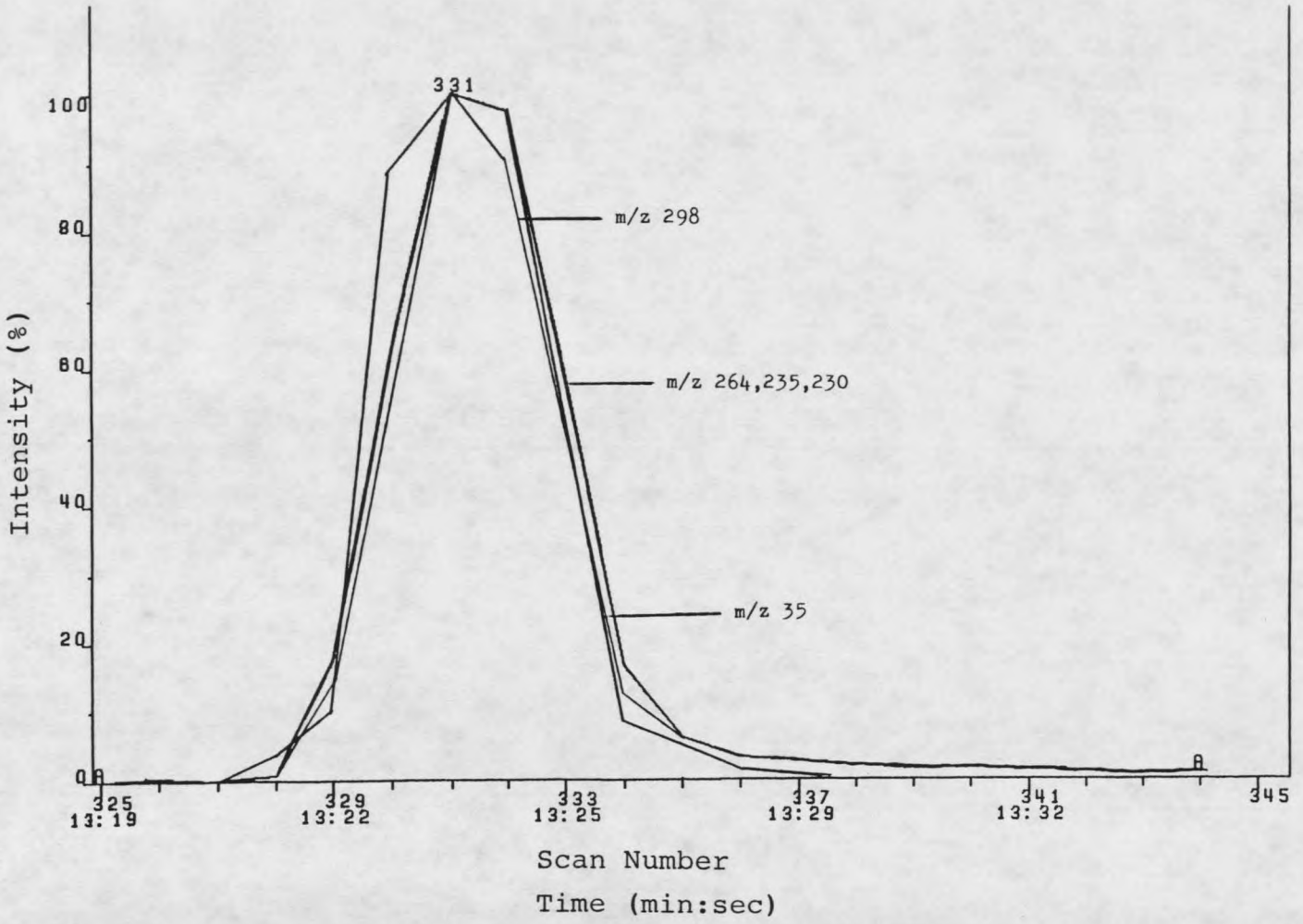


Figure 25. NRSIC for Heptachlor at 175°C and 0.45 Torr.

The suggested route for the formation of negative ions observed in the HPEC mass spectra of heptachlor is shown in Figure 26. This figure takes into account the fact that each reaction with the source wall takes a given amount of time, thus putting the reconstructed chromatograms for successive losses of 34 mass units one after the other.

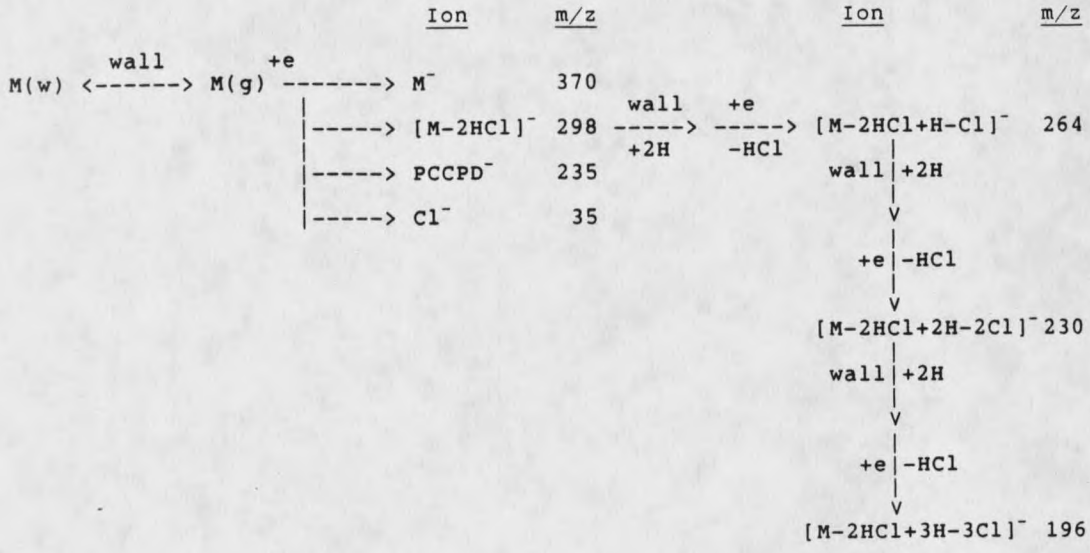


Figure 26. Suggested Mechanism for the Formation of Negative Ions from Heptachlor.

Endrin

The HPEC mass spectrum of endrin at 80°C and 0.3 Torr methane is displayed in Figure 27. The spectrum of this compound is very similar to that of its isomer, dieldrin, with one exception. That is that instead of an ion appearing at m/z 310 as with dieldrin, endrin displays an

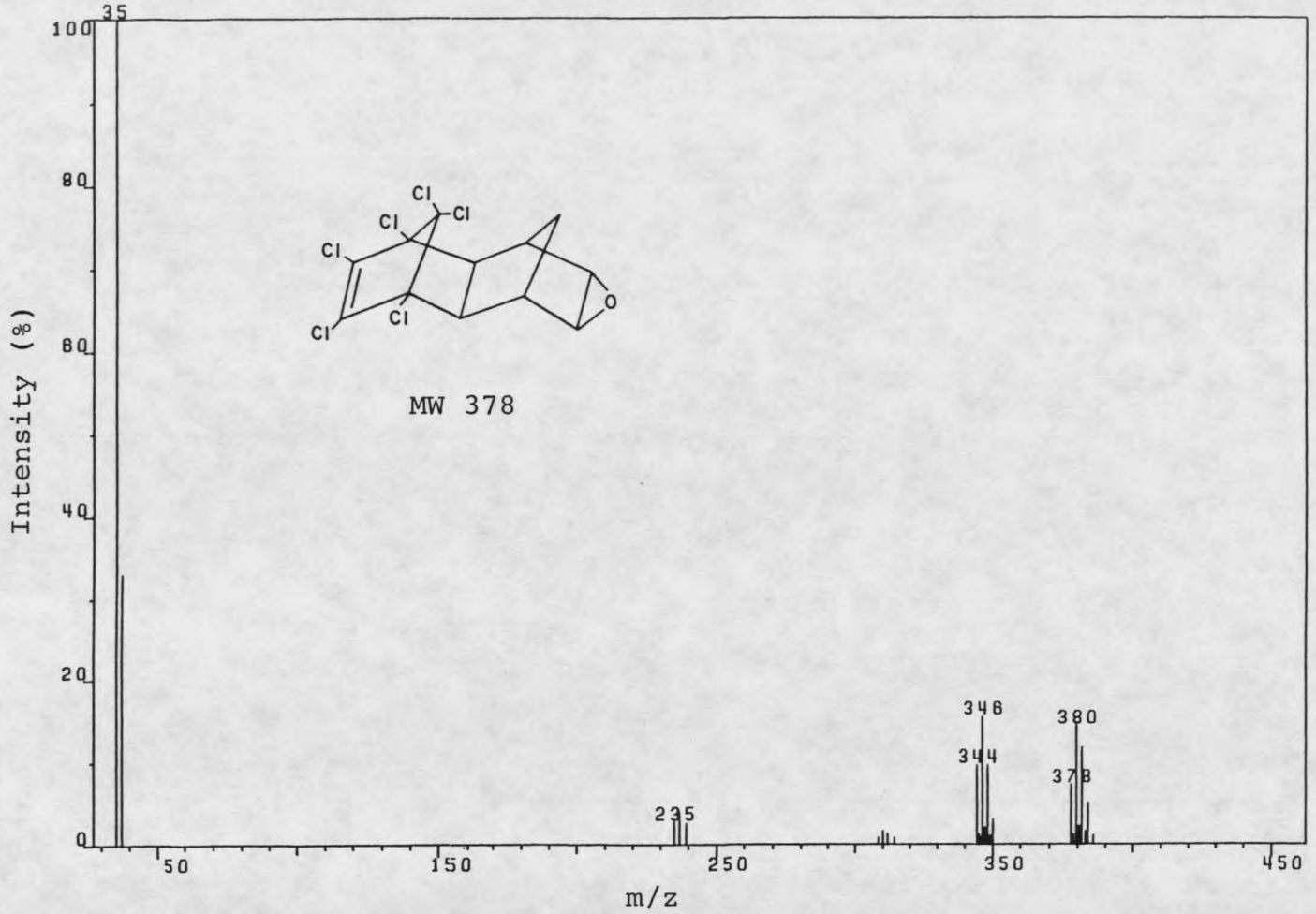


Figure 27. HPEC Mass Spectrum of Endrin at 80°C and 0.3 Torr.

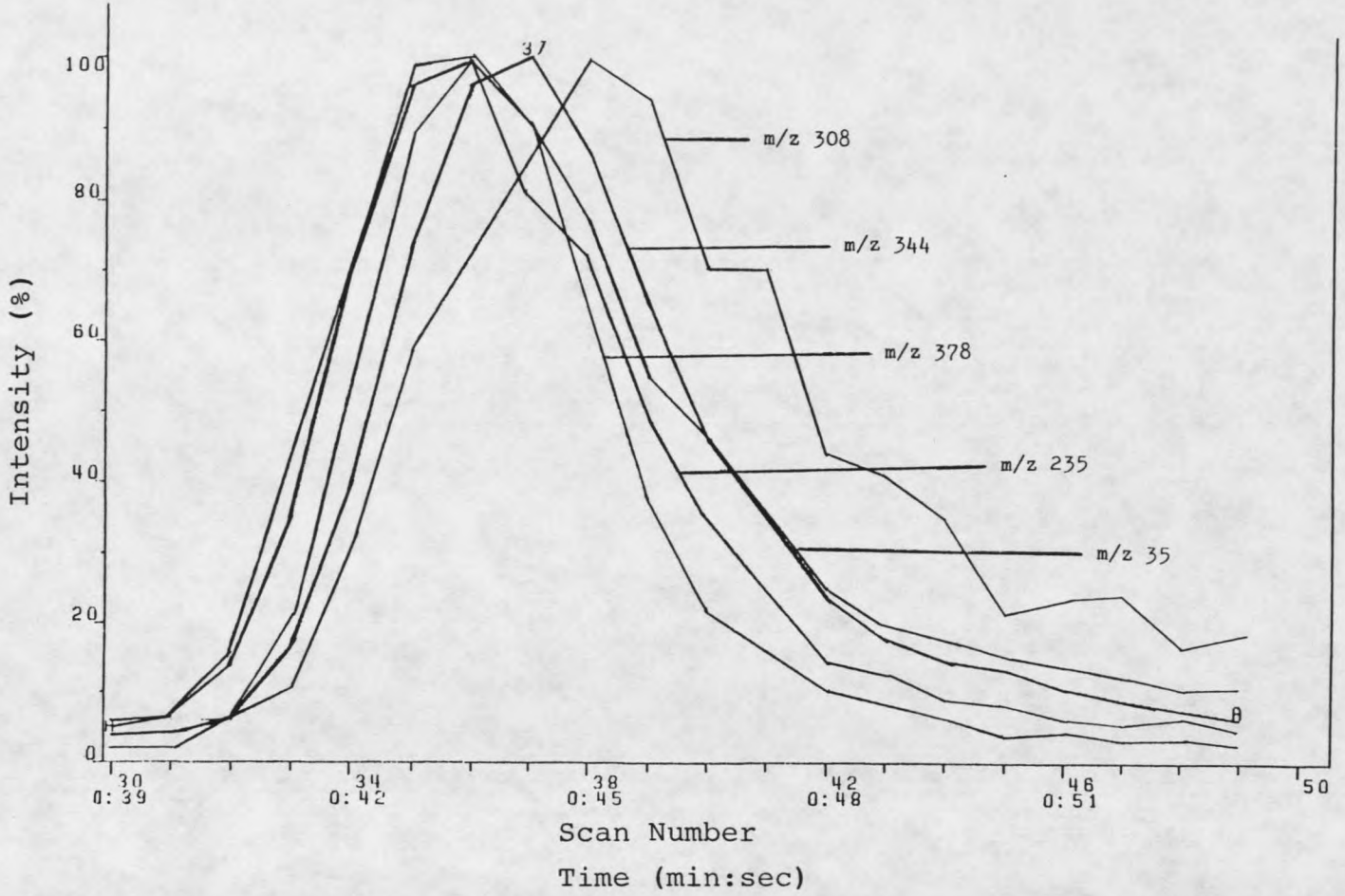


Figure 28. NRSIC for Endrin at 80°C and 0.3 Torr.

ion at m/z 308. The tabulated spectra of this compound at different ion source conditions are presented in the Appendix.

The NRSIC for endrin at 80°C and 0.3 Torr are shown in Figure 28. This figure suggests that the ion at m/z 344 is an unusual ion of the type $[M+H-Cl]^-$, whereas m/z 308 is also an ion which resulted from a species which had been adsorbed on the source surface. Figure 29 is the suggested mechanism for the production of the negative ions found in the HPEC mass spectra of endrin. This figure shows the ion at m/z 308 being converted into an unknown species, Q, upon adsorption on the ion source surface. This unknown species could then capture an electron and then dissociatively lose two chlorines. Figure 29 also suggests that m/z 35 and m/z 235 were formed from species which were structurally altered upon contact with the ion source wall.

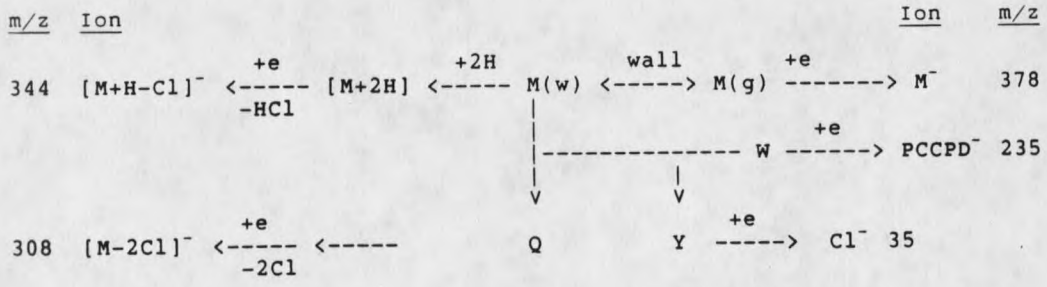


Figure 29. Suggested Mechanism for the Formation of Negative Ions from Endrin.

Endosulfan Sulfate

Figure 30 is the HPEC mass spectrum of endosulfan sulfate at 100°C and 0.3 Torr methane. This is the most complicated spectra produced by any of the compounds investigated in this study. The complications arise from the fact that in addition to the six chlorine atoms there is a sulfur atom connected to four oxygen atoms. Both of these groups stabilize negative charge, and the resulting HPEC mass spectrum reflects this. Only the significant ions will be addressed when discussing this compound. The tabulated spectra of endosulfan sulfate at various ion source conditions are shown in the Appendix.

From Figure 30 the molecular anion is shown at m/z 420 followed by m/z 384 which resulted from a loss of an HCl unit from m/z 420. The next ion to appear in the spectrum, when taking the ion of next highest mass, is m/z 351 which is followed by m/z 350. The ion at m/z 351 corresponds to $[M-HCl+2H-Cl]^-$, which has not previously been shown to have been produced for any of the other compounds. The ion at m/z 350 corresponds to $[M-HCl+H-Cl]^-$ and is an unusual ion. The $PCCPD^-$ ion can be seen at m/z 235 while an ion corresponding to $[M-PCCPD]^-$ appears at m/z 185. This is the only compound discussed in this work that displays the $[M-PCCPD]^-$ ion and can be contributed to the electron stabilizing properties of the SO_4 group. Evidence for internal rearrangement of the SO_4 group is

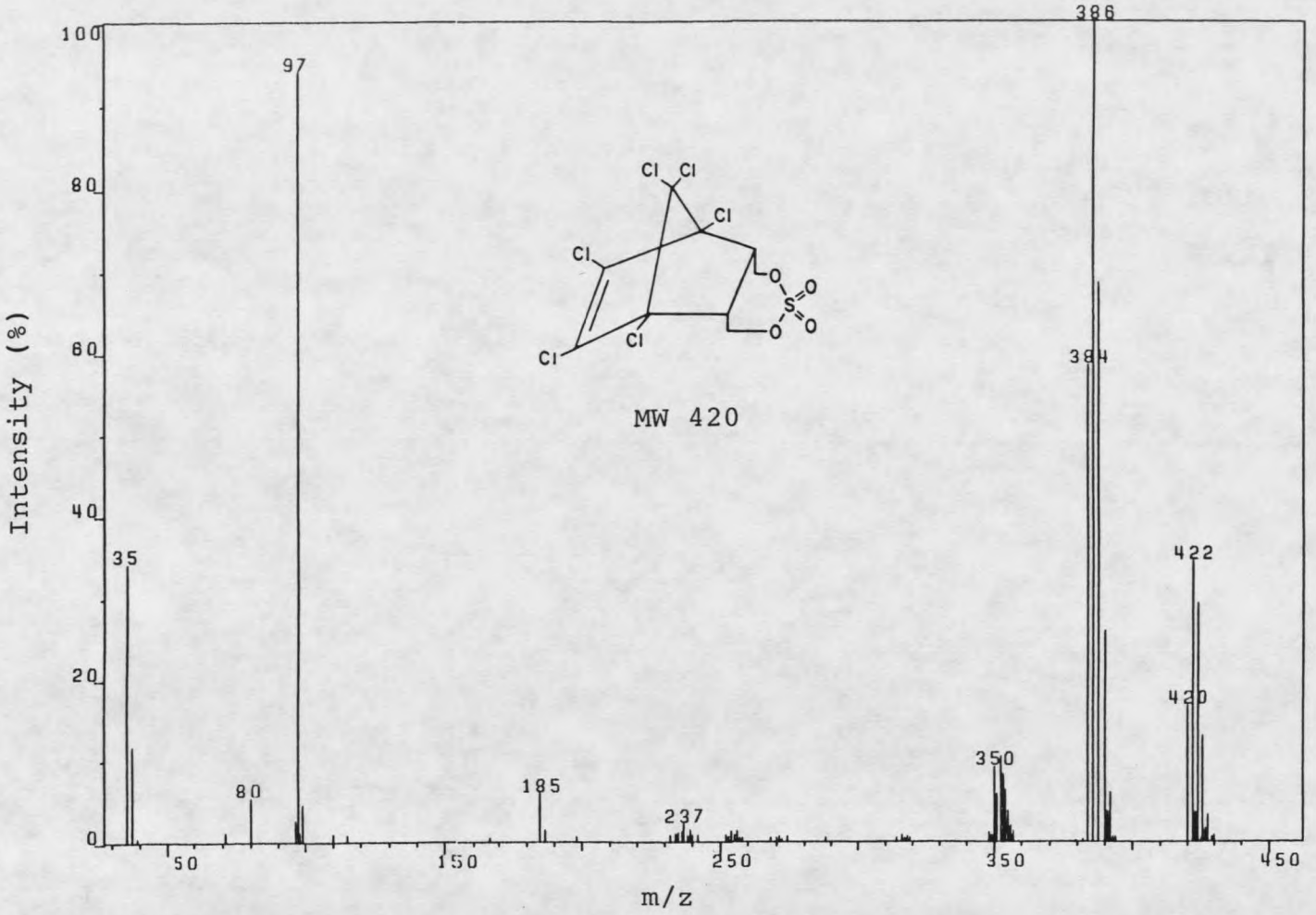


Figure 30. HPEC Mass Spectrum of Endosulfan Sulfate at 100°C and 0.3 Torr.

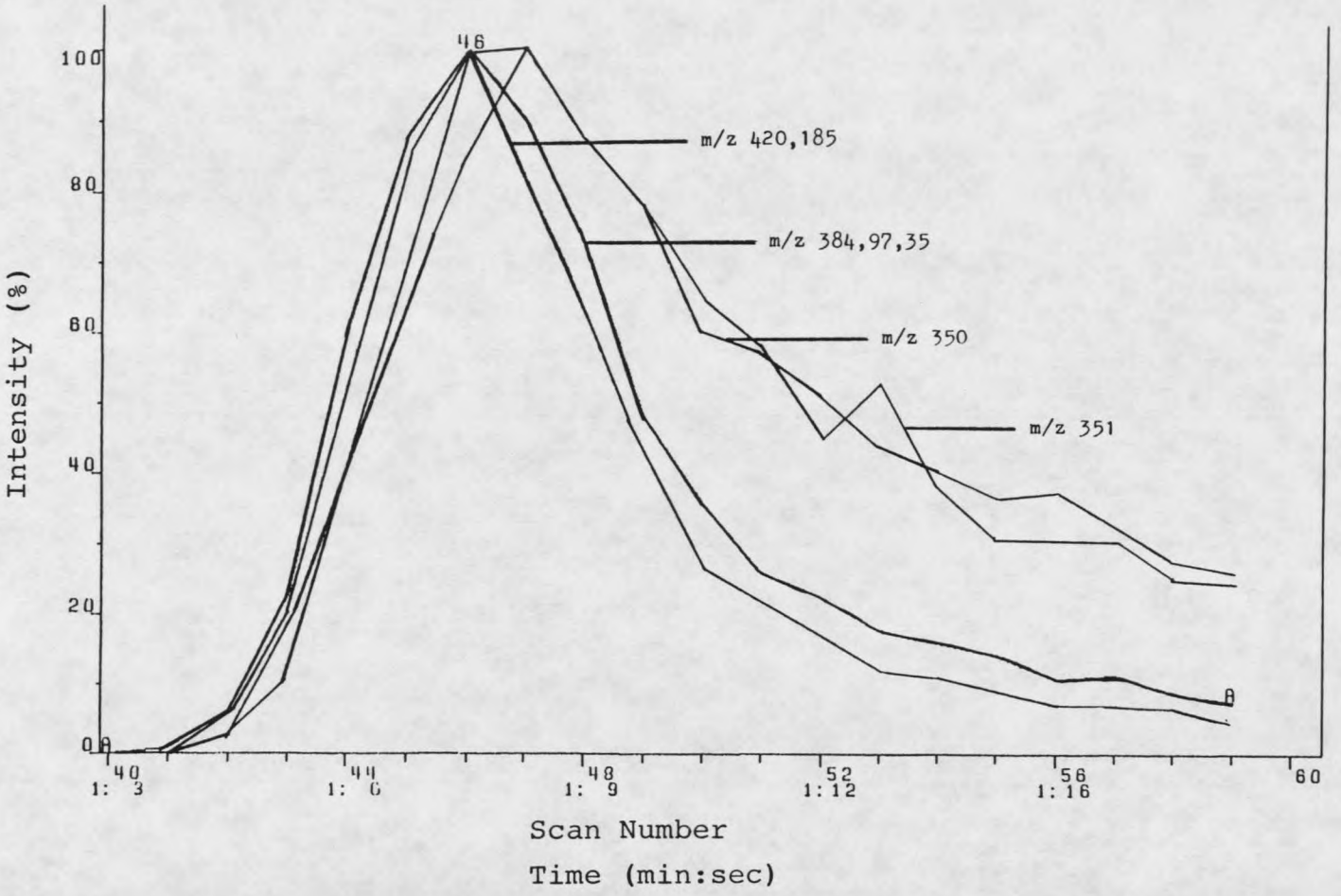


Figure 31. NRSIC for Endosulfan Sulfate at 100°C and 0.3 Torr.

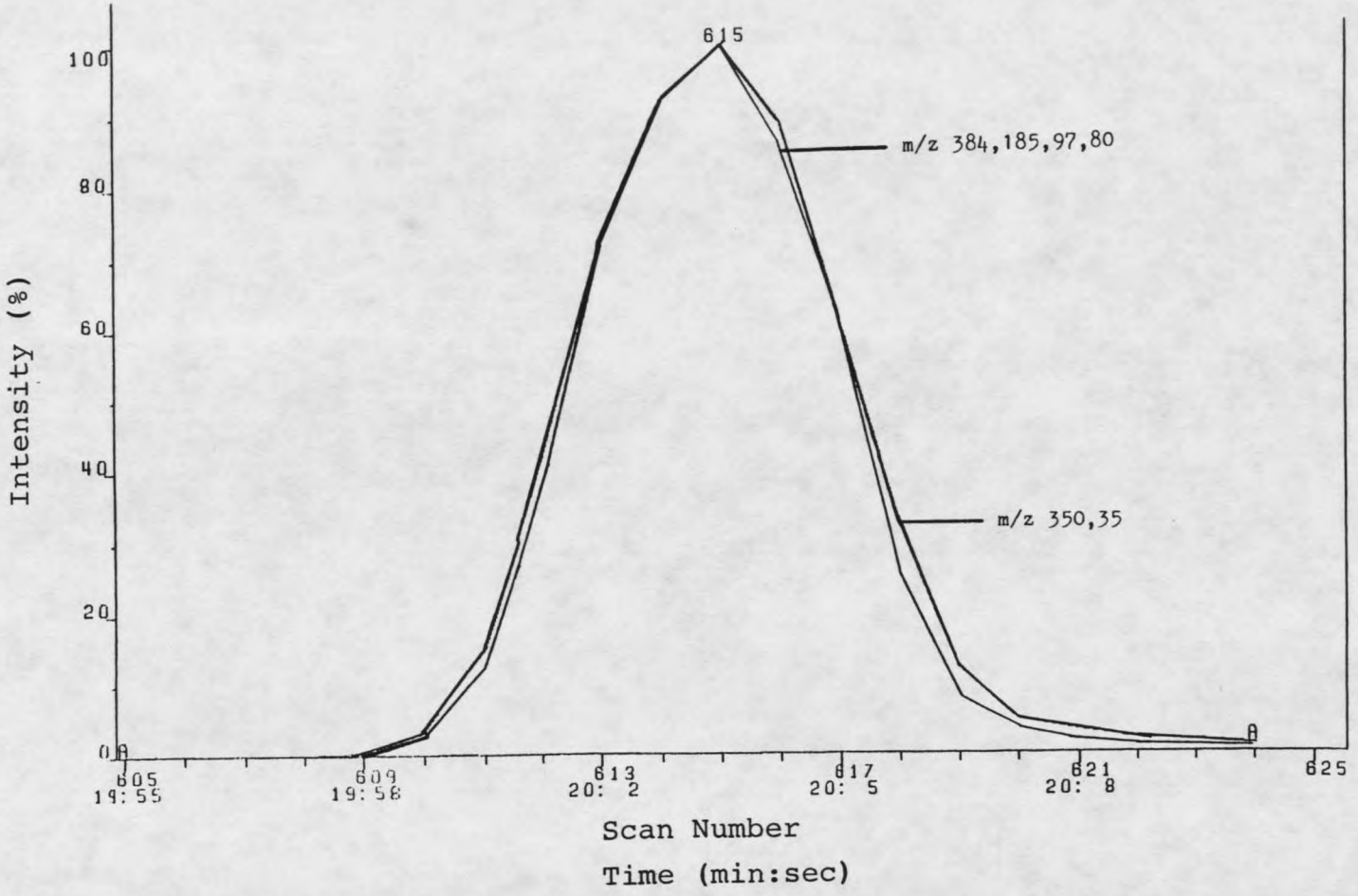


Figure 32. NRSIC for Endosulfan Sulfate at 220°C and 0.3 Torr.

shown by m/z 97 which corresponds to the HSO_4^- ion. Following this ion are ions corresponding to SO_3^- and Cl^-.

The NRSIC for endosulfan sulfate at 0.3 Torr and two different source temperatures are shown in Figures 31 and 32. Figure 31 shows that both m/z 350 and m/z 351 tail, to the same extent, well after the molecular anion has passed, suggesting that they both arose from the same neutral species. Figure 32 shows that as the temperature rises, the adsorption-desorption rate must have increased to the point that the NRSIC can no longer distinguish the ions m/z 350 and m/z 351 from the others. The suggested mechanism for the ionization of endosulfan sulfate is shown in Figure 33. The mechanism shown in this figure is the result of observations made from Figure 31 that m/z 350 and m/z 351 are presisting inside the ion source for a longer period of time than any of the other ions. Because the reconstructed chromatograms for ions other than m/z 350 and m/z 351 are so close to one another, Figure 33 shows them as arising from the same species.

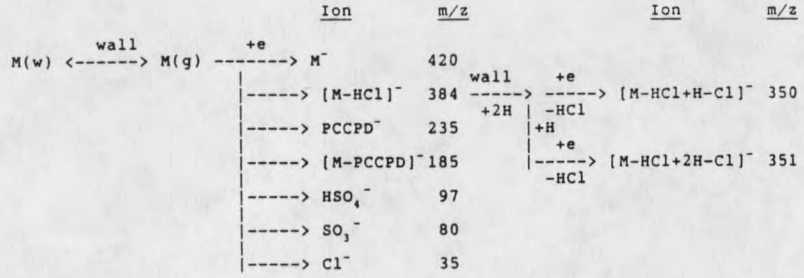


Figure 33. Suggested Mechanism for the Formation of Negative Ions from Endosulfan Sulfate.

Hexachlorocylopentadiene

The HPEC mass spectrum of hexachlorocyclopentadiene at 90°C and 0.3 Torr methane is shown in Figure 34. The ions in this figure have been normalized to m/z 237 which, other than Cl^-, is the most intense ion. This was done because of the very low abundance of all ions other than Cl^- ions. The spectrum of this compound displays its ion of highest mass at m/z 235 which corresponds to $PCCPD^-$. Following the $PCCPD^-$ ion, two consecutive losses of 34 mass units are observed at m/z 201 and m/z 167 and correspond to $[M-Cl+nH-nCl]^-$ ions where n equals 2. All other ions observed in Figure 34 have abundances less than 0.5% of the Cl^- ion.

The NRSIC for hexachlorocyclopentadiene are presented in Figure 35. Only the three ions at m/z 235, m/z 201, and m/z 167 are shown in Figure 35. It is apparent from this figure that there are consecutive wall reactions that produce the ions shown. Figure 36 is the suggested mechanism for the production of negative ions by HPECMS. This figure depicts the unusual ions arising from the $PCCPD^-$ ion.

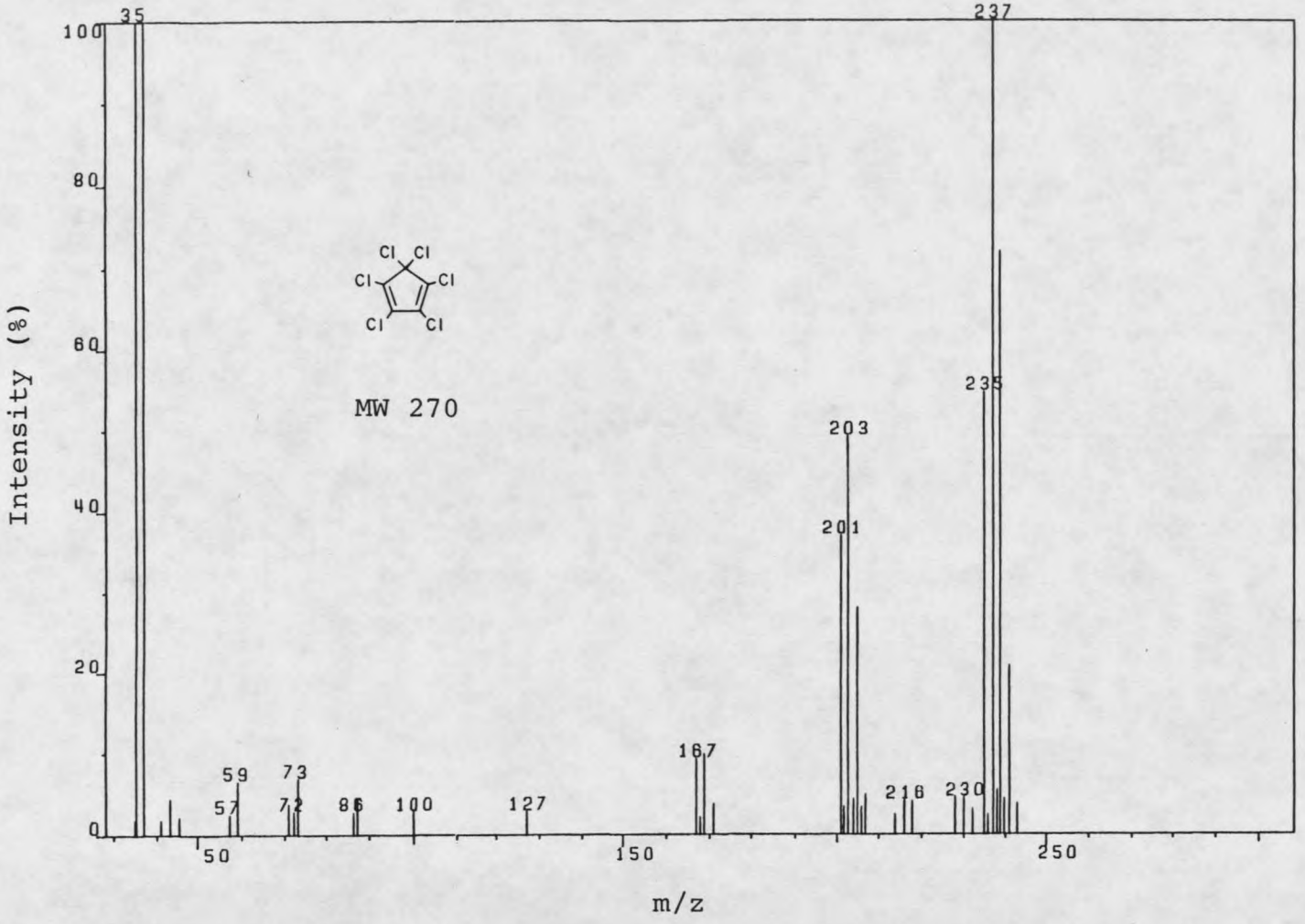


Figure 34. HPEC Mass Spectrum of Hexachlorocyclopentadiene at 90°C and 0.3 Torr.

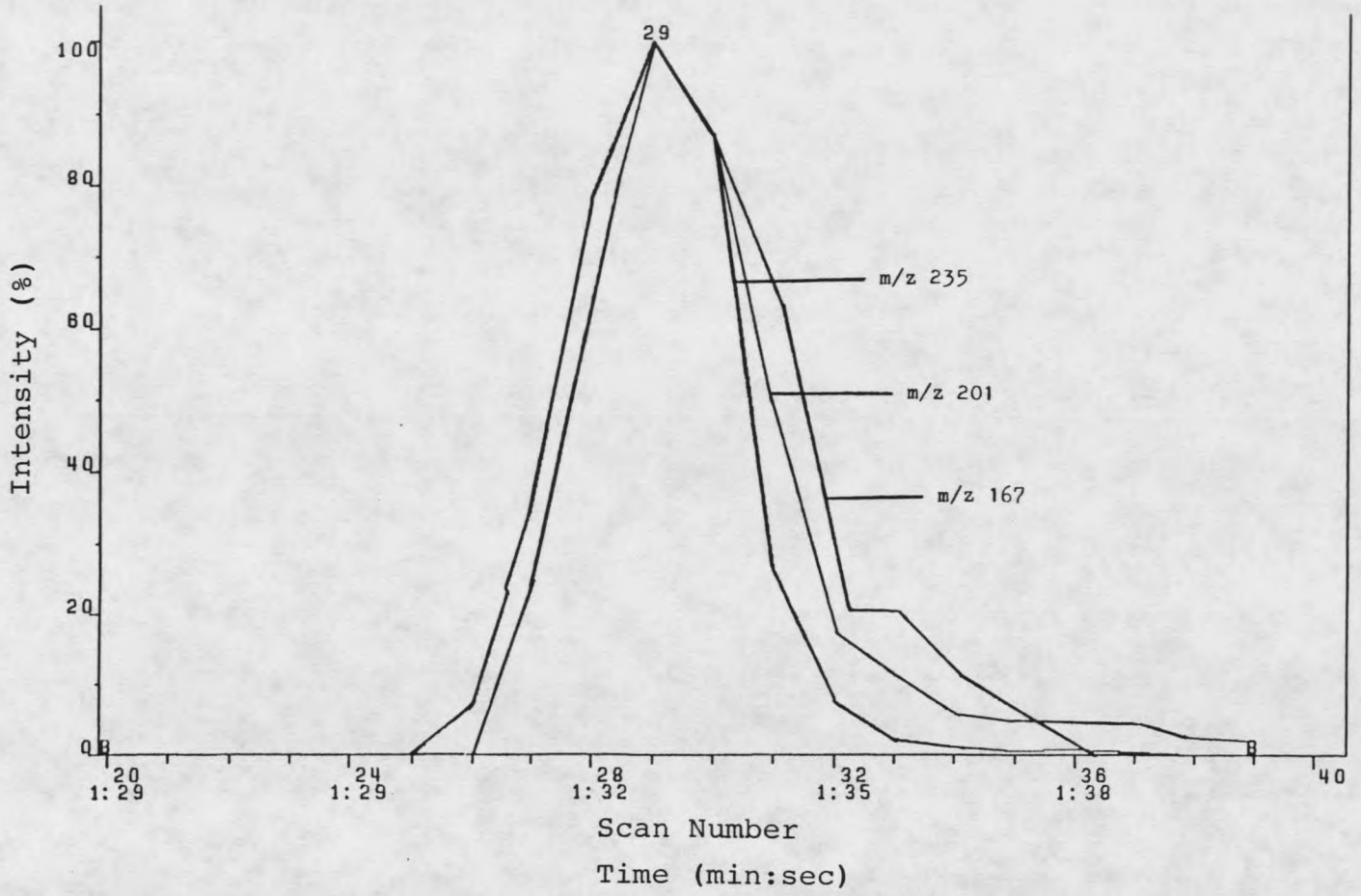


Figure 35. NRSIC for Hexachlorocyclopentadiene at 90°C and 0.3 Torr.

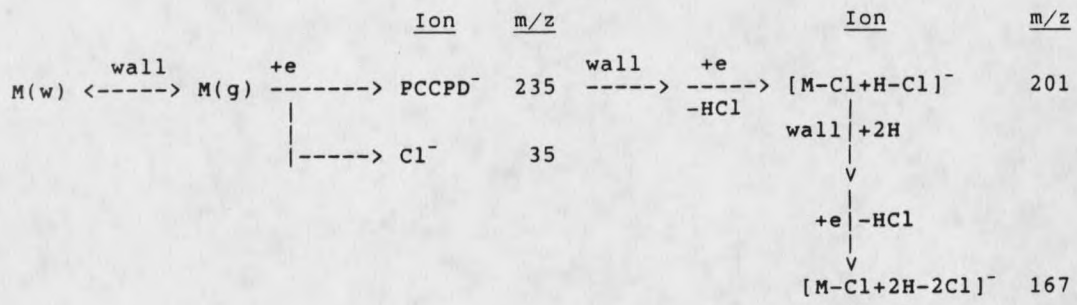


Figure 36. Suggested Mechanism for the Formation of Negative Ions from Hexachlorocyclopentadiene.

Mirex

The next compound that will be of interest in this study is mirex. The HPEC mass spectrum of this compound at 175°C and 0.2 Torr is shown in Figure 37. Mirex is not a compound on the EPA Priority Pollutant list, but because it is also a derivative of hexachlorocyclopentadiene it was investigated. The ion of highest mass appears at m/z 435 and corresponds to $[M-3Cl]^-$. Following m/z 435 appears m/z 400 and corresponds to the $[M-4Cl]^-$ ion. After the $[M-4Cl]^-$ species shown in Figure 37 comes a series of ions corresponding to $[M-4Cl+nH-nCl]^-$ where n equals 5. The tabulated spectra of mirex are shown in the Appendix.

The NRSIC for mirex at 175°C and 0.2 Torr are presented in Figure 38. This figure clearly shows that each ion differing by 34 mass units from the previous ion of higher mass tails after it. The fact that m/z 400

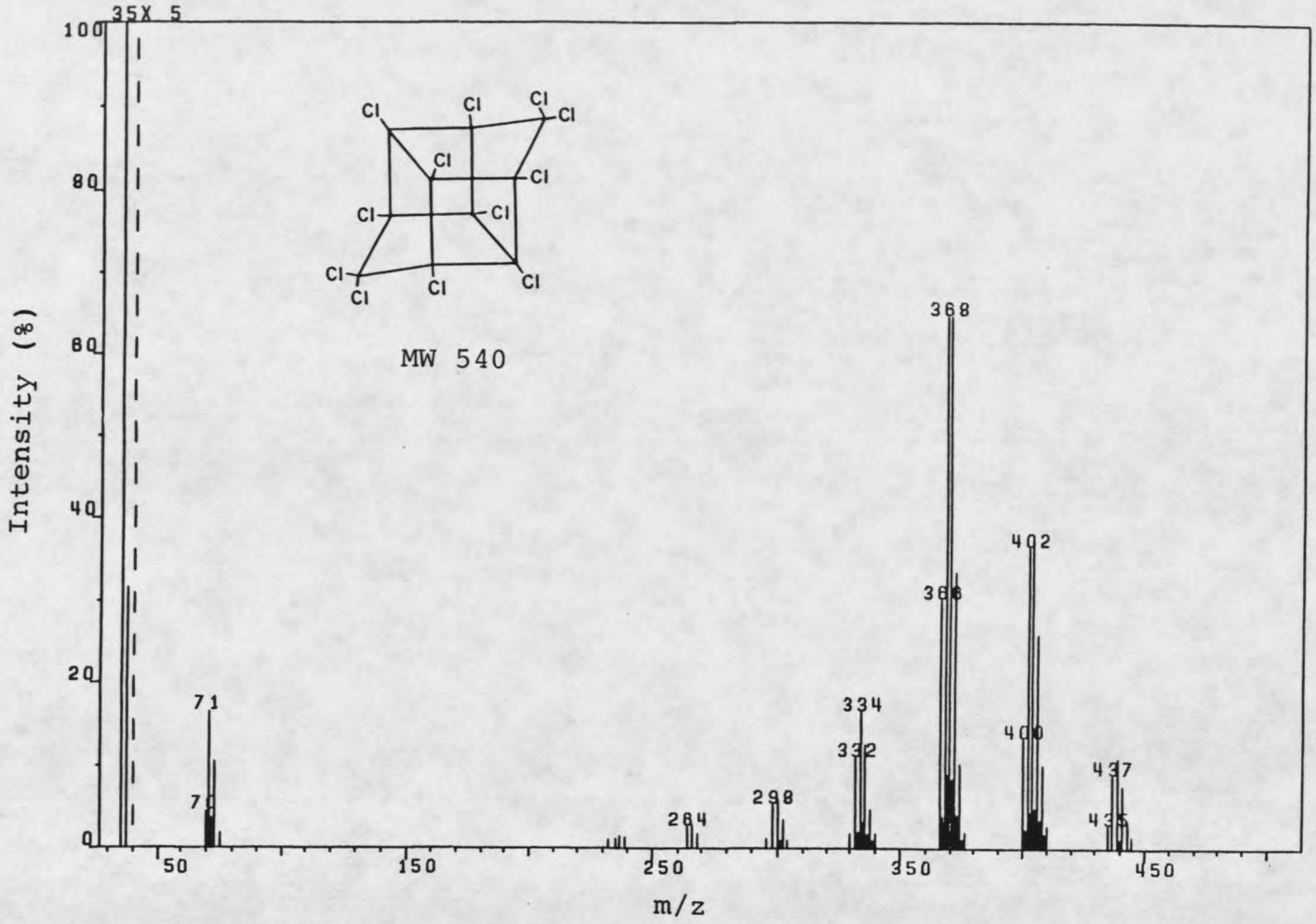


Figure 37. HPEC Mass Spectrum of Mirex at 175°C and 0.2 Torr.

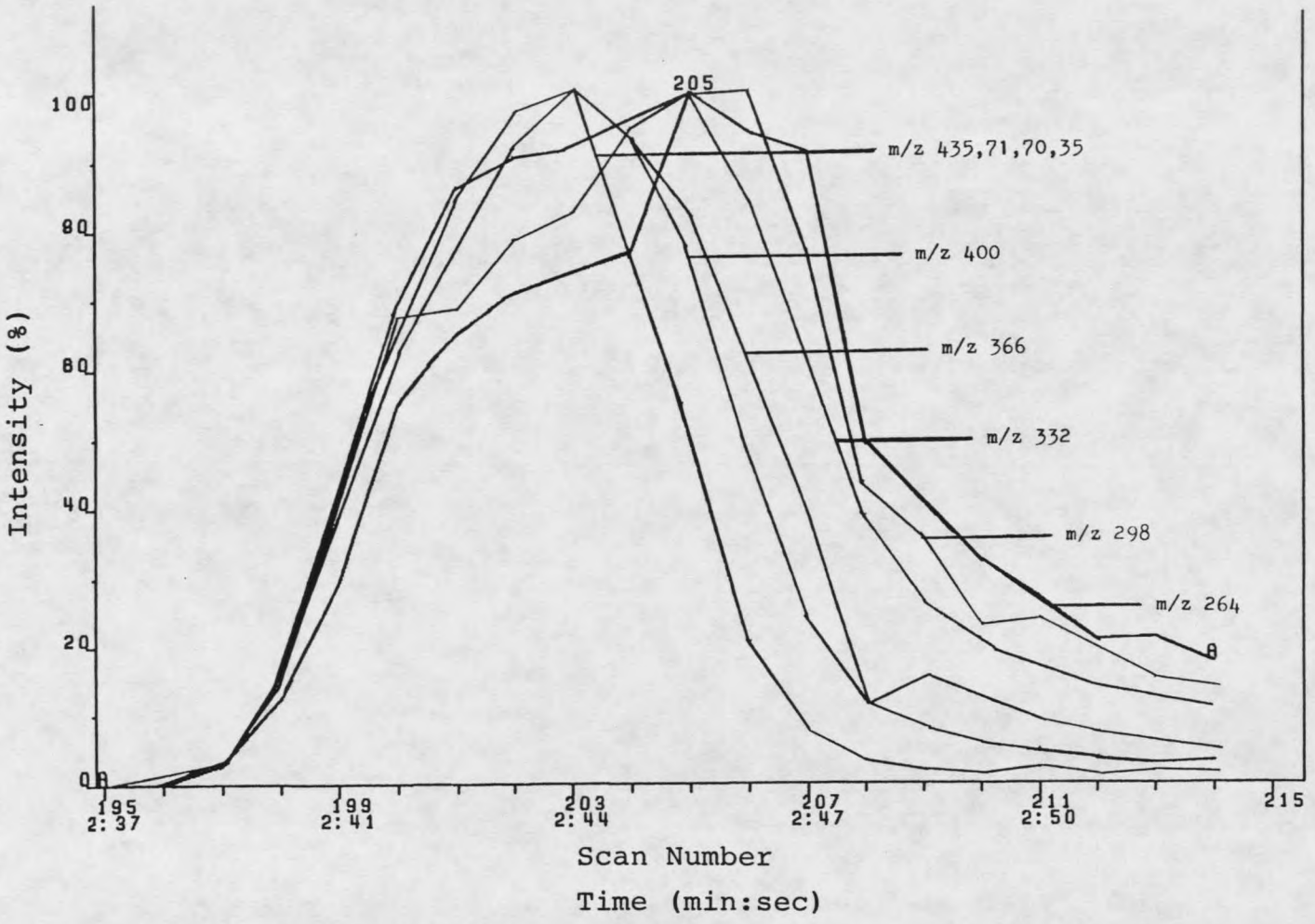


Figure 38. NRSIC for Mirex at 175°C and 0.2 Torr.

appears to tail after m/z 435 in Figure 38 suggests that it, too, may be the result of reaction taking place at the ion source walls. The suggested mechanism for the production of negative ions from mirex is shown in Figure 39. This figure shows the ion at m/z 400 arising from a wall reaction. The unusual ions, $[M-4Cl+nH-nCl]^-$ where n equals 5, are shown to be produced by a repetitive reaction sequence involving the $[M-4Cl]^-$ ion.

Pentac

Pentac is another compound that is not an EPA priority pollutant but was investigated because it also shows ions of the type $[M-Z+nH-nCl]^-$. The tabulated spectra of this compound are shown in the Appendix for two different experimental conditions. The HPEC mass spectrum of this compound at 100°C and 0.3 Torr is presented in Figure 40. This spectrum is very similar to that of mirex suggesting these two compounds follow a closely related decomposition pattern. The ion of highest mass in Figure 40 is m/z 435 and corresponds to the $[M-Cl]^-$ ion. Following this ion there appears one at m/z 400 corresponding to $[M-2Cl]^-$. After the ion at m/z 400 comes a series of unusual ions having the form $[M-2Cl+nH-nCl]^-$ where n is 5. One interesting feature that should be pointed out from Figure 40 is that there is an ion appearing at m/z 201. This ion is probably the result of

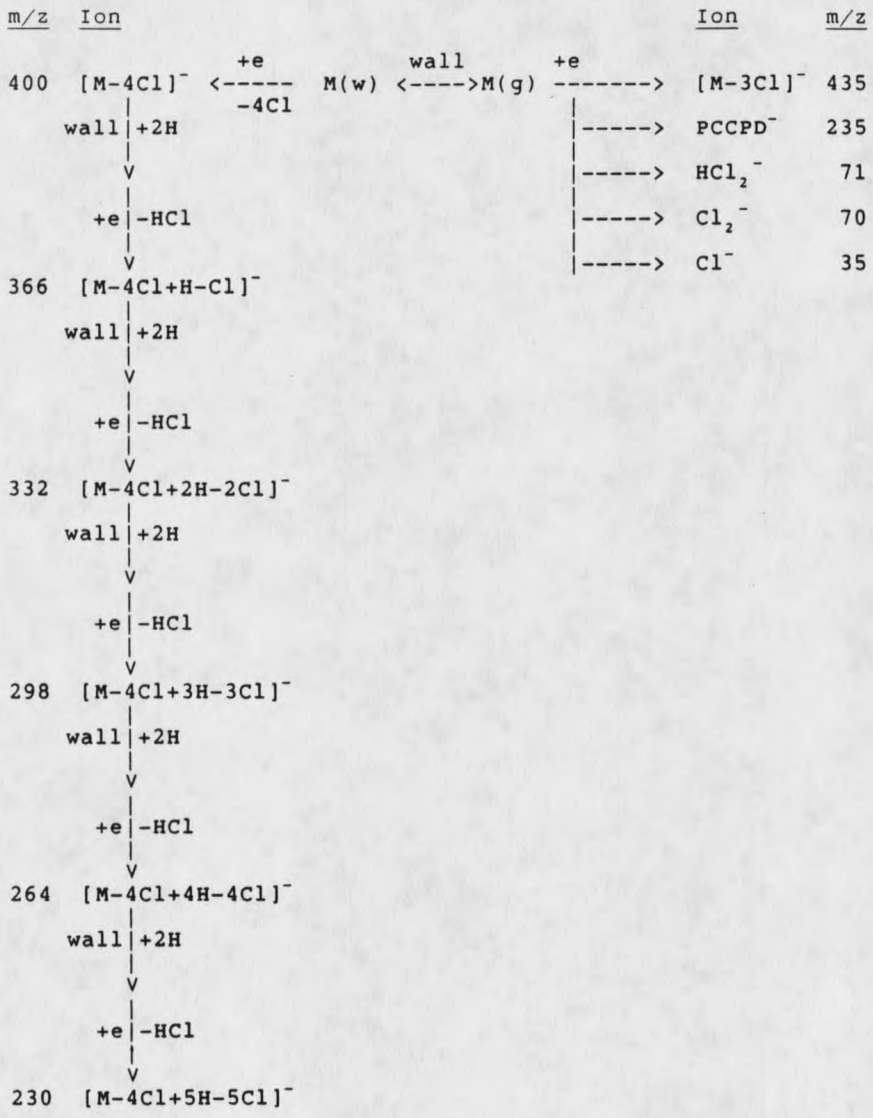


Figure 39. Suggested Mechanism for the Formation of Negative Ions from Mirex.

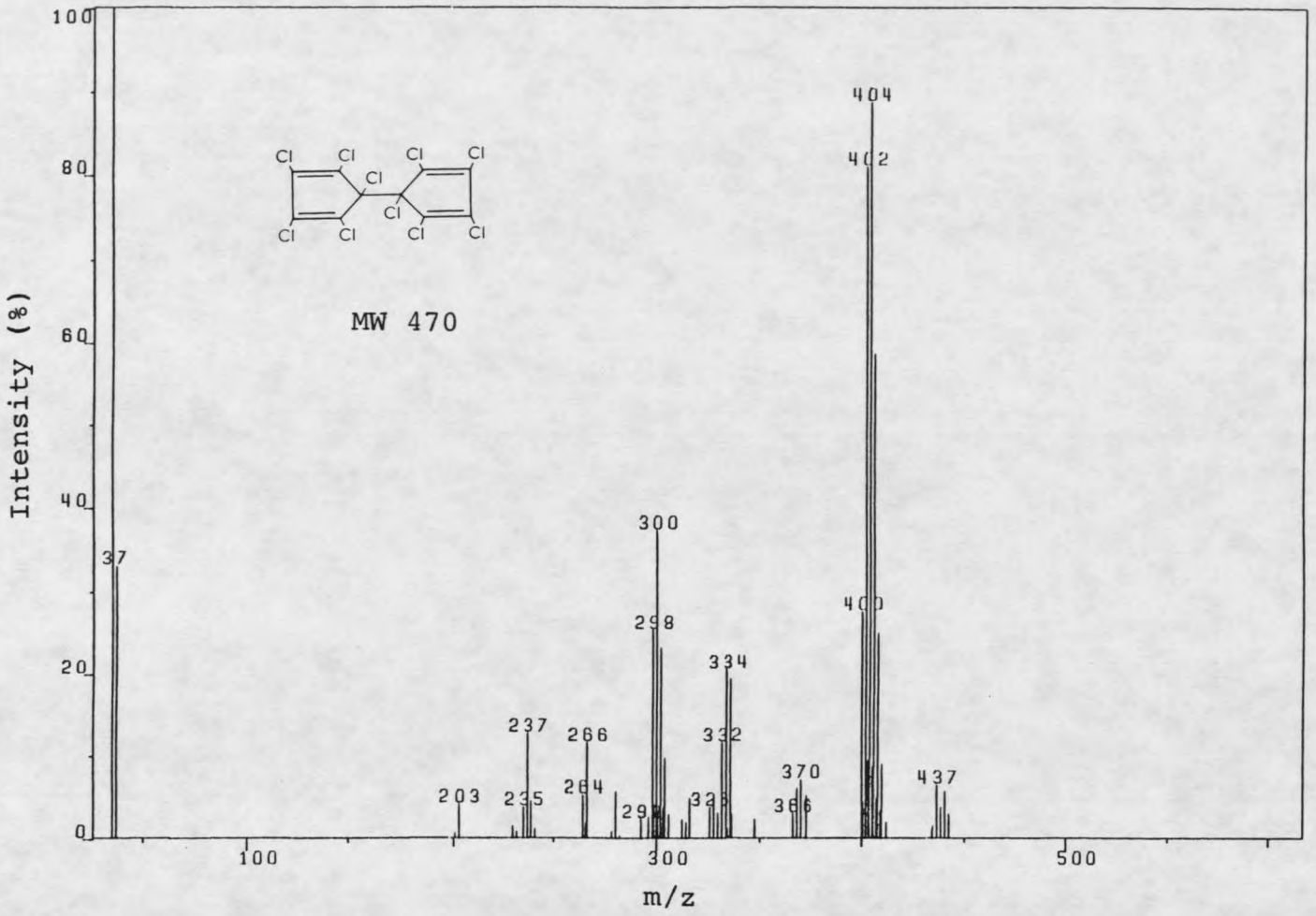


Figure 40. HPEC Mass Spectrum of Pentac at 100°C and 0.3 Torr.

a wall reaction of the $PCCPD^-$ ion produced by direct bond cleavage of the two rings in pentac.

The NRSIC for pentac are shown in Figure 41 at 100°C and 0.3 Torr methane. The ions at m/z 435 and m/z 235 appear to follow the same chromatogram suggesting that they left the ion source at the same time. The rest of the ions all tail after the ions just mentioned. The suggested mechanism for the production of negative ions for pentac is shown in Figure 42 based on the observations from Figure 41.

Hexachlorobenzene

The HPEC mass spectrum of hexachlorobenzene at 100°C and 0.3 Torr is presented in Figure 43. The tabulated spectra of this compound are shown in the Appendix. Figure 43 displays the molecular anion of this compound as the base peak of the spectrum. Following the molecular anion at m/z 282 are ions at m/z 248, m/z 247, and m/z 35 corresponding to $[M+H-Cl]^-$, $[M-Cl]^-$ and Cl^- respectively.

The NRSIC for hexachlorobenzene are shown in Figure 44 at 100°C and 0.3 Torr methane. Only the unusual ion corresponding to $[M+H-Cl]^-$ appears to lag after the other ions have left the ion source. The suggested mechanism for the formation of negative ions from this compound is shown in Figure 45.

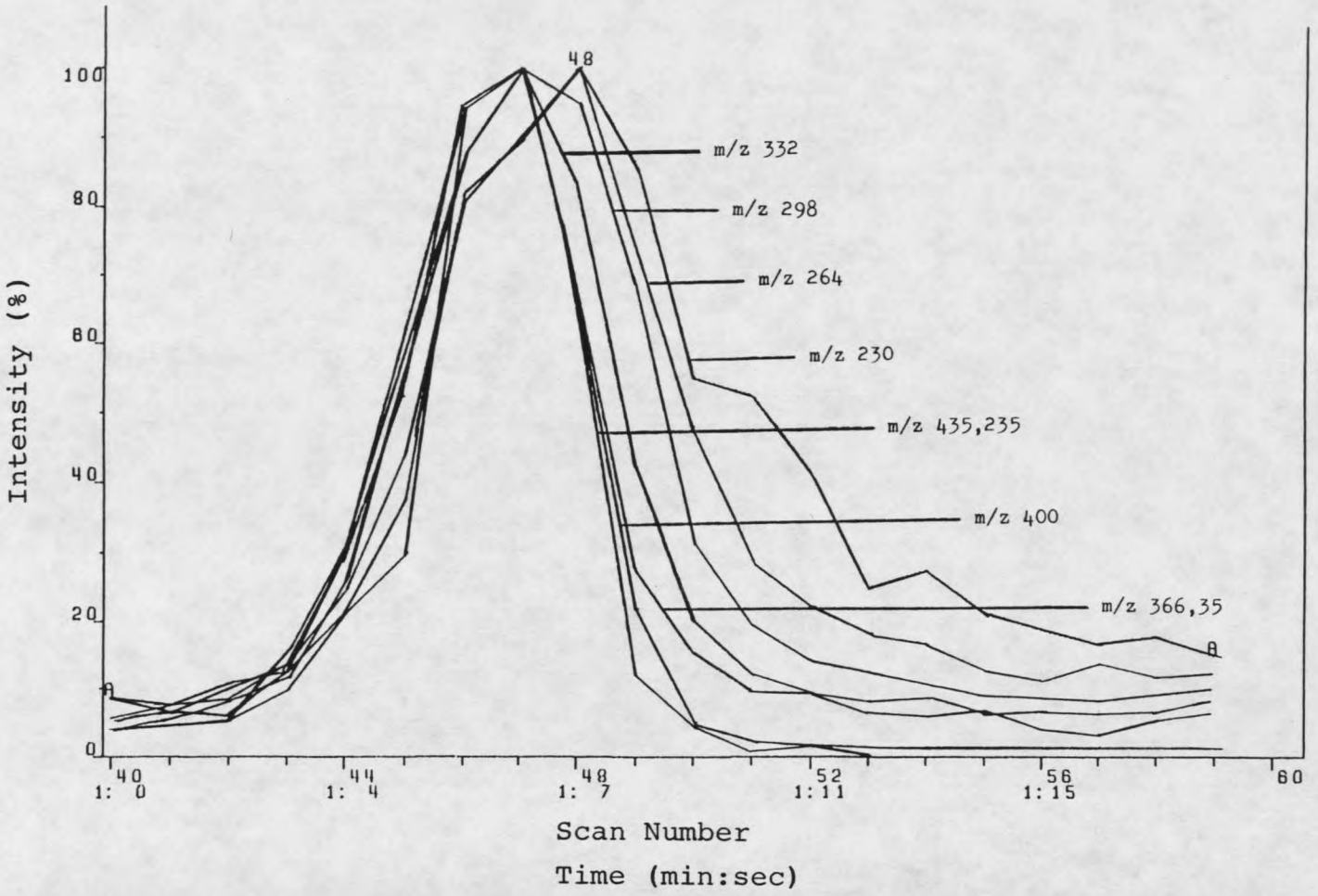


Figure 41. NRSIC for Pentac at 100°C and 0.3 Torr.

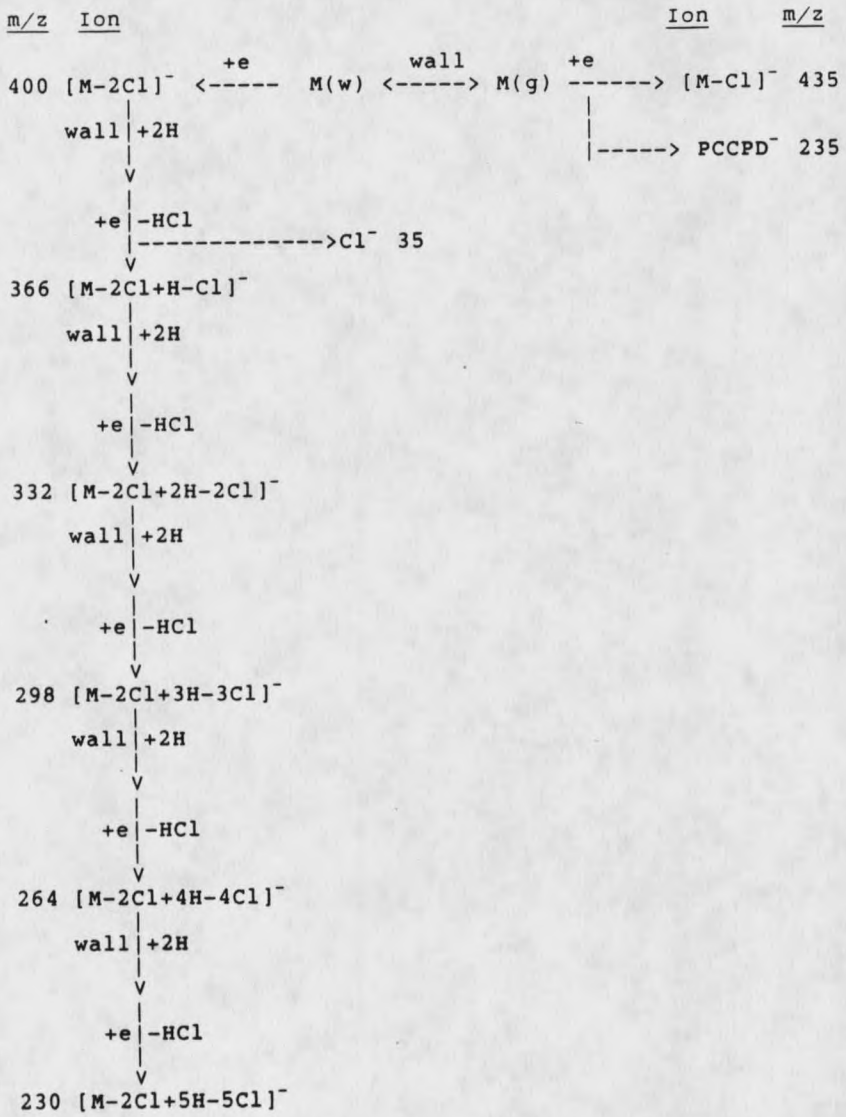


Figure 42. Suggested Mechanism for the Formation of Negative Ions from Pentac.

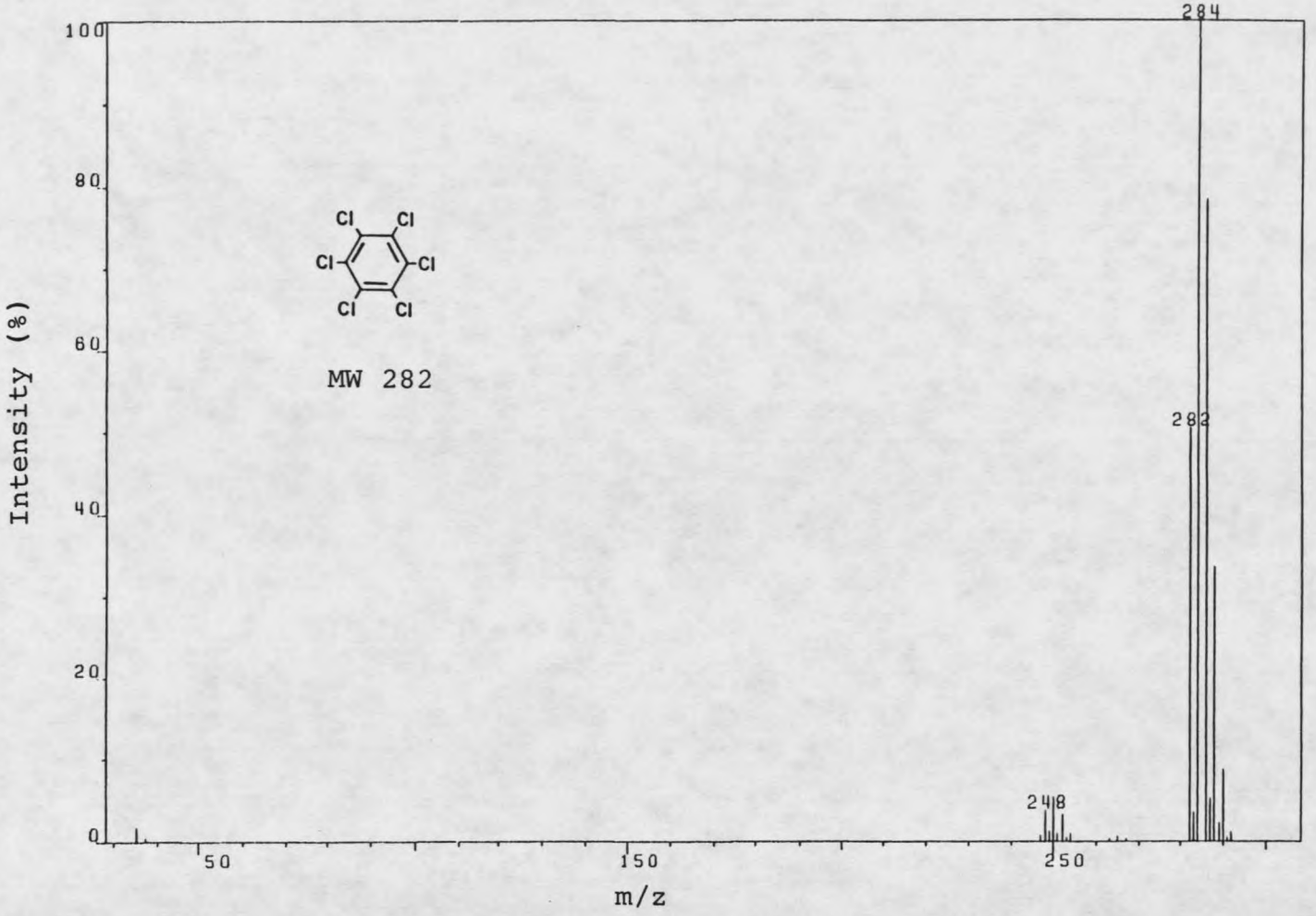


Figure 43. HPEC Mass Spectrum of Hexachlorobenzene at 100°C and 0.3 Torr.

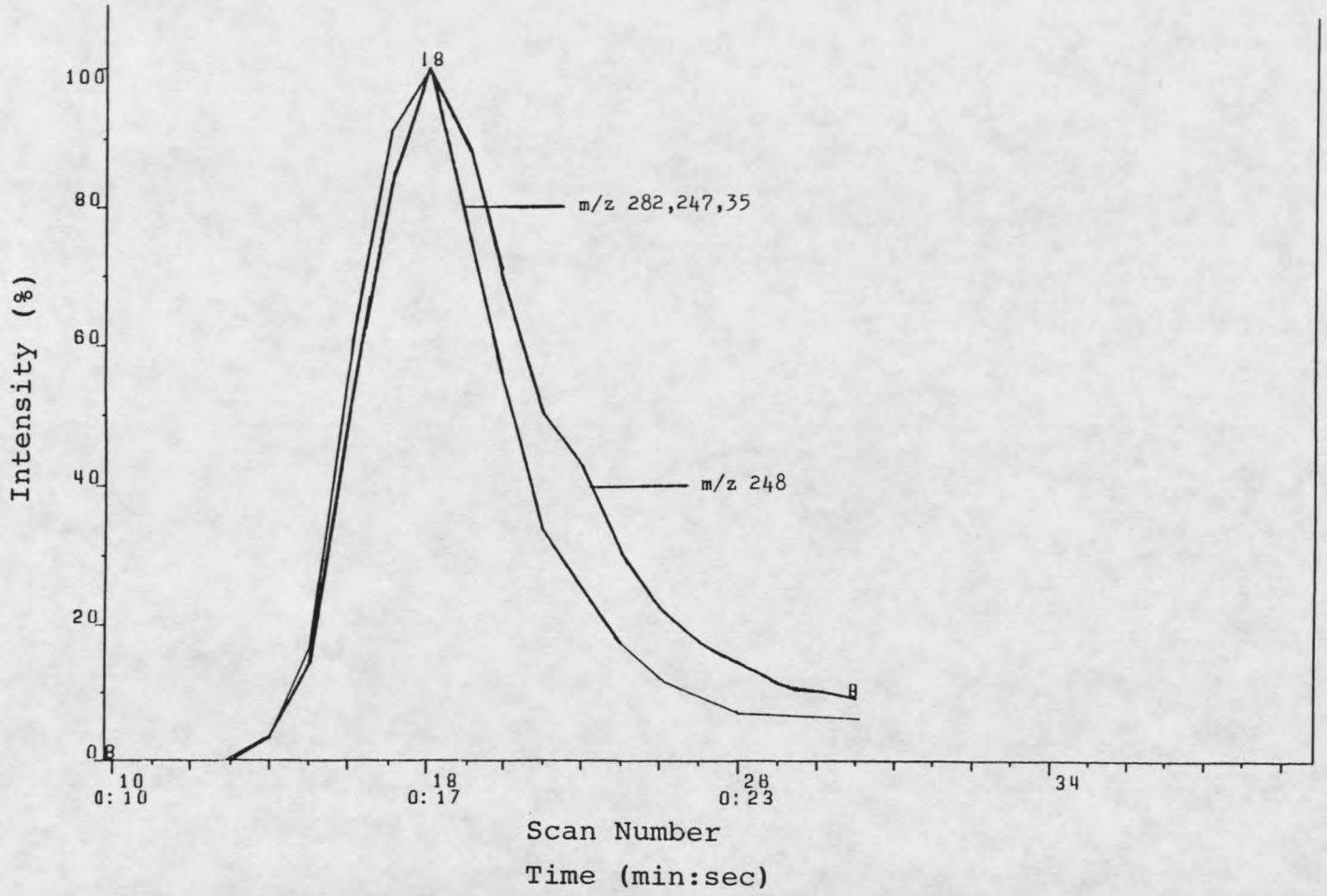


Figure 44. NRSIC for Hexachlorobenzene at 100°C and 0.3 Torr.

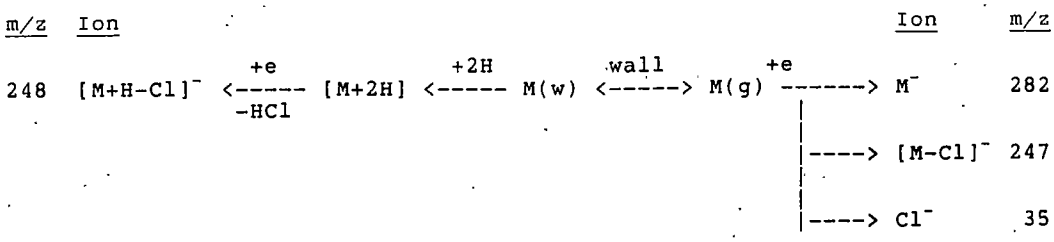


Figure 45. Suggested Mechanism for the Formation of Negative Ions from Hexachlorobenzene.

Polychlorinated Biphenyls (PCB's)

The last example of unusual ions of the type $[M-Z+nH-nCl]^-$ that will be investigated is produced by the PCB's. These compounds have the general formula $C_{12}H_xCl_y$ where y ranges from 1 to 10 and x+y must equal 10. As was shown by other investigators[17] and found to be true also in this investigation, the HPEC mass spectra of PCB's containing between 1 and 5 chlorines are dominated by the dissociative electron capture product, Cl^- ion. PCB's containing between 6 and 10 chlorines show the molecular anion in their spectra. Figure 46 is a typical HPEC mass spectrum of a PCB containing 8 chlorines at 100°C and 0.3 Torr. At least one unusual ion appears in Figure 46 and corresponds to $[M+H-Cl]^-$.

The NRSIC for the PCB mentioned above are shown in Figure 47 at 100°C and 0.3 Torr methane. Only the ions at m/z 426 and m/z 392 are shown in this figure because the ions at m/z 358 and m/z 35 are of so little abundance that

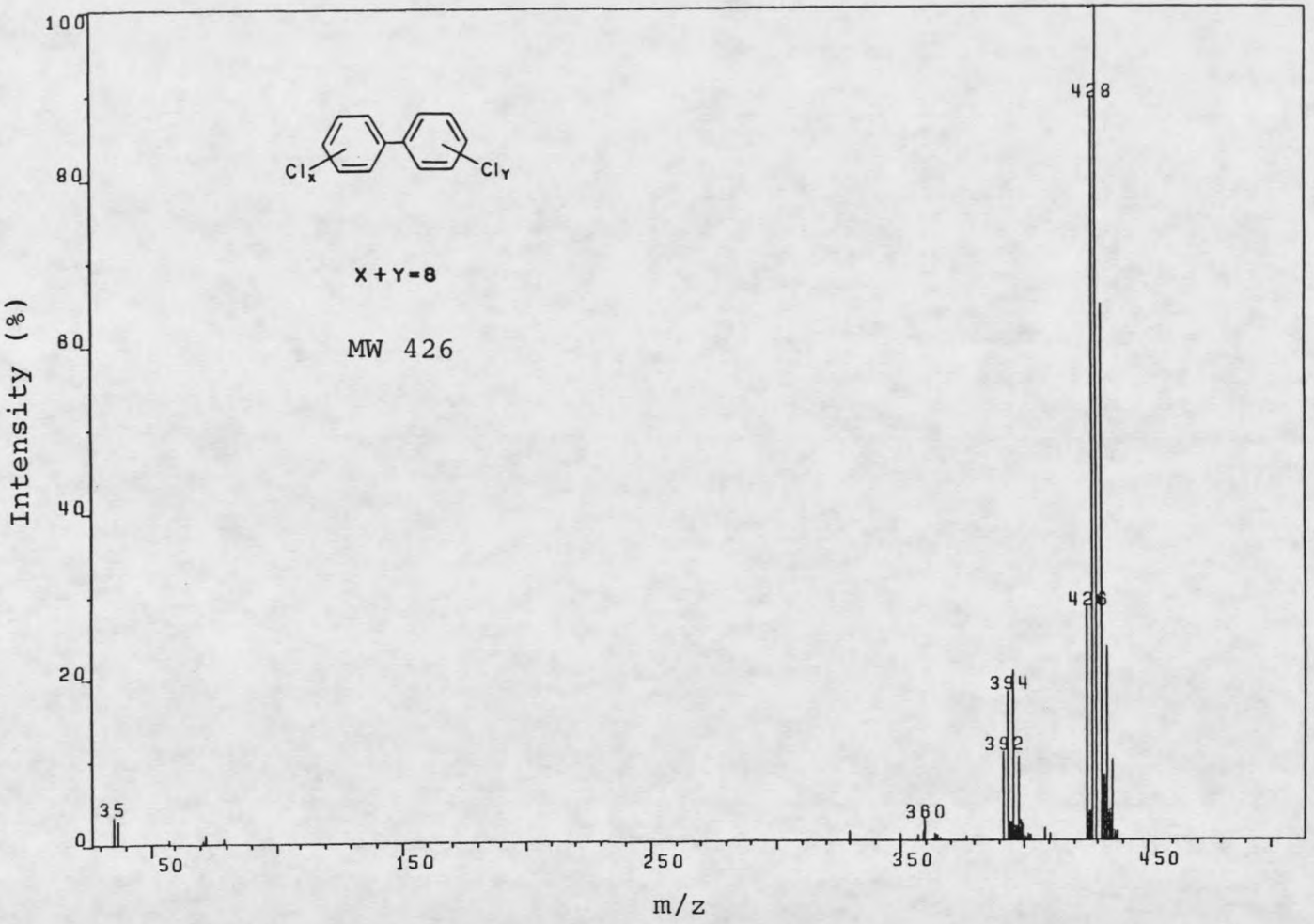


Figure 46. HPEC Mass Spectrum of a PCB containing 8 Chlorines at 100°C and 0.3 Torr.

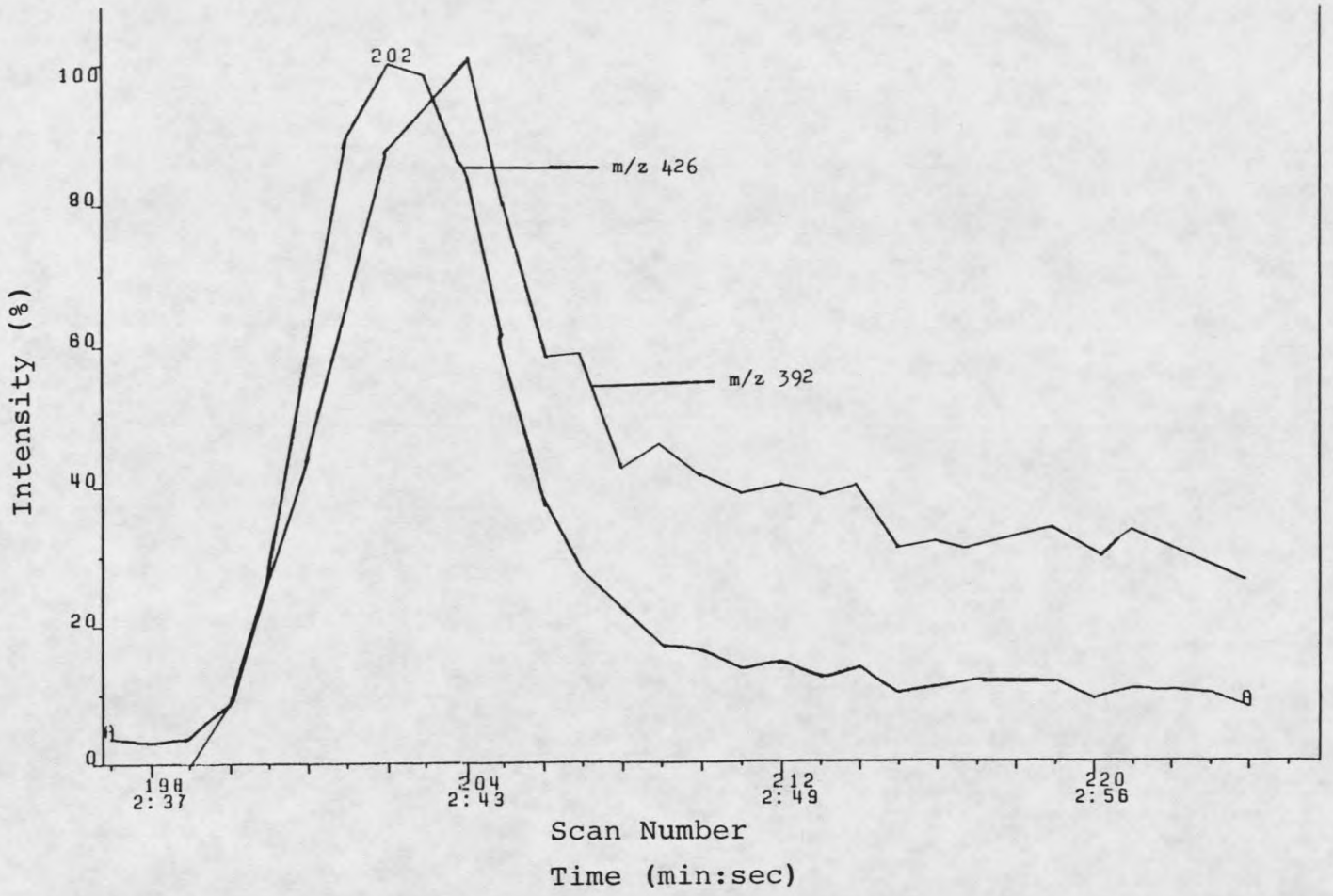


Figure 47. NRSIC for a PCB Containing 8 Chlorines at 100°C and 0.3 Torr.

the chromatograms produced were useless. Figure 48 is the suggested mechanism for the production of negative ions from the 8 chlorine-containing PCB.

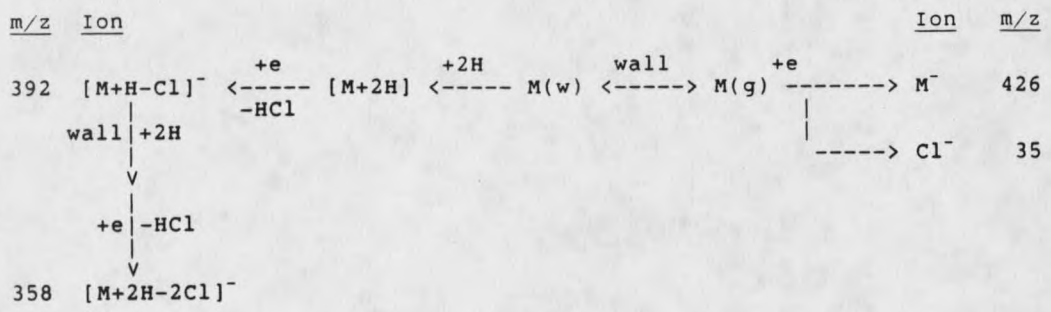


Figure 48. Suggested Mechanism for the Formation of Negative Ions from a PCB Containing 8 Chlorines.

Ions of the Type $[M+R]^-$

A number of the EPA priority pollutants examined in this study displayed HPEC mass spectra that included unusual ions of the type $[M+R]^-$, where R is thought to be H, CH_2, CH_3 or some other carbon containing species. Most of the polycyclic aromatic hydrocarbons (PAH's) in Table 4 showed, at least to some degree, ions of the type $[M+R]^-$. Table 9 presents the tabulated HPEC mass spectra for a selected group of PAH's at various ion source conditions. The compounds listed in Table 9 will now be discussed

Table 9. Tabulated HPEC Mass Spectra for Four PAH's.[a]

Source Conditions					Negative Ions								
Compound	mw	T(°C)	P(Torr)	E(μA)	M-2	M-1	M	M+1	M+14	M+15	M+28	M+29	Other Ions
Fluorene	166	175	0.3	500	2.0	100	15.0[b]	2.8	1.5	—	—	—	24.3(M+12) 4.6(M+13 1.5(M+26) 1.1(M+27)
Fluorene	166	200	0.3	200	—	100	17.8[b]	2.4	1.8	—	—	—	16.7(M+12) 2.6(M+13)
Fluorene	166	220	0.2	500	3.1	100	16.1[b]	2.4	2.2	—	—	—	30.9(M+12) 5.4(M+13) 2.0(M+26) 2.8(M+27) 1.3(M+40)
Fluorene	166	260	0.3	500	2.0	100	15.8[b]	1.1	14.86	2.37	—	—	11.7(M+12) 1.6(M+13) 0.6(M+27)
Fluoranthene	202	100	0.2	500	—	0.5	100	18.0	2.3	0.9	—	—	—
Fluoranthene	202	180	0.2	500	—	1.2	100	18.8	5.9	1.7	—	—	—
Fluoranthene	202	220	0.2	500	—	3.7	100	21.7[b]	6.0	2.3	—	—	—
Fluoranthene	202	220	0.3	200	—	4.1	100	19.3[b]	5.4	1.5	0.4	0.4	—
Fluoranthene	202	260	0.3	200	0.6	4.9	100	22.0[b]	8.9	3.2	1.0	0.9	0.4(M+42) 0.6(M+43)
Fluoranthene	202	260	0.3	500	—	5.9	100	27.2[b]	8.7	3.5	—	—	—
Benzo(b)fluoranthene	252	220	0.2	500	—	1.0	100	22.9	2.1	1.4	—	—	0.5(M+16)
	252	250	0.3	500	—	—	100	22.5	0.9	0.6	—	—	—
Benzo(k)fluoranthene	252	220	0.2	500	—	1.2	100	21.9	4.1	2.3	—	—	—
	252	250	0.3	500	—	—	100	25.6[b]	8.1	3.5	0.5	0.7	0.3(M+30)

a. These values are not correct for ^{13}C contribution

b. Higher than expected for ^{13}C contribution

one at a time. The use of NRSIC will prove of value once again.

Fluorene

Fluorene will be the first of the compounds listed in Table 9 to be presented. The HPEC mass spectrum for this compound at 260°C and 0.3 Torr is shown in Figure 49. This compound displays an ion corresponding to $[M-H]^-$ as its base peak. Deprotonation induced by O_2^- and OH^- ions, which are formed from traces of O_2 and H_2O found in the ion source of some mass spectrometers, has been the suggested process which forms the $[M-H]^-$ ion found in certain polycyclic aromatic hydrocarbon HPEC mass spectra.[25,26] Ions corresponding to O_2^- and OH^- were not observed in the mass spectrometer used in this study. One possible explanation for the $[M-H]^-$ ion is that it is the result of a dissociative electron capture reaction where a neutral hydrogen atom was lost. Figure 49 also shows an ion appearing at $[M-2H]^-$. This ion has also appeared in the literature of PAH's[26] but without explanation. Again, dissociative electron capture cannot be ruled out for the formation of $[M-2H]^-$ ions. In the four different source conditions applied to this compound (Table 9) there appears to be, at least to some degree, evidence of a molecular anion. Ions corresponding to unusual ions of the type $[M+R]^-$ appear at m/z 178 and m/z 180. While the

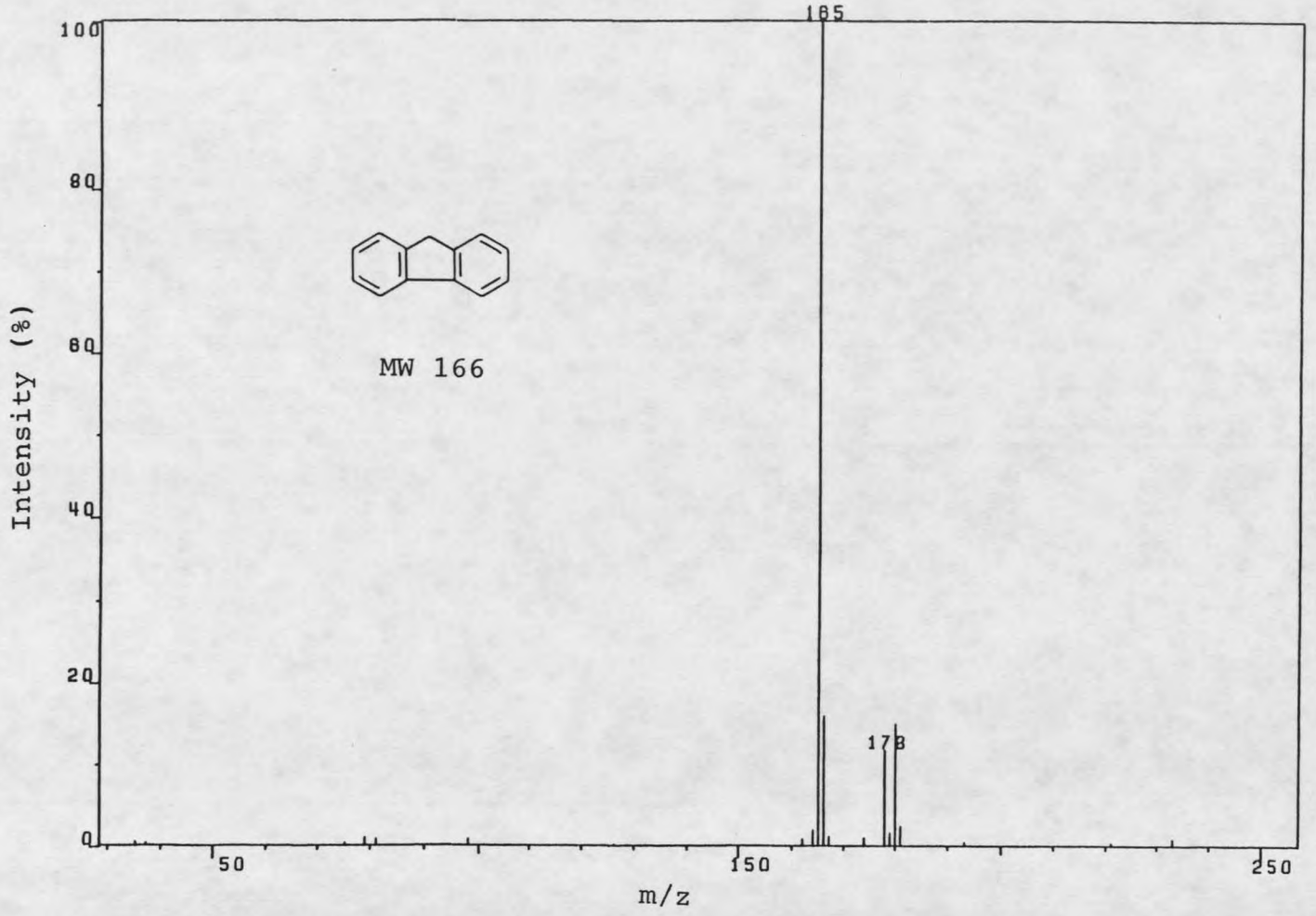


Figure 49. HPEC Mass Spectrum of Fluorene at 260°C and 0.3 Torr.

$[M+14]^-$ ion (m/z 180) is common in the HPEC mass spectra of PAH's, the $[M+12]^-$ ion (m/z 178) is not.

The NRSIC for fluorene at three different sets of ion source conditions are shown in Figures 50 through 52. Figures 50 and 51 at 175°C and 200°C both show the $[M+12]^-$ ion persisting in the ion source after m/z 165. In Figure 52 the temperature of the ion source was 260°C and the abundance of m/z 180 was high enough that a good chromatogram could be reconstructed for this ion. It would appear that the $[M+12]^-$ and $[M+14]^-$ ions of fluorene resulted from the ion source wall, at least in part, and not solely from the gas phase as some investigators had previously thought. If these ions were formed at the source surface, then the gas phase radical-molecule reaction time of 5 msec (compared to the 3 msec of ventilation) does not apply here and the reaction becomes more favorable. The question of whether the unusual ions of the type $[M+R]^-$ originated from the $[M-H]^-$ ion or the parent molecule now arises. The time it takes for a dissociative electron capture, diffusion to the walls, and the electron capture sequence to take place is well within the time frame of ventilation. If the analyte molecule did not capture electrons readily and the [M+R] species did, then the $[M+R]^-$ ion could be of higher abundance than the molecular anion as is the case with fluorene. In the suggested mechanism for the production of unusual ions of

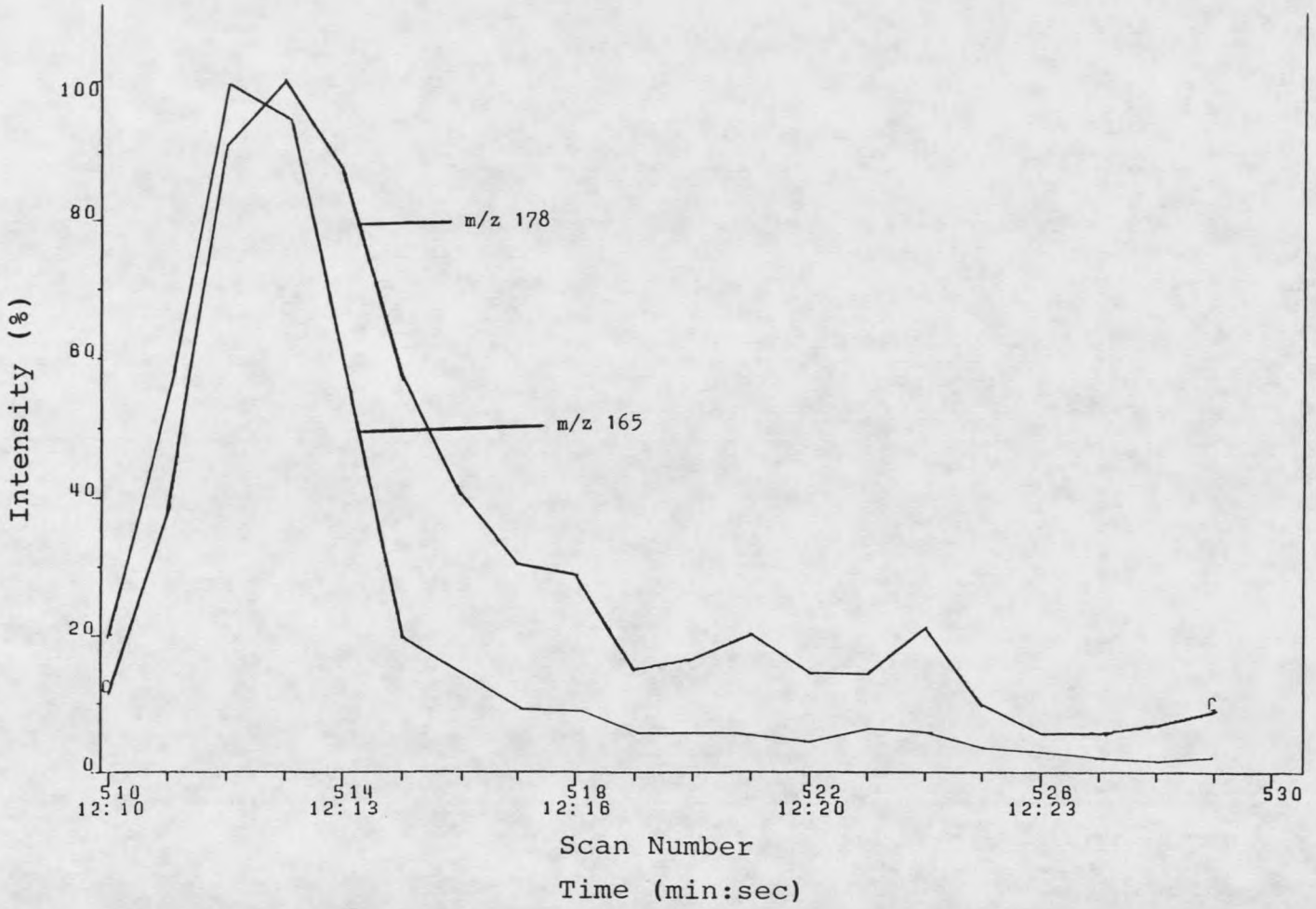


Figure 50. NRSIC for Fluorene at 175°C and 0.3 Torr.

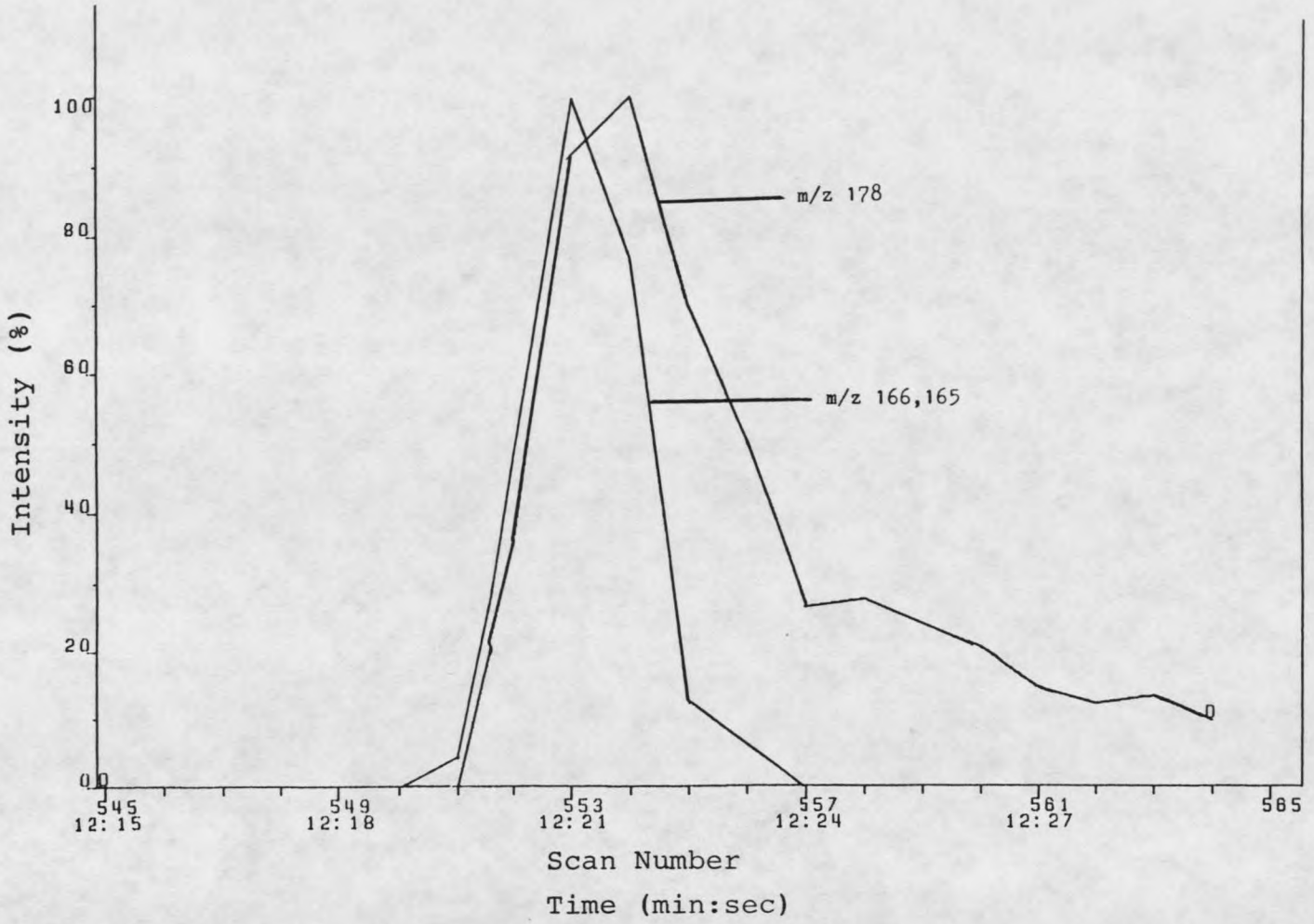


Figure 51. NRSIC for Fluorene at 200°C and 0.3 Torr.

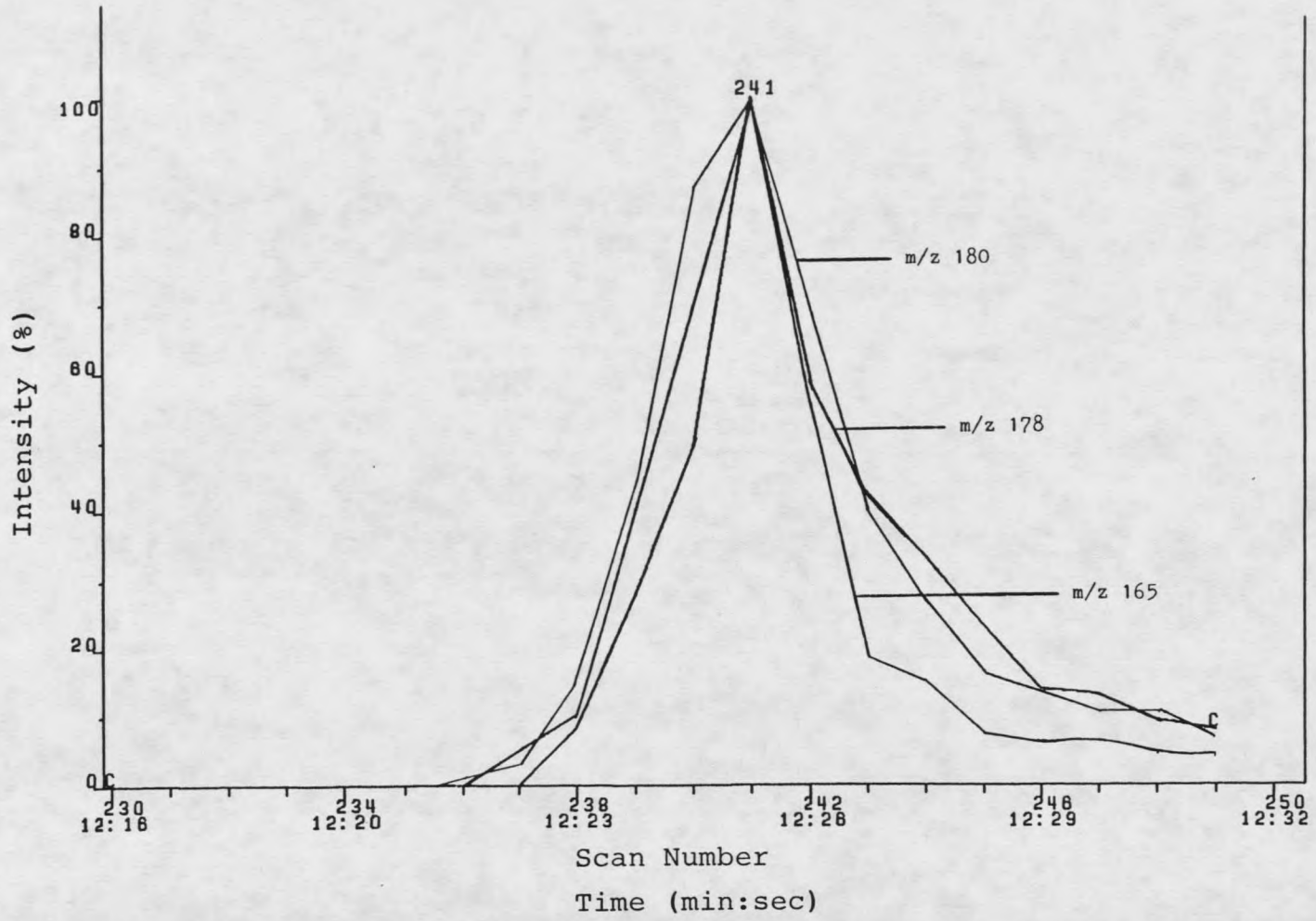


Figure 52. NRSIC for Fluorene at 260°C and 0.3 Torr.

the type $[M+R]^-$ it will be assumed that they originated from the parent-molecular species. Figure 53 is the suggested mechanism for the formation of negative ions from fluorene.

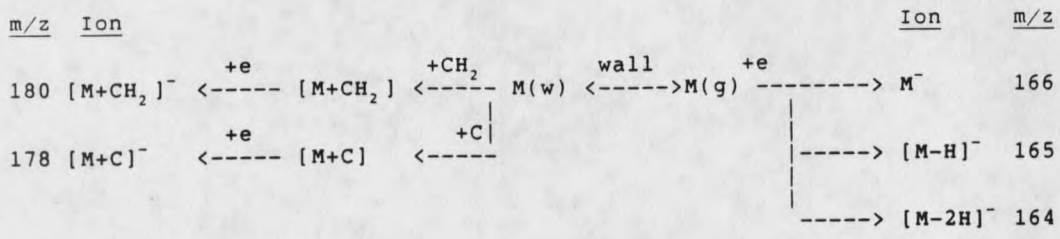


Figure 53. Suggested Mechanism for the Formation of Negative Ions from Fluorene.

Fluoranthene

The next compound to be shown that produces ions of the type $[M+R]^-$ is fluoranthene. The HPEC mass spectrum of this compound at 260°C and 0.3 Torr is shown in Figure 54. The base peak in the spectra of fluoranthene is the molecular anion. As is shown in Table 9, an ion corresponding to $[M-H]^-$ increases with increasing temperature, possibly indicating that this ion results from dissociative electron capture. Also, as shown in Table 9 an ion corresponding to $[M+H]^-$ appears and grows in intensity with increasing temperature. This ion could be the result of gas phase proton transfer or a hydrogen radical addition followed by electron capture. The $[M+H]^-$ ion could also result from the ion source wall, but

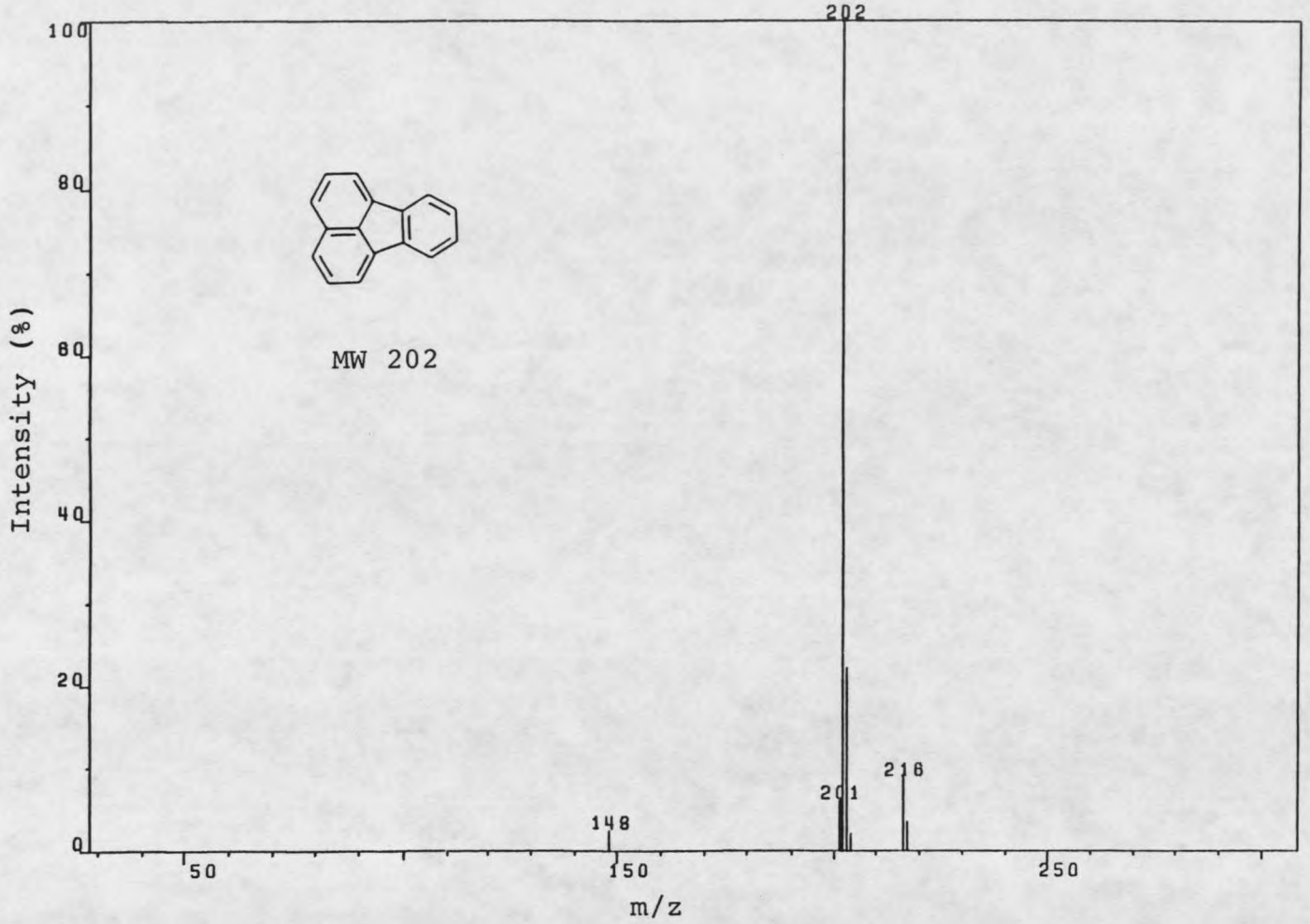


Figure 54. HPEC Mass Spectrum of Fluoranthene at 260°C and 0.3 Torr.

evidence to be given shortly does not confirm this. Unusual ions of the type $[M+R]^-$ at m/z 216 and m/z 217 are present in all cases shown for fluoranthene in Table 9. In two of the reported spectra in Table 9 ions at m/z 230 and m/z 231, corresponding to $[M+28]^-$ and $[M+29]^-$, were observed while one spectrum shows ions at m/z 244 and m/z 245 which correspond to $[M+42]^-$ and $[M+43]^-$.

The NRSIC for fluoranthene at three different sets of ion source conditions are shown in Figures 55 through 57. These figures only show the chromatographic traces for ions with a strong enough intensity to produce a usable trace. Figures 55 and 56 show NRSIC for fluoranthene at 100°C and 180°C. In both figures the $[M+14]^-$ ion at m/z 216 is remaining inside the ion source for a longer period of time than the molecular anion, suggesting this unusual ion had its origins on the ion source surface. The NRSIC shown in Figure 57 suggests that the $[M+28]^-$ ion might actually be the result of two consecutive wall reactions by the same species where an $\cdot CH_2$ radical is picked off the wall each time. The suggested ion forming mechanism for a selected number of ions present in the HPEC mass spectra of this compound is shown in Figure 58.

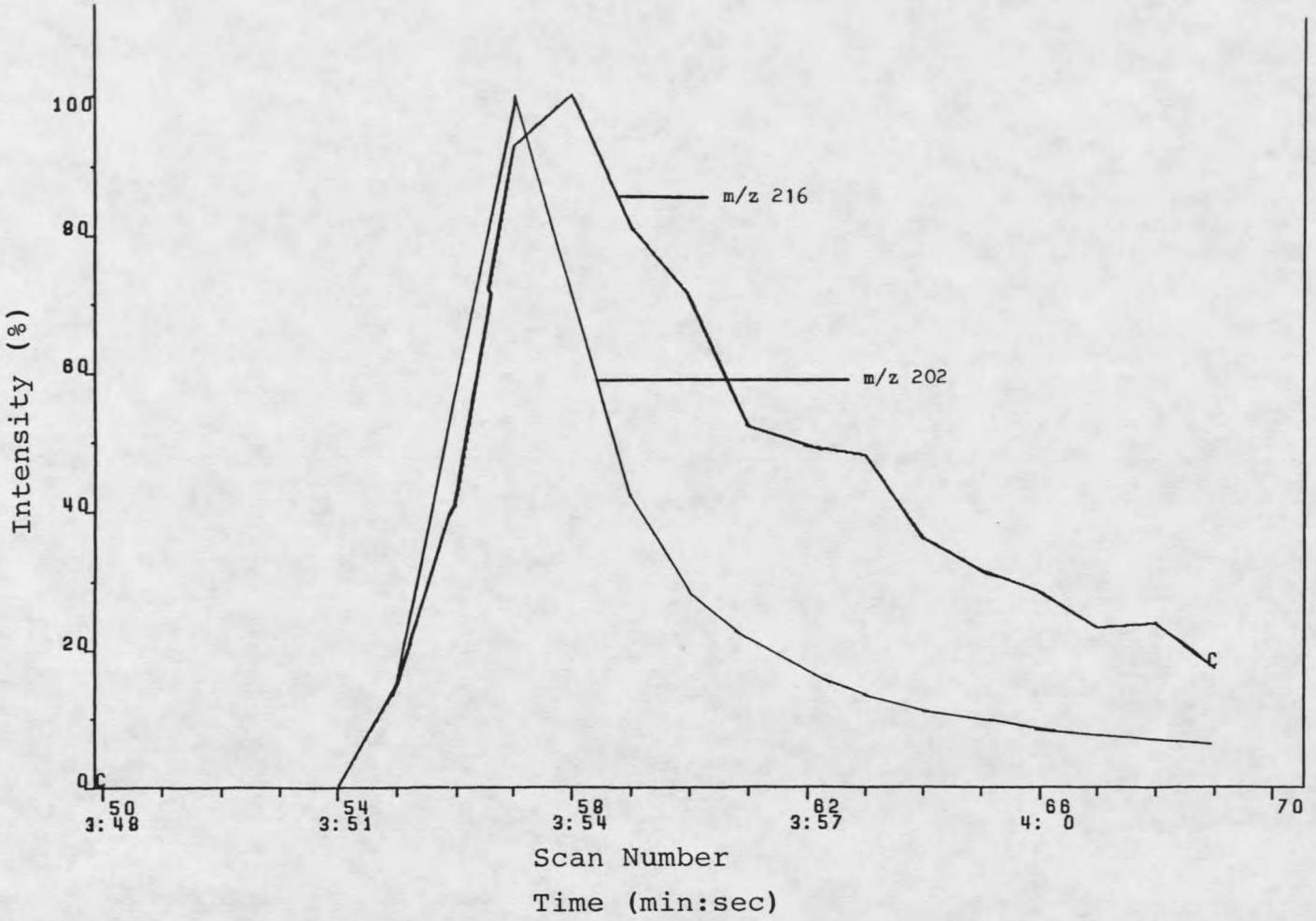


Figure 55. NRSIC for Fluoranthene at 100°C and 0.2 Torr.

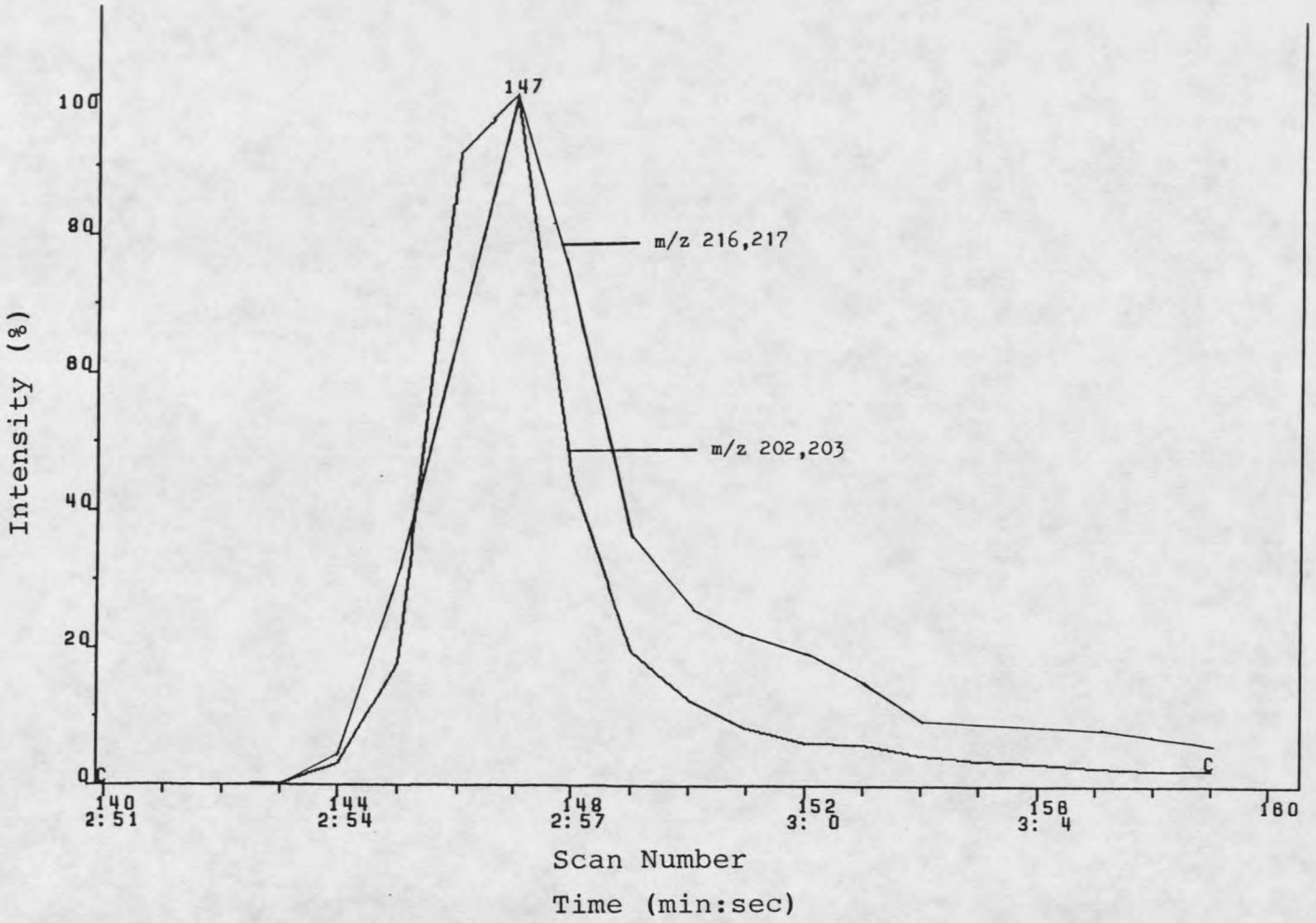


Figure 56. NRSIC for Fluoranthene at 180°C and 0.2 Torr.

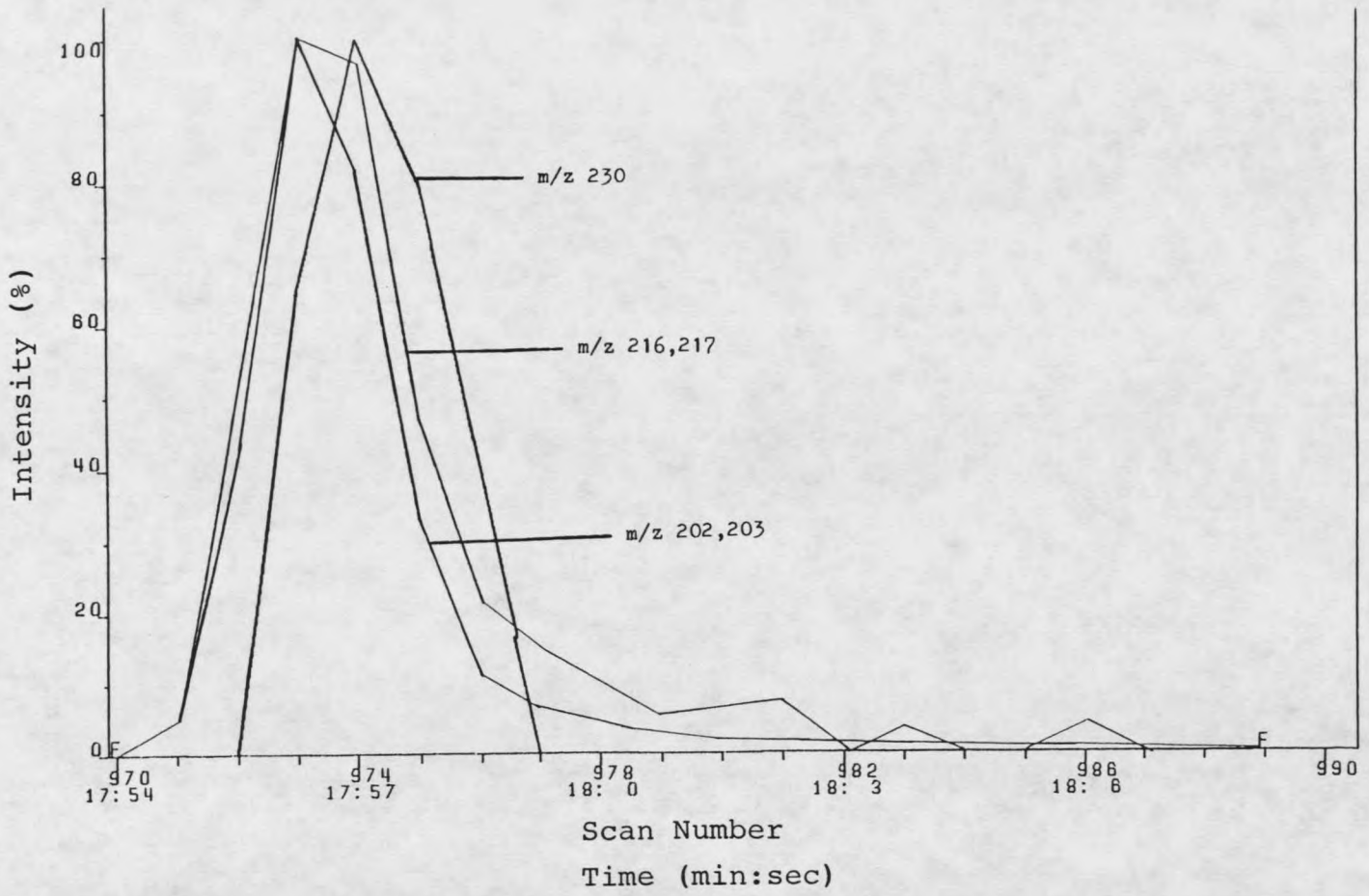


Figure 57. NRSIC for Fluoranthene at 200°C and 0.3 Torr.

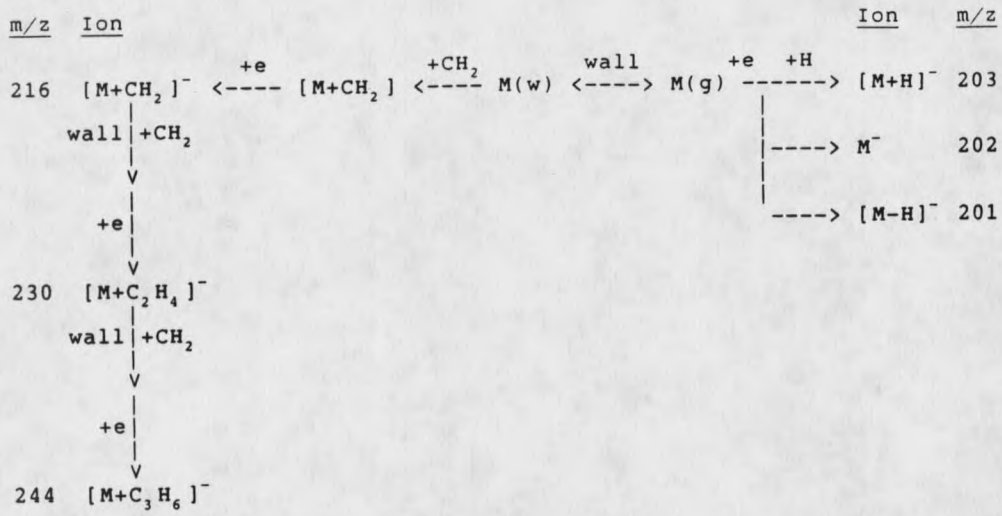


Figure 58. Suggested Mechanism for the Formation of Negative Ions from Fluoranthene.

Benzo(b)fluoranthene

The HPEC mass spectrum of benzo(b)fluoranthene at 250° and 0.3 Torr methane is shown in Figure 59. This compound shows a predominant M^- ion and ions of the type $[M+14]^-$ and $[M+15]^-$ only in very small abundance, as shown in Table 9. The NRSIC for benzo(b)fluoranthene at 220°C and 0.2 Torr are shown in Figure 60. As was the case for the previous PAH's discussed, the unusual ion $[M+14]^-$ is remaining in the ion source much longer than the molecular anion, m/z 252. The suggested mechanism for the formation of negative ions from this compound is shown in Figure 61.

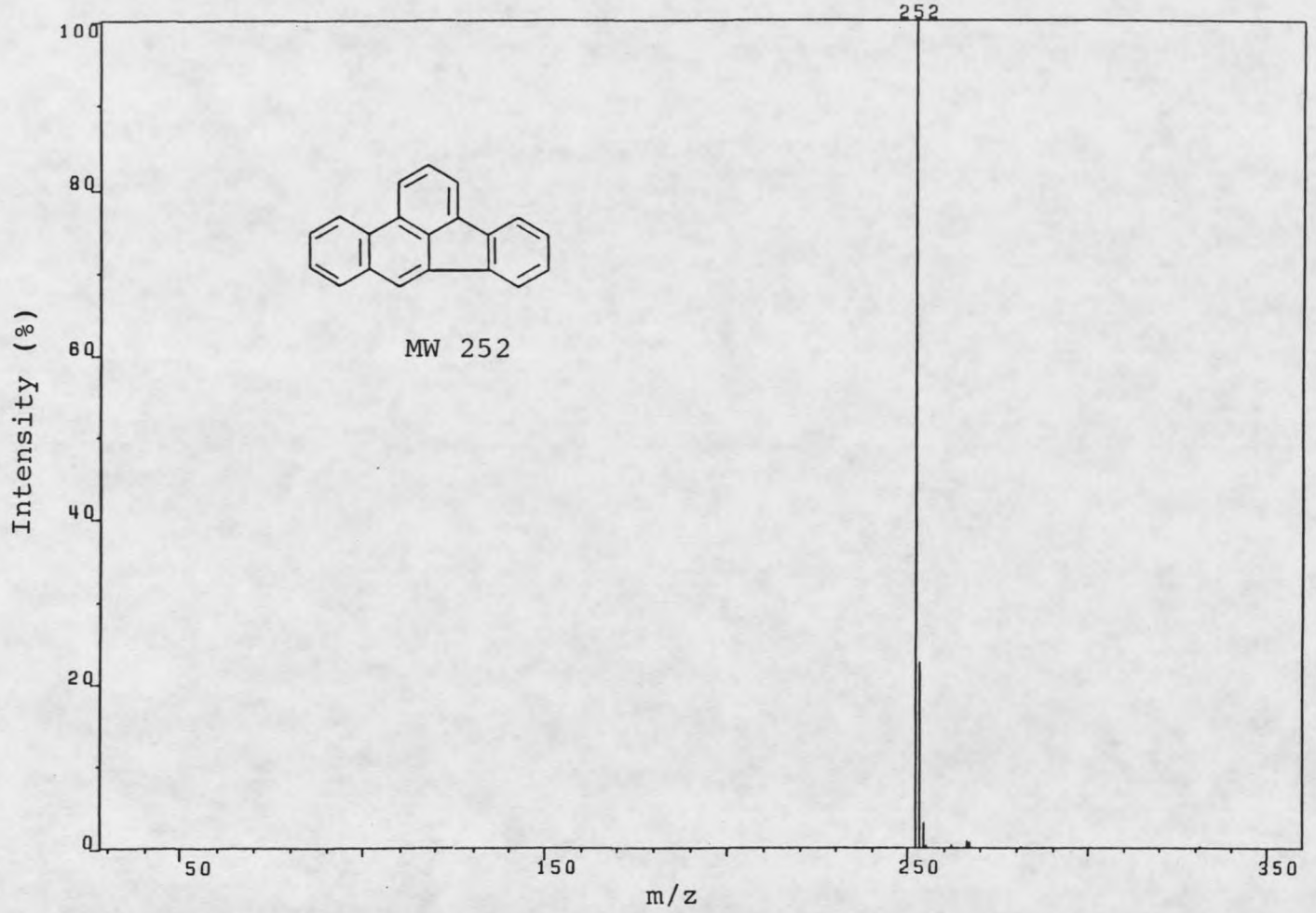


Figure 59. HPEC Mass Spectrum of Benzo(b)fluoranthene at 250°C and 0.3 Torr.

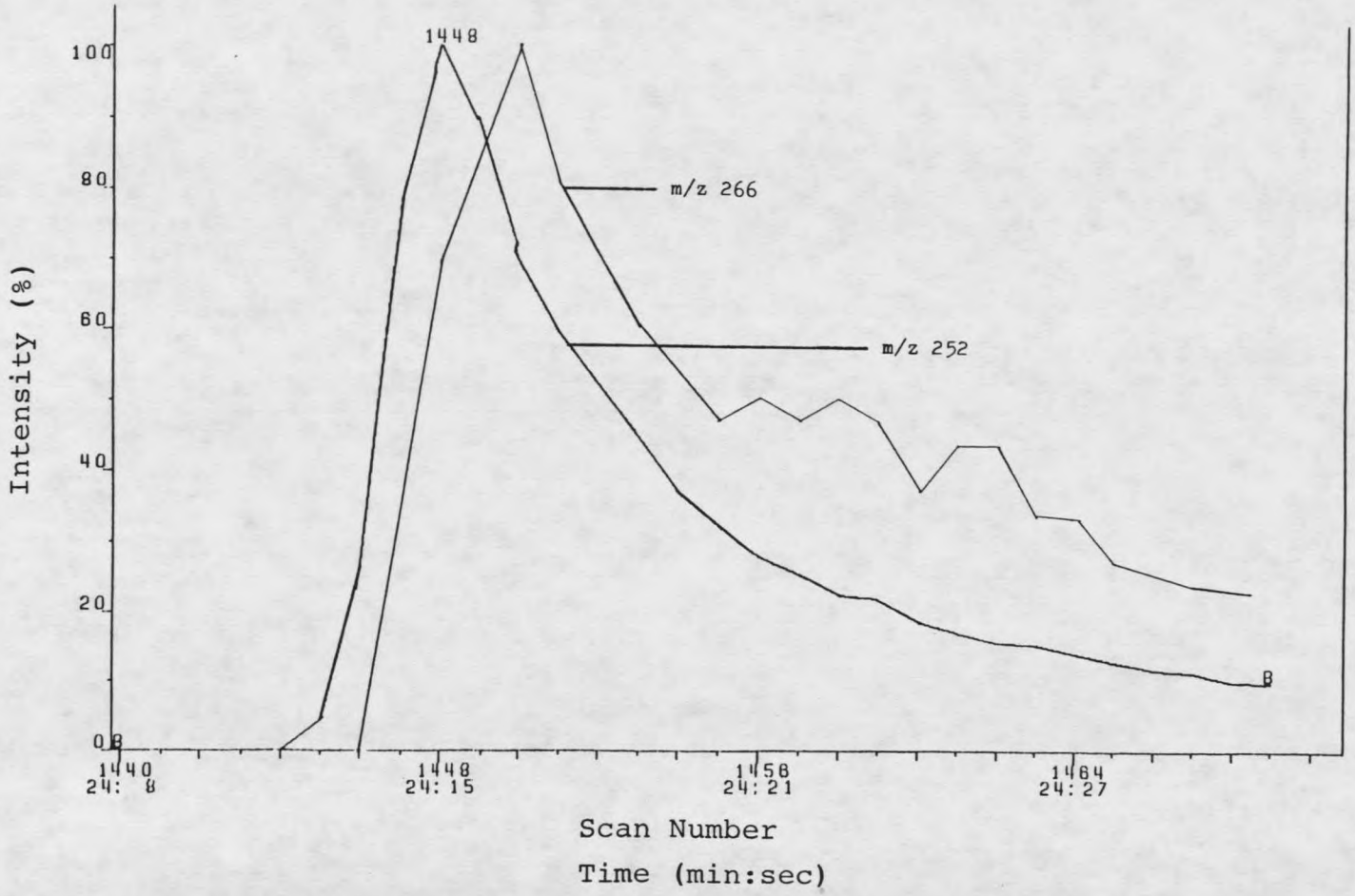


Figure 60. NRSIC for Benzo(b)fluoranthene at 220°C and 0.2 Torr.

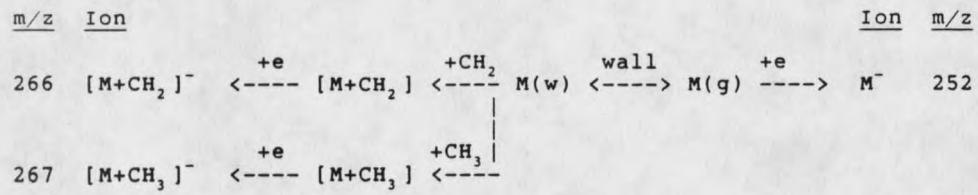


Figure 61. Suggested Mechanism for the Formation of Negative Ions from Benzo(b)fluoranthene.

Benzo(k)fluoranthene

The last example of a compound that produces ions of the type $[M+R]^-$ that will be presented is benzo(k)-fluoranthene. Figure 62 is the HPEC mass spectrum of this compound at 250°C and 0.3 Torr methane. The molecular anion is the base peak of this compound as shown in Figure 62. Table 9 shows that the unusual ions $[M+14]^-$ and $[M+15]^-$ are produced by this compound. The NRSIC for benzo(k)fluoranthene at 250° and 0.3 Torr are shown in Figure 63. The suggested negative ion production mechanism for this compound is shown in Figure 64.

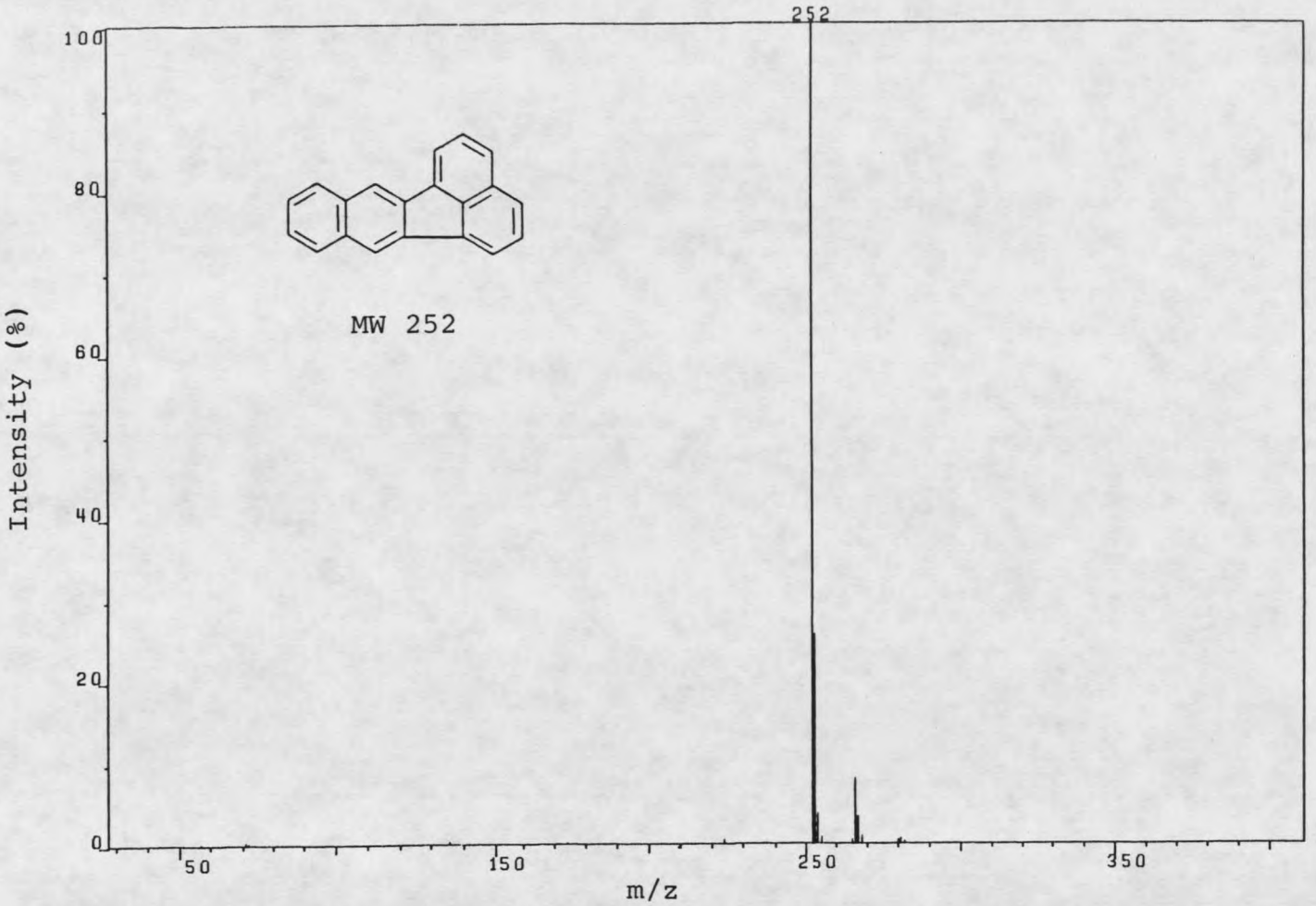


Figure 62. HPEC Mass Spectrum of Benzo(k)fluoranthene at 250°C and 0.3 Torr.

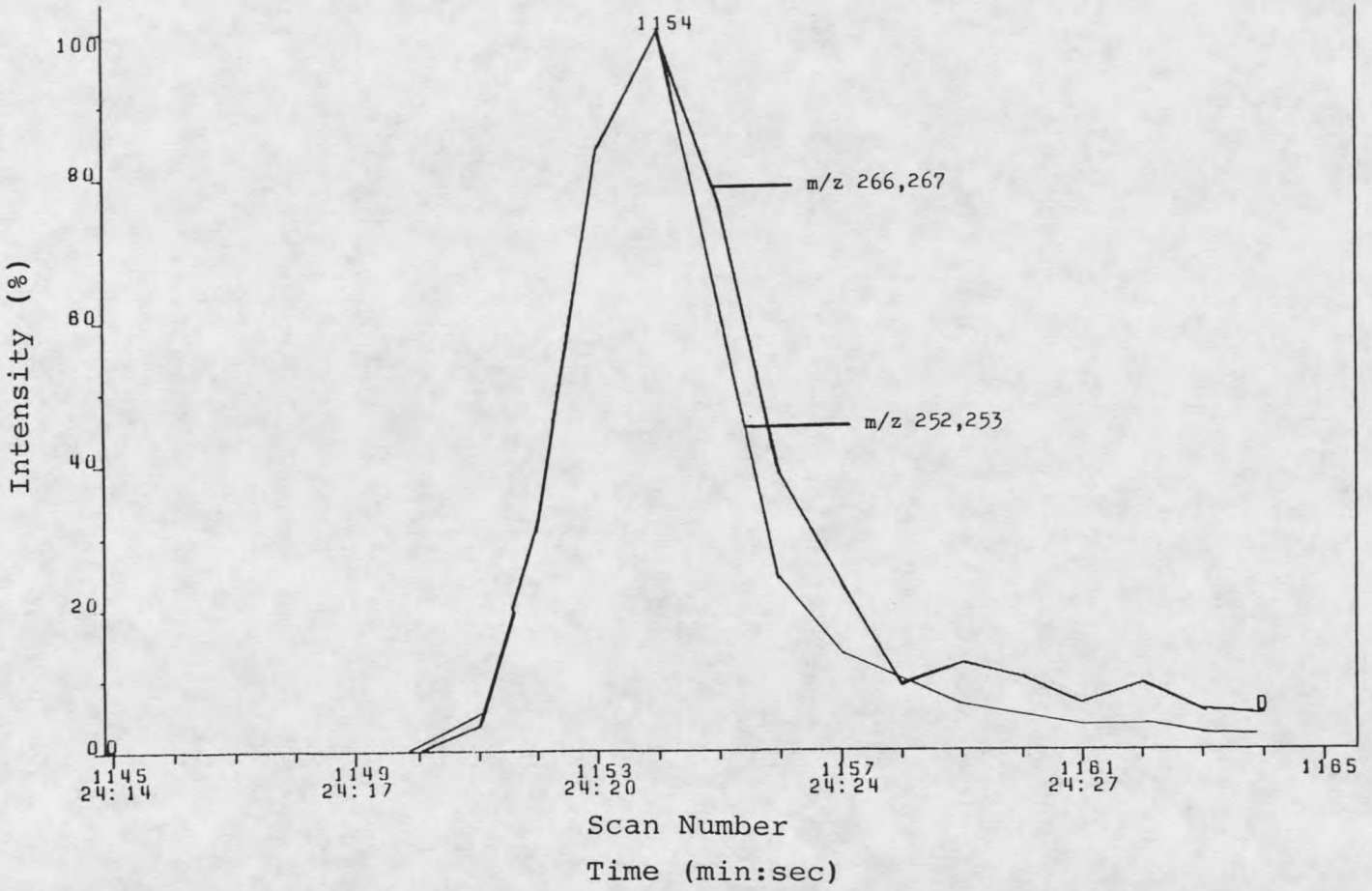


Figure 63. NRSIC for Benzo(k)fluoranthene at 250°C and 0.3 Torr.

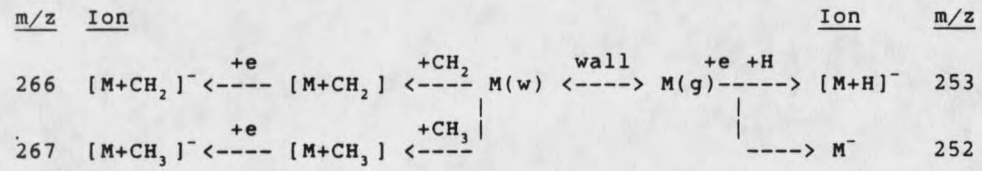


Figure 64. Suggested Mechanism for the Formation of Negative Ions from Benzo(k)fluoranthene.

SUMMARY

The high pressure electron capture mass spectra of 61 of the EPA priority pollutants were initially examined for evidence of negative ions that were the result of chemical processes in addition to resonance and dissociative electron capture. As a result of this initial investigation, two general types of unusual negative ions were discovered. The first corresponded to ions of the type $[M-Z+nH-nCl]^-$ where Z is either a fragment of M whose mass depends on its composition or is zero. The value of n was found to be as great as 5 in some cases. Many of the polychlorinated species investigated were shown to produce ions of the type $[M-Z+nH-nCl]^-$. The second type of unusual ions observed corresponded to ions of the type $[M+R]^-$, where R was thought to be H, CH_2, CH_3 or some other carbon based species. Most of the polycyclic aromatic hydrocarbons investigated were found to produce ions of this type.

Strong evidence was presented which indicated that both types of unusual ions were the result, at least to a fair degree, of interactions of analyte species with the ion source surface. The evidence for ion source wall activity was displayed through normalized reconstructed

single ion chromatograms (NRSIC) which were proven to be an excellent indicator of neutral species leaving the ion source walls at different times. Both the background and theory in Chapter 1 support the idea of chemical reactions taking place on the ion source walls.

The HPEC mass spectra and NRSIC were examined at various temperatures, pressures, and emission currents of the ion source. The dependence of the spectra and NRIC on the ion source conditions were discussed for some compounds.

A mechanism was proposed for each compound that produced unusual ions in HPECMS. The mechanisms include both gas phase and surface assisted reactions for both types of unusual ions observed in the HPEC mass spectra of EPA priority pollutants.

Finally, the results suggest that the ion source surface is a complex region where reactions can take place. The time an analyte species spends adsorbed to the walls of the ion source seems dependent on the structure of the analyte molecule. Further studies in the area surface activities of the mass spectrometer ion source could prove to be worthwhile in examining not only HPEC mass spectra, but mass spectra produced by other modes of ionization.

REFERENCES CITED

1. Munson, M. S. B., and F. H. Field, J. Amer. Chem. Soc. **88**, 2621 (1966).

2. Dougherty, R. C., and J. Dalton, Org. Mass Spec. **6**, 1171 (1972).

3. Siegel, M. W., in Practicle Spectroscopy Series, Vol. 3, Part B, Chapter 4, ed. by Merrit, Jr., and C. N. McEwen. Marcel Dekker, New York (1980).

4. Harrison, A. G., Chemical Ionization Mass Spectrometry, Chapter 2, CRC Press, Inc., Boca Raton, Florida (1983).

5. Szulejko, J. E., et. al., Organic Mass Spectrometry **15**, 263 (1980).

6. Laramee, J. A., B. C. Arbogast, and M. L. Deinzer, Anal. Chem. **58**, 2907 (1986).

7. Christophorou, L. G., Environmental Health Perspectives **36**, 3 (1980).

8. Sears, L. J., J. A. Campbell, and E. P. Grimsrud, Biomedical and Environmental Mass Spectrometry **14**, 401 (1987).

9. Dougherty, R. C., Anal. Chem. **53**, 625A (1981).

10. Hunt, D. F., and F. W. Crow, Anal. Chem, **50**, 1781 (1978).

11. Ibrahim, K. E., et. al., Anal. Chem. **56**, 1695 (1984).

12. Stockl, D., and H. Budzikiewicz, Organic Mass Spectrometry **17**, 470 (1982).

13. Gregor, I. K., and M. Guilhaus, Int. J. Mass Spec. & Ion Processes **56**, 167 (1984).

14. Stockl, D., and H. Budzikiewicz, Organic Mass Spectrometry **17**, 376 (1982).

15. McEwen, C. N., and M. A. Rudat, J. Amer. Chem. Soc. **103**, 4343 (1981).

16. Stemmler, E. A., et. al., Biomedical and Environmental Mass Spectrometry, submitted for publication, June 1987.

17. Crow, F. W., et al., Anal. Chem, 53, 619 (1981).

18. Grimsrud, E. P., S. Chowdhury, and P. Kebarle, Int. J. Mass. Spec. & Ion Proc. **68**, 57 (1986).

19. Stemmler, E. A., and R. A. Hites, Anal. Chem. **57**, 684 (1985).

20. Kassel, D. B., K. A. Kayganich, and J. T. Watson, American Society for Mass Spectrometry, 34th Annual Conference, Cincinnati, Ohio (1986), Abstracts, page 523.

21. Jones, R. G., Surface Science **88**, 367 (1979).

22. Deinzer, M., et. al., Biomed. Mass Spec. **9**, 85 (1982).

23. Rappe, C., et. al., Nature (London), **292**, 524 (1981).

24. Hilpert, L. R., G. D. Byrd, and C. R. Vogt, Anal. Chem. **56**, 1842 (1984).

25. Oehme, M., Anal. Chem. 55, 2290 (1983).

26. Iida, Y., and S. Daishima, Chemistry Letters 273 (1983).

27. American Institute of Physics Handbook, 3rd edition, ed. by J. B. Marion and D. E. Gray, p. 184, McGraw-Hill, New York (1972).

28. Pellizzari, E. D., J. Chromatogr. **98**, 324 (1974).

29. Mitchell, J. B. A., and J. W. McGowan, in Physics of Ion-Ion Collisions, ed. by F. Brouillard and J. W. McGowan, p. 279. Plenum Press, New York (1983).

30. Smith, D., and N. G. Adams, in Physics on Ion-Ion and Electron-Ion Collisions, ed. by F. Brouillard and J. W. McGowan, p. 501. Plenum Press, New York (1983).

31. Kerr, J. A., in Free Radicals, ed. by J. K. Kochi, Vol. 1, Chapter 1, John Wiley & Sons, New York (1973).

32. Langmuir, I., Phys. Rev. 33, 954 (1929).

33. McDaniel, E. W., Collision Phenomena in Ionized Gasses, pp. 503-506, Wiley, New York (1964).

34. Dushman, S., in Scientific Foundations of Vacuum Techniques, ed. by J. M. Lafferty, p. 91. John Wiley and Sons, Inc., New York (1962).

35. Morris, M. A., M. Bowker, and D. A. King, in Comprehensive Chemical Kinetics, Vol. 19, Chapter 1, ed. by C. H. Bamford, et. al., Elsevier Science Publishing Company, Inc., New York (1984).

36. Grabke, H. J., Metallurgical Transactions 1, 2972 (1970).

37. Mason, R., F. R. S. and M. Textor, Proc. R. Soc. Lond. 365A, 47 (1977).

38. Dushman, S., Scientific Foundations of Vacuum Techniques, ed. by J. M. Lafferty, p. 66. John Wiley, New York (1962).

39. Telliard, W. A., Spectra 10, 4 (1986).

APPENDIX

Table 10. Tabulated HPEC Mass Spectra for Heptachlor Epoxide.

Source Conditions			Negative Ions						
T°C	P(Torr)	Ec(mA)	386	352	316	280	235	71	35
80	0.3	0.2	6	1	4	3	4	4	100
100	0.1	0.5	1	<1	2	2	-	2	100
100	0.3	0.2	4	1	9	6	8	12	100
100	0.5	0.2	3	1	4	3	3	5	100
175	0.2	0.5	-	-	5	5	2	5	100
175	0.3	0.2	-	-	2	3	2	3	100
175	0.45	0.2	-	-	4	4	10	4	100
175	0.45	0.5	<1	-	4	4	11	4	100
220	0.3	0.2	-	-	1	2	<1	2	100

Table 11. Tabulated HPEC Mass Spectra for Dieldrin.

Source Conditions			Negative Ions					
T°C	P(Torr)	Ec(mA)	378	344	310	235	71	35
85	0.3	0.2	10	15	2	4	-	100
100	0.3	0.2	8	16	2	5	1	100
100	0.5	0.2	5	7	<1	3	1	100
175	0.2	0.5	1	5	1	1	<1	100
175	0.3	0.2	-	1	-	1	2	100
175	0.45	0.2	<1	2	1	9	1	100
175	0.45	0.5	<1	2	<1	8	<1	100
220	0.3	0.2	-	-	-	1	1	100

Table 12. Tabulated HPEC Mass Spectra for Heptachlor.

Source Conditions			Negative Ions						
T°C	P(Torr)	Ec(mA)	370	298	264	235	230	71	35
80	0.3	0.2	-	2	3	1	1	2	100
100	0.3	0.2	-	4	6	3	3	5	100
175	0.2	0.5	-	4	4	1	2	2	100
175	0.3	0.2	-	2	3	1	1	1	100
175	0.45	0.2	-	3	7	3	2	1	100
175	0.45	0.5	-	4	11	2	4	-	100
220	0.3	0.2	-	2	3	1	1	1	100

Table 13. Tabulated HPEC Mass Spectra for Endrin.

Source Conditions			Negative Ions							
T°C	P(Torr)	Ec(mA)	378	344	308	270	235	71	70	35
80	0.3	0.2	11	10	-	-	2	-	-	100
100	0.3	0.2	4	7	1	<1	4	2	4	100
175	0.2	0.5	1	1	3	3	1	2	5	100
175	0.3	0.2	<1	1	2	2	1	3	6	100
175	0.45	0.2	2	3	7	6	10	5	15	100
175	0.45	0.5	<1	<1	1	1	3	1	4	100
220	0.3	0.2	-	-	2	3	-	3	5	100

Table 14. Tabulated HPEC Mass Spectra for Endosulfan Sulfate.

Source Conditions			Negative Ions									
T°C	P(Torr)	Ec(mA)	420	384	351	350	349	348	185	97	80	35
100	0.3	0.2	17	58	6	9	1	1	6	94	5	34
175	0.2	0.5	1	35	9	11	1	1	8	100	5	-
175	0.3	0.2	1	29	9	13	1	1	7	100	5	<1
175	0.45	0.2	2	33	7	10	1	1	7	100	6	12
175	0.45	0.5	2	28	5	8	1	1	6	100	6	19
220	0.3	0.2	-	10	6	8	1	1	7	100	6	3

Table 15. Tabulated HPEC Mass Spectra for Mirex.

Source Conditions			Negative Ions										
T°C	P(Torr)	Ec(mA)	435	400	366	332	298	264	235	230	71	70	35
100	0.3	0.2	1	3	6	2	1	-	-	-	6	1	100
175	0.2	0.5	1	3	6	2	1	1	<1	-	3	1	100
175	0.3	0.2	3	6	12	13	7	4	1	2	10	8	100

Table 16. Tabulated HPEC Mass Spectra for Pentac.

Source Conditions			Negative Ions									
T°C	P(Torr)	Ec(mA)	435	400	366	332	298	264	235	230	201	35
100	0.3	0.2	-	27	3	11	25	5	4	1	1	100
175	0.3	-	1	16	2	4	11	13	6	7	1	100

Table 17. Tabulated HPEC Mass Spectra for Hexachlorobenzene.

Source Conditions			Negative Ions			
T°C	P(Torr)	Ec(mA)	282	247	248	35
100	0.3	0.2	51	1	4	2
175	0.2	0.5	51	-	2	7
220	0.3	0.2	51	1	1	26

MONTANA STATE UNIVERSITY LIBRARIES
3 1762 10023613 0